**Response to the**
**Reviewer comments on**

"Changes in glacier dynamics at the northern Antarctic Peninsula since 1985"

By Thorsten Seehaus et al.

**Anonymous Referee #1**
**Received: 04 August 2017**

**First of all we want to thank the reviewer for constructive comments on our manuscript. All comments have been taken into account and a list of answers and undertaken actions is given below. Answers are indented and in bold face type and changes in manuscript are indented in** *italic.*

1) Because this study confines itself to a rather specific portion of the whole Antarctic Peninsula 'region', the authors are cautioned to avoid vague terms such as 'region' (see Abstract, page 1, line 11) when referring to only the very northern part of the contiguous AP and none of the adjacent islands.

**We appreciate the comment and carefully revised the usage of "region" throughout the manuscript.**

2) 'Seal Nunataks' is used in the abstract to provide a geographic limit to the study area (page 1 line 13) but should refer to Fig. 1 as it is not labeled on the other maps.

**It is quite uncommon to refer to figures in the abstract. Therefore, we do not want to do it here. In the description of the study site in the Introduction we refer to Fig. 1.**

3) The authors are similarly cautioned to be specific when referring to the 'study period' given that the title states that the study period is 'since 1985' but the velocity data covers a much shorter period, especially for some glaciers, and some regions only had 'area changes' since ~1995.

**We revised the usage of "study period" and year numbers provided according to the reviewer's comment.**

4) Similar to #1, the authors must be clear that the warming that has been observed on the 'Antarctic Peninsula' must be limited to the 'northern' AP and its outlying islands given where the majority of the data sets are located (page 1 line 26).

**We rephrased this sentence to be clearer.**

*During the last century, the northern Antarctic Peninsula (AP) and its outlying islands haves undergone significant warming (Turner et al., 2005), leading to substantial glaciological changes.*

5) The use of a single reference to document the loss of ice shelves, page 2 line 10, appears a little uncharitable to the many researches who have contributed a great deal of insight and analysis to this particular topic along and across the AP. Even though additional references are added below, the list still seems inadequate and does not give the reader a useful sense of what shelf areas were lost and when.

**We revised this sentence and added reference and year numbers.**

*Numerous ice shelves along the AP have retreated widely (e.g. Müller, Wilkins, Wordie) or disintegrated in recent decades (e.g. Braun and Humbert, 2009; Cook and Vaughan, 2010; Doake and Vaughan, 1991; Rack et al., 1998; Rack and Rott, 2003; Wendt et al., 2010)*

6) Related to #5, close inspection of Figure 1 helps somewhat with this issue but the placement of the 'keys' on top of the area changes is unhelpful. Further, dashed lines would help differentiate some of the colors that are very similar. Oddly, it is only by closely reading the text that one realizes that the northern end of the contiguous AP was studied but lacked enough velocity data to be included (those basins are included in Figure 5 for area change). It isn't clear why the basins are cropped off.

**According to the reviewer's advice, we revised the "keys" and replaced some solid lines by dashed or dotted lines of Fig.1. We revised Fig. 5 and removed the "cropped off" basins at the northern end, which are not included in our study area.**

7) On page 2, line 23, given the number of studies in this section, it isn't clear which 'authors' are being discussed.

**We rephrased this sentence to be clearer.**

*Observations by Kunz et al. (2012) support this supposition. They analyzed surface elevation changes of 12 glaciers on the western AP based on stereoscopic digital elevation models (DEM) over the period 1947-2010.*

8) Similar to #1, the term 'north-eastern' appears to mean the northern AP's eastern glacier basins on page 2, line 25. Also, 'as a consequence to' on line 26 is unclear.

**This section was revised to be clearer.**

*Frontal surface lowering was found at all glaciers. Whereas, glacier area-wide surface lowering of ice shelf tributaries was observed along the north-eastern AP by various author groups (e.g. Berthier et al., 2012; Rott et al., 2014; Scambos et al., 2014).*

9) The phrase 'not homogeneous' (page 2, line 28) seems rather obvious. One assumes that the authors mean this in both space and time and this should be linked back to the different times that glaciers in the area have become marine- as opposed to shelf-terminating.

**We would like to keep the sentence as it is, since all details are already provided above.**

10) The phrase "Previous studies often only cover a specific period or region, or focus on one particular aspect of glacier change." On page 2 lines 29-30 also appears to be uncharitable to other researchers who worked with what data sets were available to them at the time. In time, this study will also be superseded by new data and techniques so I suggest rephrasing the intended meaning.

**The reviewer is right and we revised this section accordingly.**

*Previous studies often cover a specific period or area, or focus on one particular aspect of glacier change. By now, the availability of remote sensing data time series data and other data sets in this region facilitates the comprehensive analysis of glacier change.*

11) Similar to previous concerns, 'northern-most' (page 3, line 5) is quite imprecise and requires all outlying islands of the AP to be ignored. The analysis of Huber et al. 2017 makes it quite clear how much area of the AP has been excluded in this study.

**We refer her to the whole AP, since it is the introductory sentence to the section "Study site". Further down, we specify our study area more precisely. See also answer to comment #16.**

12) Please review all superscripts for consistency (page 3, line 8). Also, should 'yr' or 'a' -1 be used?

**Thank you for this advice. We revised the superscripts and replaced "yr" by "a" to be consistent.**

13) Given their prominence on the figures and also as the source areas for many glaciers, the 'plateau regions' should be referenced (page 3, line 12).

**We added the names of the plateau regions.**

*Aside from those that are ice shelf tributaries, almost all glaciers on the AP are marine terminating, and the majority of the glacier catchments extend up to the high elevation plateau regions (north to south: Laclavère, Louis Philippe, Detroit, Herbert, Foster, Forbidden, Bruce, Avery, Hemimont, Dyer).*

14) The Prince Gustav (no hyphen) shelf had left the channel before 1995 according to ADD and also the USGS I-2600A map (page 3, line 15).

**The ADD and USGS I-2600A map shows the extent of Prince Gustav ice shelf in 1993 (across the channel) and 1995 (the channel is open). However, the date of the ice shelf break up cannot be determined based on these maps.**
**The ice shelf quite likely broke up in early 1995 according to Rott et al. 1996: *"A National Oceanic and Atmospheric Administration (NOAA) image from 9 January 1995 shows that although the channel was open, major icebergs were close to the previous ice shelf, which indicated that the shelf had broken only a few days earlier."***

**To be clearer we added a literature reference. All hyphens between "Prince" and "Gustav" were removed.**

15) The phrase 'long-term' is not appropriate for ~20+ year records (see previous comment on 'study period').

**We removed the phrase "long-term" in this sentence.**

16) Given the use of percentages in a number of places in the paper is seems appropriate to contrast the '11,000 km2' area (page 3, line 26) against the whole area of the AP including its islands. Also 'altitudes' should probably be 'elevations'.

**We appreciate the reviewer's suggestion and added information on the percentage of AP area coverage by our study area. Altitudes were replaced by elevations.**

*The study area covers an area of ~11,000 km$^2$ (~11% of the whole AP including islands, Cook et al., 2014; Huber et al., 2017) with elevations stretching from sea level up to 2220 m.*

17) There are too many 'word choices' to point them all out but 'substituted' should be 'replaced' (page 3, line 29).

**According to the reviewer's advice, we changed the wording.**

18) Please revise capitalization on page 4, lines 8-9. Also line 26.

**We revised the capitalization.**

19) One assumes that the '100m' (please check spacing for units throughout the text) pixel spacing requires resampling given the native resolutions now listed in Table 2 as 'nominal ground resolution'* although one has to wonder if this is also due to incidence angle on the AP's 'jagged' topography. Please clarify.

**The resolution of the velocity fields depends on the combination of the SAR data resolution in slant-range-geometry (not the ground range resolution in Table 2) and the tracking step-size (Table 2) of the tracking process. We applied step-sizes in order to achieve approx. 100 m pixel spacing of the velocity results. The geocoding and orthorectification algorithms include a resampling process.**
**Only for the high resolution sensors (TerraSAR-X and TanDEM-X), tracking results of 50 m resolution (based on SAR resolution and step-size) were calculated and resampled to 100 m resolution, in order to use the same resolution for all sensors.**
**We added information on this issue in the manuscript.**
**As described in the manuscript, we correct for effects on the local incidence angle by the AP's "jagged" topography. (see also next answer to next comment)**

20) A requested 'summary' of the uncertainty in the ASTER DEM has been inserted on page 5, line 25. Unfortunately, a quick examination of Cook et al. (2012) Figure 5, the paper that is the source of the elevation bias, shows that the bias number is itself biased towards the much more extensive ICESat coverage far to the south (to 70°S) of this paper's study area. With the vast majority of the ICESat to DEM comparisons apparently coming from lower slope areas of the AP, it is highly unlikely that the given numbers apply to the 63-65°S portion of the AP. Further, no attempt appears to have been made to show if the bias varies as a function of slope in the study area. One has to wonder why this was not done given the importance of the DEM to the geometric aspects of the study as well as the potential to impact the velocity data. In short, a much more realistic assessment of the DEM's accuracy in the study area is not yet available. See also Huber et al's (2017) more conservative estimates.

**We appreciate the reviewer's comment and added information on Huber et al's estimates in the manuscript. Our velocity measurements are all located close to the calving front where the slope of the glacier is typically quite low and the quality of the DEM high. Therefore, we assume the impact on the velocity data to be insignificant (see also Seehaus et al. 2015, supplemental material, and Scambos et al. 2014).**

*It is currently the best available digital elevation model of the Antarctic Peninsula. It has a mean elevation bias of -4 m (±25 m RMSE) from ICESat data and horizontal accuracy better than 2 pixels. However, Huber et al. 2017 estimated the uncertainty to be ±50 m, since it varies regionally. Velocity data is analyzed close to the calving front (see further down) where the slope of the glaciers at the AP is typically quite low. Thus, the impact of the DEM accuracy on the velocity fields is insignificant (see Seehaus et al., 2015 supplemental material).*

21) The text on page 6, line 15 needs clarification: "close to the terminus of each glacier basin, behind the maximum retreat state of ice front position in the observation period". It is pretty clear what is meant but this phrasing is awkward.

**We rephrased this sentence.**

*A profile is defined (red lines in Fig. 1) close to the terminus of each glacier basin, considering the maximum retreat state of ice front position in the observation period.*

22) It would be useful to quantify what is meant by 'very high' and 'significantly lower' on page 6, lines 6-8. Also, does the mass input depend at all on basin orientation or only on the hypsometry and elevation (lines 8-9).

**As requested, we added CMB values for the east and west coast.**
**The reviewer is right; the mass input also depends on the basin orientation (east coast vs. west coast, as stated in the same section of the manuscript). We changed the wording to be more precise.**

*The climatic mass balance at the northern AP shows a strong spatial variability, with very high accumulation rates along the west coast (3769 mm we a-1 in average in sector "West", 1992-2014,* *RACMO2.3), significantly lower values on the east coast (1119 mm we a-1 in average in sector "East", 1992-2014, RACMO2,3) and an increase towards higher altitudes along both coast lines (Turner, 2002; van Wessem et al. 2016). Consequently, the mass input depends on the basin orientation (east coast or west coast), elevation range and the hypsometry.*

23) The sentence at the end of page 7 and top of page 8 still needs some sort of analogy or further explanation to make it accessible to the average reader. Even the most dedicated readers will be unlikely to dive as deep as appears to be needed to see what is being done to the raw input numbers. In addition, it still seems relevant to point to any other study in glaciology that has derived useful results from a related 'sorting' technique.

**According to the reviewer's suggestion we rephrased this sentence and added literature reference of studies, which used the cluster analyses to group glaciers based on a set of variables.**

*This is a proven method to classify glaciers based on a set of variables (Lai and Huang, 1989; Sagredo and Lowell, 2012)*
*…..*
*At the start, the most similar glaciers (samples) are grouped. The resulting clusters are iteratively joined based on their similarities (distances) until only one cluster is left, resulting in a dendrogram (see Section 4.4).*

24) Area changes for the 'ice shelf loss glaciers' needs to be separately called out on page 8, line 5, given that are 'after 1995' not since '1985-1989'. Interestingly, this date range suggests the variability in temporal resolution of the area change values going into the cluster analysis, also an issue with the temporally variable velocity values as shown in S1-74.

**We appreciate this comment and revised the date specification in this section and also in Table S1 and Table 5. We are sorry, but we do not understand the second part of the comment.**

25) See previous comment on 'percentages' but the actual area change values should be given on page 8, lines 11-13.

**We added the actual area change values.**

*In total, 238.81 km² of glacier area was lost in the survey areas in the period 1985-2015, which corresponds to a relative loss of 2.2%. All sectors show glacier area loss (Table 5), of which the area loss by 5.7% (208.59 km²) at sector "East-Ice-Shelves" clearly dominates. The glaciers in sector "West" and "East" recessed by 0.2% (9.14 km²) and 1.4% (21.07 km²), respectively*

26) The use of the word 'trends' when referring to what are simply plots of the velocity data is problematic for a number of reasons. In some case, there simply isn't enough data to even estimate a trend (e.g. S4, S6, S8) and even when there is more data, it is often so unevenly temporally sampled (S27, S28, S56) as to be impossible to discern a trend (or as is discussed later, a pattern). Further, there is also a great deal of concern that signal vs noise (apparent pattern vs error bars) is not being taken into account in the results section of this paper.

**We appreciate this comment and revised the usage of the word "trends" and "pattern" throughout the manuscript.**
**We added some information regarding the signal to noise ratio in Section 4.2.**

*In order to analyze the quality of obtained velocity change signal, the ratio of the maximum measured velocity difference (maximum velocity minus minimum velocity) divided by the average error of the velocity measurements is calculated for each glacier. An average signal to noise ratio of 14.6 is found. At three glaciers (DGC14, DGC22 and Orel) a signal to noise ratio of less than 2 is observed. These glaciers are characterized as "stable", which justifies the low signal to noise* *ratio.*

27) Please clarify "On average the ice flow in the study region increased by 1.6%, but the glaciers in the individual sectors showed on average significant change." on page 9, lines 7-8. Please give velocity change values as well as % so as to save to save the reader from having to also read the supplement.

**We changed the wording to be clearer ad added the velocity change values.**

*On average the ice flow in the whole studied area increased by 1.6% (0.008 m/d), but the average changes of the individual sectors are more pronounced. Along the west coast an average acceleration by 41.5% (0.177 m/d) occurred and the former ice shelf tributaries on the east coast accelerated by 16.8% (0.081 m/d). In the sector "East" the glaciers decelerated resulting in a mean velocity change of -69% (-0.688 m/d).*

28) The sentence "The presented average flow speed change values are based on the observed changes of all glaciers in the respective sector (Table S1), ignoring the different size of the individual glaciers." leads to wondering if size classes in each sector might provide more insight?

**In our opinion an average value weighted by the flux-gate size rather the catchment size could be applied. However, the ice thickness data at the AP (e.g. from Huss and Farinotti 2014) also has got significant uncertainties, which might bias the calculation. Therefore, we decided to keep it simple and comprehensible.**

29) Please change the term 'shrinkage' throughout as it suggests a 3-dimensional change in volume rather than a change in area alone (page 10, line 3).

**We revised the usage of "shrinkage" throughout the manuscript. Thank you for this advice.**

30) The term 'theory' should be replaced with 'hypothesis' and given how speculative this is, given the large distances to the nearest met stations, I think the editor should consider excising this speculative section. Note, unpublished (as of yet) studies are suggesting that the 'cooling' was a problematic sampling of the longer-term record now that 2016 and 2017 data is becoming available.

**We replaced "theory" with "hypothesis". Well, in this section we are not talking about the cooling trend in the 21$^{st}$ century. We talk about a warming between 1986 and 2005. However, if the editor wants to excise this section, we can remove it.**

31) The 'clear positive velocity trend' (page 10, lines 16-17) does not appear to be supported by the figures in S57-74 in my opinion. See the previous comments on 'trend' and signal vs noise'.

**We rephrased this sentence, in order to not over-interpret the results and observed trends. Regarding signal vs noise; see answer to comment 26.**

*This spatial trend corresponds to our observations, since most of the glaciers which accelerated are located at the southern end of sector "West".*

32) Please explain how Skvarca et al. (1998) saw a cooling trend in the 21st century (page 11, line 6).

**Sorry, this reference was displaced.**

33) The 'peaked' trend for TPE10 Glacier (page 11, line 15, is a very clear example of over-interpreting insufficient data as is Aitkenhead Glacier (S3).

**The reviewer is right TPE10 Glacier has got only a few velocity measurements. However, we**

**added the graphs obtained from the 2nd velocity measuring approach (measured at maximum ice thickness at the terminus profiles) in the revised version of the supplement. These results also support the velocity change classification of TPE10 Glacier as "peaked". As well for Aitkenhead Glacier, the same classification is obtained by both measuring approaches.**
**We added a reference to the respective figures in the manuscript.**

34) Perhaps I don't understand what 'frontal advance' means (page 11, line 22) given 5-year averaging but the glaciers mentioned both show continued area losses in the referenced plots.

**Both glaciers accelerated and gained area (frontal advance) in the period 2010-2015. We added data specification to be clearer.**

*Diplock and Victory glaciers (Fig. S5 and S13) show a decrease of flow speed during retreat (1995-2010) followed by an acceleration combined with frontal advance (2010-2015).*

35) Please give the 'comparable values' for the two analyses on page 12, line 11.

**We added the observed values of both analyses exemplarily for two dates.**

36) A 'potential peak in flow speed' (page 12, line 25) appears to be unnecessary speculation as it 'cannot be detected'.

**According to the reviewer's suggestion we removed this sentence**

37) Pyke Glacier is within the APPE group so a reference to Table 1 seems useful (page 12, line 28).

**We appreciate this advice and added a reference to Table 1.**

*Rott et al., (2014) also found nearly constant flow velocities at Pyke Glacier (part of the APPE basin, Table 1).*

38) The opening paragraph on page 13 seems muddled. Also, the term 'jagged' for the western coastline seems inadequate given the point is to give context for the 'heterogeneous' changes observed in sector 'West'. See the previous review for a concern about the potential orographic impact of large islands on the west side as well as an earlier comment here on slope aspect vs solely elevation/hypsometry.

**We rephrased and condensed this paragraph to be clearer. Moreover, we added a statement on the potential impact of the islands on the climate on AP's mainland.**
**We are sorry, but we do not exactly understand the part regarding "slope aspect vs. solely elevation/hypsometry". The general aspect of the glaciers (east coast vs. west coast) is taken into account by dividing the study site in sectors. In our opinion, to use the average slope of the glaciers at the AP as a geometry variable is less reasonable, since the glacier tongues are usually dynamically separated by steep cliffs from the plateau section. Therefore, we decided to use maximum elevation and Hypsometric Index since the accumulation (which influences the ice dynamics) shows a significant elevation gradient (especially along the west coast).**

*The glacier geometries differ strongly along the west coast. In the southern part of sector "West" the shoreline is more ragged and islands are near the coast. An impact of the islands on the climatic conditions at the AP mainland's coastline (e.g. orographic barrier) is not obvious (visual inspection of RACMO2.3 5.5 km grid cell model results (Van Wessem et al., 2016)). However, the climatic conditions on the AP show strong spatial and temporal variability (see Section 1.2 and 3.3). These factors cause the heterogeneous spatial pattern of area and flow speed changes in sector "West" as compared to the eastern sectors.*

39) Group1 ‘needs some space’ (page 13, line 21).

**Corrected**

40) There is something missing around ‘dissimilarities’ on page 13, line 18, perhaps ‘matrix analysis’ would be appropriate to add here.

**We changed the wording to be clearer.**

*The large number of glaciers in this sector is analyzed by means of a hierarchical cluster analysis (Section 3.4) and assorted into four groups based on the resulting dendrogram (Fig. 6).*

41) It seems odd not to reference the previous study by the lead author at the end of the first sentence of the Conclusions.

**With previous work (along the west coast) we mean the work by Pritchard and Vaughan (2007). We added the lit. reference to be clearer.**

42) It would appear to be more accurate to say higher ‘overall’ glacier flow given the heterogeneous response (page 15, line 7) and there is also a problematic use of ‘trends’ here as well.

**We changed the wording according to the reviewer's suggestion. The use of “trends” was also revised.**

*The results are in general in line with findings of the previous studies, however along the west coast higher overall glacier flow was determined and on the eastern side temporal evolution of ice dynamics of 21 glaciers were observed for the first time.*

43) It was my understanding from the paper that ‘Larsen Inlet, Larsen A’ glaciers had area changes assessed since ~1995 (not relative to 1985), page 15, lines 10-11.

**The Larsen A and Prince Gustav Ice Shelf tributaries had area changes assessed since 1995. We added this information to be clearer.**

*On the east side all glacier fronts retreated in the study period (relative to 1985, relative to 1995 for former Larsen-A and Prince Gustav Ice Shelf tributaries, see also Section 5.2), with highest retreat rates observed at former tributaries of the Prince Gustav, Larsen Inlet and Larsen A ice shelves.*

44) The phrase ‘cooling since the mid-2000s’ (page 15, line 16) is inconsistent with what Turner and Oliva et al. published. Also, ‘1960s’ seems incorrect. Please check.

**In the previous review, the reviewer suggested to use the term “mid-2000s”, considering Turner and Oliva et al.**
**1960s refer to Skvarca et al. (1998) (see also Section 1). The authors analyzed temperature measurements at the norther-eastern AP between 1961 and 1996.**

45) There would usefully be some discussion of what is and is not possible with the data sets available to date in the last paragraph. It is clear to this reader that even with a very serious effort to understand the variability of this region, there are pretty significant deficiencies in our data sets.

**We appreciate the reviewer's comment. In our opinion, most significant is the lack of recent high quality region wide surface elevation change data at the AP, since measurements obtained by Cryosat are strongly limited due to the complex topography and measurements using TanDEM-X data is only available for some sections. We added a statement on this issue.**

*Upcoming sensor probably facilitate the region wide measurement of recent surface elevation, since current estimates have got only partial coverage or have got some serious issues due to the complex topography of the AP.*

Figures showing LIMA need not have a copyright symbol, just a credit to the agencies involved.

**We removed the copyright symbol, according to the reviewer's advice.**

Figure 2 has an order of magnitude of velocity difference between panels C and E and I remain concerned that this makes it very difficult to interpret these plots.

**We understand the concerns of the reviewer, but we analyzed a large variety of glaciers of different sizes and geometries, therefore the variability of the velocity magnitudes is large. In our opinion it is more useful to adjust the y-axis scale to the individual magnitude in order to better interpret the temporal evolution.**

Figure 3 is improved but is still very difficult to read even with much magnification of the pdf files.

**If the editor agrees, we could also upload a high resolution version of the image as a supplement.**

Figure 4, check the caption for a typo 'lest'? Also, please darken the area labels on the Y1 axis to emphasize how much area remains in each sector.

**We appreciate the reviewer's advice and changed the left y-axis (and labels) color to black. We replaced "lest" by "left".**

Figure 5's key should not have dashes and minus signs, please find some other way to show the ranges and consider adding a '+' for the one positive color. Also remove 'regional' before 'sector' in the caption.

**According to the reviewer's advice we revised the keys and caption**

Figure 7, one presumes 'Group N' is 'Group Number' or simpler 'Group'.

**To add "N" to Group was requested by the reviewer in the first review. Well, we removed it from the graph.**

Table 3 shows two categories 'stable' and 'fluctuating' as having the same numeric rating which makes one wonder even further about the cluster analysis. Did I miss discussion of 'fluctuating' in the text? Are these distinctions meaningful given the temporal resolution of the velocity data for many glaciers? Please clarify.

**We decided to use the same numeric rating for "stable" and "fluctuating" glaciers, since the difference is that the variability of "stable" glaciers is less than 0.25 m/d. For both types no clear temporal evolution of the flow speed is obvious. We added a statement in the manuscript to be clearer.**
*Glaciers categorized as "stable" showed a temporal variability in flow speeds of less than 0.25 m $d^{-1}$. Therefore, we used the same rating for the velocity change categories "stable" and "fluctuating" to perform the cluster analysis.*

Supplement, page 1, Figure S74 should be S75 for the Drygalski

**Thank you, we corrected it.**

S17, add a space in Arron Icefall's label, consider increasing font sizes for axis labels

**According to the reviewer's suggestion we add a space in “Arron Icefall” and increased the font size of the axis labels.**

**Referee #2: Jan Wuite**
**Received: 08 August 2017**

General Comments
The comments here concern the revised version of the manuscript by Seehaus et al. on changes in glacier dynamics in the northern Antarctic Peninsula since 1985. While I am glad to see that some of the issues seem adequately addressed, some important issues still stand that need to be addressed and clarified. Specifically, those related to methods & interpretation of results.

To illustrate my concerns, I focus here on Drygalski Glacier, because it is the largest glacier in the study region and with a significant reported mass loss, and one with ample velocity data providing a means of comparison. Across-flow velocity profiles of the terminus region are added in the authors' reply and updated manuscript (Fig. S75). While the quality of some of the profiles are up for debate, it shows very clearly that the later velocities (those from 2009/2010 in the plot) are well above pre-collapse values by orders of magnitude. Nevertheless, the authors write (Pg. 12 Ln. 13-15): "Most glaciers (Arron Icefall, Drygalski, LAB2, TPE61, TPE62) decelerated towards pre-collapse values and show almost constant flow speeds in recent years, indicating that the glaciers adjusted to the new boundary conditions." This is, in this example, clearly not the case.

**Regarding the quality of some profiles: We did not apply any smoothing or interpolation on our obtained velocity fields. Therefore, some data gaps are present in our profiles. However, profiles with erroneous measurements (noise), large data gaps and partial coverage were sorted out and not used for further analysis (see Section 3.2)**
**Regarding the flow speed and slow down: We understand the reviewer's concerns. In the respective section we are talking about the median values of flow speed along the profiles, and we are aware that the flow speed at a large section of Drygalski's terminus is still significantly higher than before the disintegration of the Larsen A Ice Shelf, however we decided to use the median values for our analysis and discussion (see also the discussion of the velocity measuring approaches which is now in the supplement). With "decelerated toward pre-collapse values" we meant that the glaciers now slowed down but not necessarily reached pre-collapse values.**
**We changed the wording of this section to be clearer**

*Most glaciers (Arron Icefall, Drygalski, LAB2, TPE61, TPE62) strongly decelerated after the initial acceleration and show almost constant flow speeds in recent years, indicating that the glaciers adjusted to the new boundary conditions, albeit significant higher flow speeds can be observe at the central sections of the terminus (see Section S1 and Fig. S149 and S150 in the supplement).*

It is, to me, unclear how the velocity profiles of this transect (Fig. S75) translate into the velocities depicted in Fig. 2C and values of Table S1. So, while the cross profiles of 2010 show a significant higher velocity than 1993 and 1995, Fig. 2C shows the median velocity of 1993 to be in the same order of magnitude and for 1995 even higher than those from 2010 and in Table S1 we find for Drygalski Glacier a reported increase in velocity of only ~15% between 1993 and 2010. It seems something is not right. Therefore, to restate my earlier comment, it is certainly not a 'comparable temporal trend' to that from Rott et al. 2014 who report a 280% higher velocity in 2013 compared to 1995, although this statement is still present in the revised version (Pg. 12 Ln 8-10).

**We appreciate the reviewer's comment and added a detailed discussion in the supplement on measuring velocities (median along profile vs. point measurement). We concluded to apply the median values in our study. Moreover we carefully revised all data sets which were selected in order to improve the quality. This led to some changes in the obtained results. Now we observe an increase in flow speed between 1993 and 2010 by ~73% at Drygalski Glacier. Considering the different measuring approaches, the results of both studies show comparable temporal trends (acceleration followed by deceleration), but different absolute values as stated in the preceding sentence and also the added discussion in Section S1 (supplement)**

**Regarding Fig. S75 (now Fig. S149).**
**We are sorry, but somehow not the whole profile was plotted in the previous version of the manuscript. We also added the median values to the graph (right side) in order to better compare the values.**
**We hope these additions (see also answer to next comment) will help to better interpret the results and explain the differences between point measurements and median values along a profile.**

Perhaps there is an issue in the calculation of the median values but it could also be the quality of the velocity data. However, as Drygalski Glacier is a rather wide/large and relatively fast glacier, the quality of velocity data for the many smaller & much slower glaciers is likely worse and in particular for the early period using ERS-1/2 feature tracking (although InSAR should provide better results, was this tested?). How do other cross profiles look like, for instance for the more extreme acceleration and deceleration cases in sector West and East? Do they have the same issue?
I stress this point, as I believe the figures (Fig. 2 & Fig. S1-S74 and the Table) form the core of the manuscript and the basis for subsequent discussions and conclusions. However, since the Drygalski example is the only velocity profile time series given in the manuscript, I think it makes it difficult to convince the reader about the validity of at least some of these plots/numbers. For a paper dealing primarily with glacier velocity we get to see very few velocity maps and/or profiles to get any real confidence in the data.

**Following the reviewer's comment and advises and to show the quality of the obtained velocity data, we added velocity maps (for different sensor) of our study site in the supplement. Some more velocity profile time series were also added to the manuscript (for all different velocity categories and for the largest (Drygalski) and smallest (DGC14) catchments as well).**
**The reviewer is right, regarding ERS-1/2 data. These data sets have got the highest uncertainties (see also last rows of Table S3) as well as the most tracking errors and data gaps (about 50% of the generated results were discharged during the quality checks, as mentioned above we carefully revised the data sets in order to improve the quality of the results). However, we did not apply InSAR to measure surface displacement. Only during ERS mission phases with 1 d and 3 d repetition cycles sufficient coherence can be retained (due to the glacier flow and changes of surface conditions). Just a small amount of the available ERS-data is suitable for this technique, which partially covers the study site. Moreover, the surface displacement can only be measured in range direction using InSAR (except at areas where ascending and descending orbits cross, which further limits the spatial coverage). By using a DEM to project the range displacement in the direction of glacier flow, certain errors can be introduced (e.g. various studies report significant surface elevation changes at the AP. Changes in the surface slopes between the date of the DEM and ERS data impact the projection of the range displacements). Thus, we decided not to use InSAR methods, in order to consistently (temporal and spatially) apply only one technique to calculate surface velocity fields.**

# Changes in glacier dynamics in the northern Antarctic Peninsula since 1985

Thorsten Seehaus[1], Alison J. Cook[2], Aline B. Silva[3], Matthias Braun[1]

[1] Institute of Geography, Friedrich-Alexander-University Erlangen-Nuremberg, Wetterkreuz 15, 91058 Erlangen, Germany

[2] Department of Geography, Durham University, South Road, Durham DH1 3LE, United Kingdom

[3] Laboratório de Monitoramento da Criosfera, Universidade Federal do Rio Grande, Av. Itália, km 8, 96203-900, Rio Grande - RS Brazil

Correspondence to: Thorsten Seehaus (*thorsten.seehaus@fau.de*)

**Abstract.** The climatic conditions along the northern Antarctic Peninsula have shown significant changes within the last 50 years. Here we present a comprehensive analysis of temporally and spatially detailed observations of the changes in ice dynamics along both the east and west coastlines of ~~this region~~the northern Antarctic Peninsula. Temporal evolutions ~~trends~~ of glacier area (1985-2015) and ice surface velocity (1992-2014) are derived from a broad multi-mission remote sensing database for 74 glacier basins on the northern Antarctic Peninsula (<65° S along the west coast and north of the Seal Nunataks on the east coast). A recession of the glaciers by 238.81 km² is found for the period 1985-2015, of which the glaciers affected by ice shelf disintegration showed the largest retreat by 208.59 km². Glaciers on the east coast north of the former Prince Gustav Ice Shelf extent in 1986 receded by only 21.07 km² (1985-2015) and decelerated by about 58~~69~~ % on average (1992~~85~~-2015~~4~~). A dramatic acceleration after ice shelf disintegration with a subsequent deceleration is observed at most former ice shelf tributaries on the east coast, combined with a significant frontal retreat. In 2014, the flow speed of the former ice shelf tributaries was ~~16.8~~26 % higher than before 1996~~at the beginning of the study period~~. Along the west coast the average flow speeds of the glaciers increased by 41~~.5~~ %. However, the glaciers on the western Antarctic Peninsula revealed a strong spatial variability of the changes in ice dynamics. By applying a hierarchical cluster analysis we show that this is associated with the geometric parameters of the individual glacier basins. The heterogeneous spatial pattern of ice dynamic evolutions~~trends~~ at the northern Antarctic Peninsula shows that temporally and spatially detailed observations as well as further monitoring are necessary to fully understand glacier change in regions with such strong topographic and climatic variances.

## 1 Introduction

During the last century, the northern Antarctic Peninsula (AP) and its outlying islands have~~s~~ undergone significant warming (~~Carcass et al., 1998;~~ Turner et al., 2005), leading to substantial glaciological changes. Skvarca et al. (1998) reported a significant increase in surface air temperatures at the north-eastern AP in the period 1960-1997 and correlated it with the recession of the Larsen and Prince~~-~~ Gustav Ice shelves (Fig. 1) and the observed retreat of tidewater glaciers on James Ross

Island in the period 1975-1995 (Skvarca et al., 1995). However, a recent cooling trend on the AP was revealed by Oliva et al. (2017) and Turner et al. (2016) since the late 1990s. Shepherd et al. (2012) compiled a comprehensive glacier mass balance database of the polar ice sheets. The authors estimated a mass loss on the whole AP (<73° S) of -36±10 Gt a$^{-1}$ for the period 2005-2010, which corresponds to 35% of the total mass loss of Antarctica. A projection of sea level rise contribution by the AP ice sheet amounts to 7-16 mm sea-level equivalent by 2100 and 10-25 mm by 2200 (Barrand et al., 2013a). However, along the western AP and on the higher elevation ~~regions~~ areas an increase in snow accumulation in the late 20th century was derived from ice cores (e.g. at Palmer Land, 73.59° S, 70.36° W, Thomas et al., 2008; Detroit Plateau, 64.08°S, 59.68° W, Potocki et al., 2011; at Bruce Plateau, 66.03°S, 64.07°W, Goodwind, 2013) and climate models (e.g. Dee et al., 2011), whereas van Wessem et al. (2016) obtained insignificant trends in precipitation.

Numerous ice shelves along the AP ~~(e.g. Larsen A/B, Prince Gustav and Wordie)~~ have retreated widely (e.g. Müller, Wilkins, Wordie) or disintegrated in recent decades (e.g. Larsen A in 1995, Larsen B in 2002) (Braun and Humbert, 2009; Cook and Vaughan, 2010; Doake and Vaughan, 1991; Rack et al., 1998; Rack and Rott, 2003; Wendt et al., 2010)~~Cook and Vaughan, 2010)~~. As a consequence to the reduced buttressing, former tributary glaciers showed increased ice discharge and frontal retreat (e.g. De Angelis and Skvarca, 2003; Rack and Rott, 2004; Rignot et al., 2004; Seehaus et al., 2015; Wendt et al., 2010). For the northern AP (<66° S), a mass loss rate of -24.9±7.8 Gt a$^{-1}$ was reported by Scambos et al. (2014) for the period 2003-2008, indicating that major ice mass depletion happened at the northern part of the peninsula, especially along the eastern side where numerous glaciers have been affected by ice shelf collapses. Seehaus et al. (2015, 2016) quantified the ice loss of former ice shelf tributaries. Mass loss rates of -2.14±0.21 Gt a$^{-1}$ (1995-2014) and -1.16±0.16 Gt a$^{-1}$ (1993-2014) were found at Dinsmoor-Bombardier-Edgeworth Glacier System and Sjögren-Inlet glaciers, respectively. Glaciers that were not terminating in an ice shelf also showed considerable changes. Cook et al. (2005, 2014) have analyzed the variations of tidewater glacier fronts since the 1940s. The authors reported that 90% of the observed glaciers retreated, which they partly attributed to atmospheric warming. A more recent study revealed a mid-ocean warming along the southwestern coast of the AP, forcing the glacier retreat in this region (Cook et al., 2016). Pritchard and Vaughan (2007) observed an acceleration of ice flow by ~12% along the west coast of the AP (1995-2005) and linked it to frontal retreat and dynamic thinning of the tidewater glaciers. Observations by Kunz et al. (2012) support this supposition. They ~~authors~~ analyzed surface elevation changes of 12 glaciers on the western AP based on stereoscopic digital elevation models (DEM) over the period 1947-2010. Frontal surface lowering was found at all glaciers~~,~~. Whereas,~~whereas~~ glacier~~ area~~-wide surface lowering of former ice shelf tributaries was observed ~~on~~along the north-eastern AP by various author groups (e.g. Berthier et al., 2012; Rott et al., 2014; Scambos et al., 201~~0~~4~~; Wuite et al., 2015~~) ~~as a consequence to ice shelf disintegration.~~

The collected observations suggest that the ice masses on the AP are contributing to sea level rise and show that glaciers' response to climate change on the AP is not homogeneous and that more detailed knowledge of various aspects on the glacier changes are required. Previous studies often~~often only~~ cover a specific period or ~~region~~area, or focus on one

**Formatiert:** Hochgestellt

**Formatiert:** Hochgestellt

particular aspect of glacier change. By now, the availability of remote sensing data time series data and other datasets in this region facilitates the comprehensive analysis of glacier change. Therefore, we study the changes in glacier extent in combination with detailed investigations on ice dynamics as well as other derived geometrical attributes of glaciers on the northern AP (<65° S along the west coast and north of the Seal Nunataks on the east coast, Fig. 1b colored polygons) between 1985 and 2015. We analyze various multi-mission remote sensing datasets in order to obtain methodologically consistent and temporally detailed time series of ice dynamic ~~trends~~changes of 74 glacier basins. The observations are individually discussed for the sub regions, considering the different atmospheric, glaciological and oceanic conditions and changes.

## 2 Study site

The AP is the northern-most region of Antarctica and stretches from 63-75°S (Huber et al., 2017). It covers only 3% of the entire continent in area, but receives 13% of the total mass input (van Lipzig et al., 2002, 2004). The AP's mountain chain (typically 1500-2000 m high) acts as an orographic barrier for the circumpolar westerly air streams leading to very high precipitation values on the west coast and on the plateau region of up to 5000 mm we a~~yr~~$^{-1}$, as well as frequent foehn type wind occurrences on the east coast (Cape et al., 2015, Marshall et al., 2006, van Wessem et al. 2016). The foehn events are characterized by strong winds and high air temperatures. Consequently, the climatic mass balance ($b_{clim}$) shows a strong gradient across the mountain chain (Turner, 2002; van Wessem et al., 2016). Aside from those that are ice shelf tributaries, almost all glaciers on the AP are marine terminating, and the majority of the glacier catchments extend up to the high elevation plateau regions (north to south: Laclavère, Louis Philippe, Detroit, Herbert, Foster, Forbidden, Bruce, Avery, Hemimont, Dyer). Typically the AP plateau is separated from the outlet glaciers by escarpments and ice-falls. Glaciers on the west coast drain into the Bellingshausen Sea and on the east coast into the Weddell Sea. Since the 1980s, the ice shelves along the east coast have substantially recessed and disintegrated (Larsen Inlet in 1987-89, Prince Gustav and Larsen A in 1995 and Larsen B in 2002) (Cook and Vaughan, 2010; Rott et al., 1996; Skvarca et al., 1999), which Scambos et al. (2003) attributed to higher summer air temperatures and surface melt. A more recent study by Holland et al. (2015) discovered that significant thinning of the Larsen C Ice Shelf is caused by basal melting and that ungrounding from an ice rise and frontal recession could trigger its collapse. The northern AP has a maritime climate and is the only region of Antarctica that frequently experiences widespread surface melt (Barrand et al., 2013b; Rau and Braun, 2002).

Our study site stretches approximately 330 km from the northern tip of the AP mainland southwards to Drygalski Glacier on the east coast and Grubb Glacier on the west coast (Fig. 1). This facilitates the analyses of the ~~long-term~~ temporal evolution (~20 years) of the response ~~(~20 years)~~ of tributary glaciers to ice shelf disintegration at the former Larsen A and Prince~~-~~ Gustav ice shelves on the east coast, the investigation of glaciers north of the former Prince~~-~~ Gustav Ice Shelf, where no information on change in ice flow is currently available, and the comparison with temporal variations ~~trends~~ in ice dynamics

**Formatiert:** Hochgestellt

along the west coast at the same latitude. The study area~~region~~ covers an area of ~11,000 km² (~11% of the whole AP including islands, Cook et al., 2014; Huber et al., 2017) with ~~altitudes~~ elevations stretching from sea level up to 2220 m. The glacier basin delineations are based on the Antarctic Digital Database ADD 6.0 (Cook et al., 2014). Glacier names are taken from the Global Land Ice Measurements from Space (GLIMS) project database. The local GLIMS glacier IDs (e.g. TPE62, LAB2) are used for unnamed glaciers and further missing glacier basin names are ~~substituted~~ replaced with the ADD 6.0 glacier IDs. Neighboring basins with coalescing ice flow at the termini are merged (many are already merged in the ADD 6.0), as the delineation of the individual glacier sections is not always possible and the width can vary temporally (due to changes in mass flux of the individual glaciers). In these cases, the names of the glaciers are also merged (e.g. Sikorsky-Breguet-Gregory – SBG, see Table 1 for abbreviations of glacier names). Due to the sparse data coverage (fewer than three good quality velocity measurements), no time series analysis of the glaciers at the northern tip of the AP or at some capes and peninsulas (e.g. Sobral Peninsula, Cape Longing) is possible. Therefore, the northern-most analyzed catchments are Broad-Valley Glacier on the east coast and TPE8 Glacier on the west coast, resulting in 74 studied glacier basins. Furthermore, the study site~~region~~ is divided into three sectors, taking into account the different climatic settings and drainage orientation as well as former ice shelf extent: sector "West" - ~~G~~glaciers on the west coast, draining into the Bransfield and Gerlache Strait; sector "East" – ~~G~~glaciers on the east coast, draining into the Prince Gustav Channel; and sector "East-Ice-Shelf" – ~~G~~glaciers on the east coast, that were former tributaries to the Larsen A, Larsen Inlet and Prince Gustav Ice Shelf.

## 3 Data & Methods

A large number of various remote sensing datasets are ~~analyzed~~analyzed in order to obtain temporally and spatially detailed information on changes in ice dynamics in the study area. Glacier area changes are derived from satellite and aerial imagery. Repeat-pass Synthetic Aperture Radar (SAR) satellite acquisitions are used to compute surface velocity fields in order to obtain information on changes in glacier flow speed. Auxiliary data from sources such as a digital elevation model and glacier inventory are included in the further analyses and discussion of the results.

**Formatiert:** Englisch (USA)

### 3.1 Area changes

Changes in glacier area are derived by differencing glacier outlines from various epochs. All observed glaciers are tidewater glaciers and only area changes along the calving front were considered. Information on the positions of the glacier fronts in the area studi~~y~~ed region are taken from Cook et al. (2014), and are available for the whole AP in the ADD 6.0 (1945-2010). This coastal-change inventory is based on manually digitized ice front positions using imagery from various satellites (e.g. Landsat, ERS) and aerial photo campaigns. This dataset is updated (up to 2015) and gaps are filled by manual mapping of the ice front positions based on SAR and optical satellite images. Consistent with Cook et al. (2014), the ice-front positions are assigned to 5-year intervals in order to analyze temporal trends in glacier area changes in the period 1985-2015. Before

1985, only sparse information on ice front positions for the whole study site ~~region~~ is available, and the coverage by SAR data for analyzing glacier flow starts in 1992. Additionally, the analysis of the area changes for the Larsen A and Prince Gustav Ice Shelf tributaries is limited to the period 1995-2015, as the ice shelves disintegrated in 1995.

The uncertainties of the glacier change measurements strongly depend on the specifications of the imagery used (e.g. spatial resolution, geodetic accuracies) as well as the methods used. To each record in the coastal-change inventory from the ADD 6.0, a reliability rating is assigned according to Ferrigno et al. (2006). The rating ranges from 1 to 5 (reliability within 60 m to 1 km) and takes into account errors due to manual digitization and interpretation (see Ferrigno et al., 2006 for a detailed description). This approach is also applied on the updated ice-front positions. Nearly all mapped ice fronts in the area studied~~y region~~ have a good reliability rating of 1 (76%) and 2 (21%). Only a few glacier fronts (3%) have a rating of 3. No ice fronts with reliability ratings of 4 and 5 are mapped in the study area.

### 3.2 Surface velocities

Surface velocity maps are derived from repeat-pass Synthetic Aperture Radar (SAR) acquisitions. SAR image time series of the satellite missions ERS-1/2, Envisat, RadarSAT-1, ALOS, TerraSAR-X (TSX) and TanDEM-X (TDX) are analyzed, covering the period 1992-2014. Specifications of the SAR sensors are listed in Table 2. The large number of SAR images was provided by the German Aerospace Center (DLR), the European Space Agency (ESA) and the Alaska Satellite Facility (ASF). To obtain displacement fields for the glaciers, the widely used and well approved intensity offset tracking method is applied on co-registered single look complex SAR image pairs (Strozzi et al., 2002). In order to improve the co-registration of the image pairs, we mask out fast moving and unstable regions such as outlet glaciers and the sea during the co-registration processes. Furthermore, single SAR image tiles acquired during the same satellite flyover are concatenated in the along-track direction. This helps to further improve the co-registration in coastal regions (by including more stable areas in the co-registration process) but also simplifies the analysis of the final results as no mosaicking of the results is needed. Image pairs with low quality co-registration are filtered out. A moving window technique (step-size see Table 2) is used by the intensity offset tracking method to compute the cross-correlation function of each image patch and to derive its azimuth and slant range displacement. The resolution of the obtained displacement fields depends on the combination of the step-size and the resolution of the images in slant-range geometry. A resolution of the velocity fields of ~50 m for the high resolution sensors TSX, TDX and ~100 m for all other sensors was targeted. Less reliable offset measurements are filtered out by means of the signal-to-noise ratio of the normalized cross-correlation function. Moreover, we apply an additional filter algorithm based on a comparison of the magnitude and alignment of the displacement vector relative to its surrounding offset measurements. This technique removes more than 90% of incorrect measurements (Burgess et al., 2012). Finally, the displacement fields are transferred from slant range into ground range geometry, taking into account the effects on the local incidence angle by the topography. The results are then geocoded, orthorectified, resampled and converted into velocity fields (with 100 m pixel spacing for all sensors) by means of the time span between the SAR acquisitions. The mean date of the consecutive SAR acquisitions is assigned to each velocity field. The ASTER Global Digital Elevation Model of the Antarctic Peninsula (AP-DEM, Cook et al., 2012) is used as elevation reference. It is currently the best available digital elevation model of the Antarctic Peninsula. It has a mean elevation bias of -4 m (±25 m RMSE) from ICESat data and horizontal accuracy better than 2 pixels. However, Huber et al. 2017 estimated the uncertainty to be ±50 m, since it varies regionally. ~~It is currently the best available digital elevation model of the Antarctic Peninsula.~~ Velocity data is analyzed close to the calving front (see further down) where the slope of the glaciers at the AP is typically quite low. Thus, the impact of the DEM accuracy on the velocity fields is insignificant (see Seehaus et al., 2015 supplemental material).

Depending on the displacement rate and resolution of the SAR sensor, the tracking window size needs to be adapted (de Lange et al. 2007). For the fast flowing central glacier sections, larger window sizes are needed since large displacements cannot be tracked by using small correlation patches. Small tracking window sizes are suitable for the slow moving lateral sections of the outlet glaciers. Wide parts of large tracking patches cover the stable area next to the glacier, which biases the tracking results towards lower velocities. Consequently, we compute surface velocity fields of the same image pairs for different correlation patch sizes in order to get the best spatial coverage. Table 2 shows the different tracking window sizes for each sensor. The results of each image pair are stacked by starting with the results of smallest tracking window size and filling the gaps with the results of the next biggest tracking window size.

The accuracy of the velocity measurements strongly depends on the coregistration quality and the intensity offset tracking algorithm settings. The mismatch of the coregistration ${\sigma_v}^C$ is quantified by measuring the displacement on stable reference areas close to the coast line, such as rock outcrops and nunataks. Based on the Bedmap2 (Fretwell et al., 2013) and ADD 6.0 rock outcrop masks, reference areas are defined and the median displacements magnitude of each velocity field is measured at these areas. The uncertainty of the tracking process ${\sigma_v}^T$ is estimated according to McNabb et al. (2012) and Seehaus et al. (2015) depending on accuracy of the tracking algorithm *C*, image resolution *dx*, oversampling factor *z*, time interval *dt*.

$$\sigma_v^T = \frac{Cdx}{zdt} \qquad (1)$$

The accuracy of the tracking algorithm is estimated to be 0.2 pixels and an oversampling factor z=2 is applied to tracking patches in order to improve the accuracy of the tracking process. Both independent error estimates are quadratically summed to compute the uncertainties of the individual velocity fields $\sigma_v$.

$$\sigma_v = \sqrt{(\sigma_v^T)^2 + (\sigma_v^C)^2} \qquad (2)$$

Two approaches to measure and analyze the temporal changes in ice flow of the studied glacier are evaluated and the differences are discussed in the supplement Section S1. The favored measuring approach is explained in the following and its results are used for the subsequent analysis.

A profile is defined (red lines in Fig. 1) close to the terminus of each glacier basin, ~~,~~considering ~~behind~~ the maximum retreat state of ice front position in the observation period. The results are visually inspected in order to remove unreliable measurements, based on the magnitude and direction of ice flow along the profiles. Datasets with partial profile coverage or large data gaps, as well as those with still remaining tracking errors, are rejected. The changes in the ice flow of each glacier are analyzed by measuring the surface velocities along the profiles. In order to reduce the number of data gaps along the profile due to pixel size data voids in the velocity fields, the velocity data is extracted within a buffer zone of 200 m around the profiles. To minimize the impact of potential outliers, median velocities along the profiles are calculated and the temporal developments~~trends~~ are plotted. The glaciers are manually classified in six categories according to the temporal evolution of the ice flow speeds (see Table 3), since automatic classification attempts did not succeed. Only glaciers with three or more observations and an observation period of more than 10 years are considered in the categorization, resulting in 74 categorized glacier basins (colored polygons in Fig. 1b. There is a minimum of seven velocity measurements per categorized basin and the shortest observation period is 14.83 years (see Table S1; average number of velocity measurements per glacier is 33.8 and average observation period is 19.40 years). The GAMMA Remote Sensing software is used for processing of the SAR data.

### 3.3 Catchment geometries and settings

Glacier velocities and area change measurements provide information on the ice dynamics of the individual glaciers. To facilitate a better and comprehensive interpretation of these observations, additional attributes regarding the different geometries and settings of the glaciers are derived. In addition to glacier attributes derived by Huber et al. (2017), we calculated the Hypsometric Index and the ratio of the flux gate cross section divided by the glacier catchment area.

Mass input strongly affects the dynamics of a glacier. The climatic mass balance at the northern AP shows a strong spatial variability, with very high accumulation rates along the west coast (3769 mm we $a^{-1}$ in average in sector “West”, 1992-2014, RACMO2.3)~~,~~ significantly lower values on the east coast (1119 mm we $a^{-1}$ in average in sector “East”, 1992-2014, RACMO2.3) ~~–~~and an increase towards higher altitudes along both coast lines (Turner, 2002; van Wessem et al. 2016). Consequently, the mass input depends on the basin orientation (east coast or west coast), elevation range and the hypsometry. For each glacier basin a Hypsometric Index (*HI*), defined by Jiskoot et al. (2009), is calculated by means of surface elevations from the AP-DEM. Based on this index the glaciers are grouped into the five categories according to Jiskoot et al. (2009), ranging from very top-heavy to very bottom heavy (Table 4). Moreover, the maximum elevations of the

**Formatiert:** Hochgestellt

**Formatiert:** Hochgestellt

individual glacier catchments are derived from the AP-DEM, which represents the altitude range of the catchment, since all observed glaciers are marine terminating.

In order to characterize the catchment shape, the ratios (*FA)* of the flux gate cross sections divided by the glacier catchment areas are calculated. The flux gates are defined along the profiles used for the glacier flow analysis (Section 3.2). Lower values of *FA* indicate a channelized outflow (narrowing towards the glacier front), whereas higher *FA* ratios imply a broadening of the glacier towards the calving front. Ice thickness at the flux gates is taken from the AP Bedmap dataset from Huss and Farinotti (2014).

### 3.4 Cluster analysis

The glaciers in the sector "West" (Fig. 1, red shaded area) show a heterogeneous spatial pattern of ice dynamics as compared to the other sectors changes (Section 4.1, 4.2). In order to analyze the influence of the glacier geometries on the glaciological changes and to find similarities, a cluster analysis is carried out in sector "West". This is a proven method to classify glaciers based on a set of variables (Lai and Huang, 1989; Sagredo and Lowell, 2012). Variables of the glacier dynamics used are the derived area changes (in percent) and velocity changes (ratings of the categories, Table 3). Glaciers categorized as "stable" showed a temporal variability in flow speeds of less than 0.25 m d$^{-1}$. Therefore, we used the same rating for the velocity change categories "stable" and "fluctuating" to perform the cluster analysis. The glacier geometry parameters used are the Hypsometric Indexes *HI*, maximum surface elevation $h_{max}$ of the basin and the flux gate to catchment size ratio *FA*. The variables are standardized in the traditional way of calculating their standard scores (also known as z-scores or normal scores). It is done by subtracting the variables mean value and dividing by its standard deviation (Miligan and Cooper, 1988). Afterwards a dissimilarity matrix is calculated using the Euclidean distances between the observations (Deza and Deza, 2009). A hierarchical cluster analysis (Kaufman and Rousseeuw, 1990) is applied on the dissimilarities using Ward's minimum variance method (Ward, 1963). At the start, ~~for each~~ the most similar glaciers (samples) are grouped. The resulting clusters are ~~a cluster is defined and then the most similar clusters are~~ iteratively joined based on their similarities until only one cluster is left, resulting in a dendrogram (see Section 4.4). The distances between the clusters are updated in each iteration step by applying the Lance-Williams algorithms (Lance and Williams, 1967).

**Formatiert:** Hochgestellt

## 4 Results

### 4.1 Area changes

Area changes relative to the measurements in the epoch 1985-1989 (1995-2000 for the former Larsen A and Prince Gustav Ice Shelf tributaries, see Section 5.2) of ~~all~~ the observed glaciers are plotted in Fig. S1-S74 (supplement). The glaciers are classified in three groups based on the latest area change measurements, which are illustrated in Fig. 2: retreat (Fig. 2a, b, c,

f) – loss of glacier area by frontal retreat; stable (Fig. 2e) – no significant area changes (within the error bars); advance (Fig. 2d) – gain of glacier area by frontal advance. In Fig. 3 the spatial distribution of the area change classification is illustrated. All glaciers along the east coast, including the former ice shelf tributaries, retreated, whereas along the west coast, numerous glaciers show stable ice front positions and some glaciers even advanced. In total, 238.81 km² of glacier area was lost in the survey area~~study region~~ in the period 1985-2015, which corresponds to a relative loss of 2.2%. All sectors show glacier area loss (Table 5), of which the area loss by 5.7% (208.59 km²) at sector "East-Ice-Shelves" clearly dominates. The glaciers in sector "West" and "East" recessed by 0.2% (9.14 km²) and 1.4% (21.07 km²), respectively. The temporal trends of total glacier area and area loss of all observed glaciers and of each sector are presented in Fig. 4. Catchment areas and changes between 1985 and 2015 of the individual basins are listed in Table S1 (supplement) and relative changes are illustrated in Fig. 5.

### 4.2 Surface velocities

A total of 282 stacked and filtered velocity fields are derived from the SAR acquisitions covering the period from 25th December, 1992 until 16th December, 2014. Figure S157-S160 (supplement) show exemplary velocity fields of the studied area obtained for ERS, Envisat, ALOS and TSX/TDX data. The average total uncertainty of the velocity fields amounts to $0.08 \pm 0.07$ m d$^{-1}$ and the values for each SAR sensor are provided in Table 2. In Table S~~2~~3 (supplement) the error estimates of each velocity field are listed. The mean sample count to estimate the coregistration quality is 11717 and the average mismatch amounts to 0.07 m d$^{-1}$. The error caused by the tracking algorithm strongly varies depending on the source of the SAR data (sensor). A mean value of 0.05 m d$^{-1}$ is found. ERS image pairs with time intervals of one day have very large estimated tracking uncertainties, biased by the very short temporal baselines. Therefore, only the errors caused by the mismatch of the coregistration are considered in the total error computations of the seven ERS tracking results with one day temporal baselines.

All measured velocity profiles of the 74 observed glaciers are visually inspected and in total 2~~503~~256 datasets passed the quality check (on average ~31~~34~~ per glacier). Figure 2 shows by example the temporal evolution of the ice flow for each velocity change category (see Table 3)~~.~~ and Fig. S149-S156 (supplement) show surface velocity profiles across the terminus for the same glaciers as well as for the small glacier catchments DGC14 and TPE61. The temporal ~~trends~~evolution of the surface velocities at the termini of each glacier are plotted in Fig. S1-S74 (supplement) and the related categories are listed in Table S1 (supplement). The spatial distribution of the categories is illustrated in Fig. 3. At nearly all glaciers in sector "East-Ice-Shelf" a peak in ice velocities is observed. In the sector "East", most glaciers showed a decrease in flow velocities in the observation period. The glaciers on the west coast show a more irregular distribution than along the east coast, but a local clustering of accelerating glaciers can be observed at Wilhelmina Bay. In order to analyze the quality of obtained velocity change signal, the ratio of the maximum measured velocity difference (maximum velocity minus minimum velocity) divided by the average error of the velocity measurements is calculated for each glacier. An average signal to noise ratio of 14.6 is found. At three glaciers (DGC14, DGC22 and Orel) a signal to noise ratio of less than 2 is observed. These glaciers are characterized as "stable", which justifies the low signal to noise ratio.

For each glacier the flow velocities in the first $v_S$ and last year $v_E$ of the observation period as well as the absolute and relative change *dv* is presented in Table S1 (supplement). The mean values of $v_S$, $v_E$ and *dv* of all analyzed glaciers and for each sector are listed in Table 5. On average the ice flow in the whole ~~study~~studied area ~~region~~ increased by ~~11.6%~~0.061 m/d (13%), but the average changes of the ~~glaciers in the~~ individual sectors ~~showed on average~~ are more pronounced~~significant change~~. Along the west coast an average acceleration by 41~~1.5~~% (0.177 m/d) occurred and the former ice shelf tributaries on the east coast accelerated by ~~16.8~~26% (0.118 m/d). In the sector "East" the glaciers decelerated resulting in a mean velocity change of -~~69~~58% (-0.423 m/d). The presented average flow speed change values are based on the observed changes of all glaciers in the respective sector (Table S1), ignoring the different size of the individual glaciers. The shortest observation period is 14.83 years at DBC31 ~~Glacier,~~Glacier; the longest observation period is 21.99 years at TPE31 and Sjögren glaciers and on average velocity changes are analyzed over a period of 19.~~40~~25 years (σ = ~~1.97~~2.06 years).

### 4.3 Catchment geometries and settings

The spatial distribution of Hypsometric Indexes and categories of the glacier basins is presented in Fig. 3 and the values are listed in Table S1 (supplement). The HI values range between -4.6 and 9.1 (mean: 0.88, σ: 2.10). No clear spatial distribution pattern can be identified, reflecting the heterogeneous topography of the AP. The maximum elevation of the catchments and the *FA* factors are also listed in Table S1 (supplement).

### 4.4 Cluster analysis

The resulting dendrogram of the hierarchical cluster analysis is plotted in Fig. 6. Four groups are distinguished. The boxplots of each input variable are generated based on this grouping and are shown in Fig. 7. The characteristics of the groups are discussed in Section 5.3.

## 5 Discussion

Most of the observed glaciers (62%) retreated and only 8% advanced in the study period. These findings are comparable to the results of Cook et al. (2005, 2014, 2016). Only glaciers along the west coast showed stable or advancing calving fronts and all glaciers on the east coast receded since 1985. This heterogeneous area change pattern was also observed by Davies et al. (2012) on western Trinity Peninsula. Most significant retreat occurred in the sector "East-Ice-Shelf". In the period 1985-1995, the Larsen Inlet tributaries (APPE-glaciers) lost 45.0 km² of ice. After the disintegration of Prince ~~-~~Gustav and Larsen A Ice Shelf, the tributaries rapidly retreated in the period 1995-2005. The recession slowed down in the latest observation interval (2005-2010). This trend is comparable to detailed observations by Seehaus et al. (2015, 2016) at individual glaciers (DBE glaciers and Sjögren-Inlet glaciers). At sector "East" the highest area-loss is found in the earliest observation interval (1985-1990). Davies et al. (2012) also reported higher ~~shrinkage~~retreat rates for most of the glaciers in this sector in the period 1988-2001 than in the period 2001-2009. Moreover, slightly increased recession is also found in the time period (1995-2005, Fig. 4) at sector "East". Davies et al. (2012) and Hulbe et al. (2004) supposed that the disintegration of an ice shelf affects the local climate. The air temperatures would rise due to the presence of more ice free water in summers. This might explain the slightly higher retreat rates at sector "East". At Base Marambio, ~100 km east of this sector, approximately 2°C higher mean annual air temperatures were recorded in the period 1996-2005 as compared to the period 1986-1995 (Oliva et al., 2017). Unfortunately, no temperature data recorded within sector "East" is available covering this period that could be used to validate this ~~theory~~hypothesis.

The average changes of flow velocities at each sector also vary strongly (Table 5) in the observation period 1992-2014. On the west coast an increase of 41~~2~~% is found, whereas in sector "East" the glaciers slowed down by approximately 58~~69~~% and at the ice shelf tributaries the ice flow increased on average by ~~17~~26%. Pritchard and Vaughan (2007) reported an increase in mean flow rate of 7.8% in frame 4923 (the central and much of the northern part of sector "West") and 15.2% in frame 4941 (the southern part of sector "West") for the period 1992-2005 (frame numbers correspond to European Space Agency convention for identifying ERS coverage). This spatial trend corresponds to our observations, since most of the glaciers ~~with~~which accelerated ~~a clear positive velocity trend~~ are located at the southern end of sector "West". However, for the same observation period we derived a mean increase in flow velocity by 18.9 % in sector "West", which is an approximately 1.6 times higher acceleration. Pritchard and Vaughan (2007) estimated the mean velocity change by measuring the flow speed at profiles along the flow direction of the glacier, whereas we measured the velocity across glacier profiles at the terminus. If a tidewater glacier speeds up due to the destabilization of its front, the highest acceleration is found at the terminus (see Seehaus et al., 2015, Fig. 3). Consequently, the different profile locations explain the deviations between both studies.

In the following section the observed changes in the individual sectors are discussed in more detail.

### 5.1 East

The glaciers north of the former Prince~~-~~ Gustav Ice Shelf show a ~~general trend towards lower flow velocities~~general deceleration. Eyrie, Russell East, TPE130, TPE31, TPE32, TPE34, and "2731" glaciers experienced a rapid decrease and, except "2731" Glacier, a subsequent stabilization or even gentle acceleration of flow velocities (Fig. S2, S6, S7 and S9-S12). A significant retreat followed by a stabilization or slight re-advance of the calving front position is also observed at these glaciers. According to Benn and Evans (1998), a small retreat of a glacier with an overdeepening behind its grounding line (i.e. where the bed slopes away from the ice front) can result in a rapid recession into the deepening fjord. The increased calving and retreat of the ice front cause stronger up-glacier driving stress, higher flow speed as well as glacier thinning and steepening (Meier and Post, 1987; Veen, 2002). The glacier front stabilizes when the grounding line reaches shallower bathymetry and ice flow also starts to slowdown. A delay between the front stabilization and slowdown can be caused by thinning and steepening of the glacier. Additionally, the accelerated ice flow can surpass the retreat rates and cause short-term glacier advances in the period of high flow speeds (e.g. Eyrie, Russel East, TPE130 and TPE32 glaciers, Fig. S6, S7, S9 and S11) (Meier and Post, 1987). This process can be initiated by climatic forcing (Benn and Evans, 1998). Significant higher surface air temperature at the north-eastern AP and a cooling trend in the 21$^{st}$ century was reported by Oliva et al. (2017)~~, Skvarca et al. (1998)~~ and Turner et al. (2016) (see Section 1). Hence, we assume that the initial recessions of the glaciers in sector "East" were forced by the warming observed by Oliva et al. (2017) and Skvarca et al. (1998) since the 1970s. Therefore, this initial frontal destabilization and retreat led to high flow speeds at the beginning of our ice dynamics time series (earliest velocity measurements from 1992) and the subsequently observed frontal stabilization (after 1985) caused the deceleration of the ice flow. The fjord geometry significantly affects the dynamics of the terminus of a tidewater glacier (Benn and Evans, 1998; van der Veen, 2002). The tongues of Aitkenhead and "2707" glaciers are split into two branches by nunataks, resulting in rather complex fjord geometries. A retreat from pinning points (e.g. fjord narrowing) causes further rapid recession and higher flow speeds until the ice front reaches a new stable position as observed at "2707" and Aitkenhead Glacier (Fig. S1 and S3). At TPE10 Glacier (Fig. S8 and S82) a "peaked" flow velocity evolution~~trend~~ is observed as at Aitkenhead Glacier (Fig. S3 and S77). No nunatak is present at the terminus, but small rock outcrops, indicating a shallow bedrock bump, are identified north of the center of the ice front by visual inspection of optical satellite imagery. Most probably, this shallow bedrock acts as a pinning point and prevents further retreat. The front of Broad Valley Glacier (Fig. S4) is located in a widening fjord. This geometry makes the glacier less vulnerable to frontal changes (Benn and Evans, 1998). Therefore, no significant changes in flow velocities are observed as a consequence of the frontal recession and re-advance.

Diplock and Victory glaciers (Fig. S5 and S13) show a decrease of flow speed during retreat (1995-2010) followed by an acceleration combined with frontal advance (2010-2015). Surge-type glaciers, found for example in Alaska (tidewater) (Motyka and Truffer, 2007; Walker and Zenone, 1988) or Karakoram (land terminating) (Rankl et al., 2014), show similar behavior. They are characterized by episodically rapid down-wasting, resulting in a frontal acceleration and strong advance. Regarding tidewater glaciers the advance can be strongly compensated by increased calving rates in deepwater in front of the glacier. It is therefore possible that these glaciers may have experienced a surge cycle in our observation period; however, a longer time series analysis is necessary to prove this hypothesis.

**5.2 East-Ice-Shelf**

In the sector "East-Ice-Shelf" the tributary glaciers in the Larsen A embayment ("2558", Arron Icefall, DBE, Drygalski, LAB2, LAB32, TPE61 and TPE62; Fig. S14, S17, S19-S22, S25 and S26) and Sjögren-Inlet (Boydell, Sjögren and TPE114; Fig. S18, S23 and S24) lost the downstream ~~ice shelves~~Larsen A and Prince Gustav Ice Shelf in 1995. Nearly all glaciers showed a rapid and significant acceleration after ice shelf break up and a subsequent slow down. A gentle peak in flow speeds is obtained at LAB32 and TPE114 glaciers. They are classified as "stable", since the variations are below the threshold of 0.25 m $d^{-1}$, according to the categorization in Table 3. Dramatic speed up with subsequent deceleration of former ice shelf tributaries was reported by various authors; e.g. in this sector by Seehaus et al., (2015, 2016) at DBE and Sjögren-Inlet glaciers and further south at Larsen B embayment by Rott et al. (2011) and Wuite et al. (2015). The velocities reported by Rott et al. (2014) at Sjögren, Pyke, Edgeworth and Drygalski glaciers are generally higher than our findings. The authors measured the velocities at locations near the center of the glacier fronts, where the ice flow velocities are typically highest, whereas we measured the median velocities at cross profiles close to the glacier fronts (Seehaus et al. 2015). The different approaches result in different absolute values (see also Section S1 in the supplement), but comparable temporal developments~~trends~~ in glacier flow speeds are observed by both author groups. For example Rott et al. (2015, 2017) presented surface velocity measured along a central flow line of Drygalski Glacier. Figure S~~75~~149 shows our surface velocity measurements across the terminus of Drygalski Glacier and Fig S94 velocity measurements at the maximum ice thickness across the terminus profile. Both studies show comparable values (e.g. in 1995: this study ~2.7 m/d, Rott et al. (2015) ~2.8 m/d; in 2009: this study ~5.5 m/d, Rott et al. (2015) ~6.0 m/d) at the ~~center of the~~ terminus.

Highest peak values of 6.3 m $d^{-1}$ are found at TPE61 Glacier in November 1995 and January 1996. Most glaciers (Arron Icefall, Drygalski, LAB2, TPE61, TPE62) strongly decelerated ~~towards pre-collapse values~~after the initial acceleration and show almost constant flow speeds in recent years, indicating that the glaciers adjusted to the new boundary conditions, albeit significant higher flow speeds can be observe at the central sections of the terminus (see Section S1 and Fig. S149 and S150 in the supplement). At "2558", Boydell, DBE and Sjögren glaciers the deceleration is ongoing and Boydell and DBE glaciers still show increased flow speeds at the glacier fronts. We suppose that these tributary glaciers show a prolonged response to ice shelf disintegration, caused by local settings (e.g. bedrock topography or fjord geometry), and are still adjusting to the new boundary conditions, as suggested by Seehaus et al. (2015, 2016).

In the 1980s, Prince Gustav Ice Shelf gradually retreated (see Fig. 1) and "2668" Glacier (Fig. S15) has not been buttressed by the ice shelf since the early 1990s. A deceleration is found in the period 2005-2010. Hence, this glacier may also have experienced a speed up in the early 1990s due to the recession of ~~-~~Prince Gustav Ice Shelf in the 1980s. However, the earliest velocity measurement at "2668" Glacier is only available from February 1996.

The ice shelf in Larsen Inlet disintegrated in 1987-1988 and earliest velocity measurements are obtained in 1993. ~~Therefore, a potential peak in the flow speed after ice shelf break-up cannot be detected at APPE glaciers (Fig. S16).~~ As for "2668" Glacier no sufficient cloud free coverage by Landsat imagery is available which facilitates the computation of surface velocities for the 1980s. The ice flow speeds at APPE glaciers (Fig. S16) ~~shows a~~are nearly stable ~~trend~~ with short term variations in the order of 0.2-0.5 m $d^{-1}$ between 1993 and 2014. Rott et al., (2014) also found nearly constant flow velocities at Pyke Glacier (part of the APPE basin, Table 1). The authors suggest that the ice flow of APPE glaciers was not strongly disturbed by the ice shelf removal due to the steep glacier surfaces and shallow seabed topography at the glacier fronts (Pudsey et al., 2001).

### 5.3 West

~~Meredith and King (2005) reported an increase of surface summer temperatures by more than 1°C in the ocean west of the AP since the 1950s. The authors attributed this to atmospheric warming and reduced sea ice production rates. However, Cook et al. (2016) reported cool ocean temperatures along the north-western AP for the period 1945-2009, and an absence of the atmospheric warming, especially pronounced at the northern AP, since the turn of the millennium was found by Oliva et al. (2017) and Turner et al. (2016), which correlates with an increase of sea ice concentration and the cool ocean temperatures at the northern AP. Thus, t~~The glacier geometries differ strongly along the west coast. In the southern part of sector "West" the shoreline is more ragged and islands are near the coast. An impact of the islands on the climatic conditions at the AP mainland's coastline (e.g. orographic barrier) is not obvious (visual inspection of RACMO2.3 5.5 km grid cell model results (Van Wessem et al., 2016)). However, the climatic conditions on the AP show strong spatial and temporal variability ~~do not show a spatially and temporally constant trend~~(see Section 1.2 and 3.3). ~~Moreover the glacier geometries differ strongly, and especially in the southern part of sector "West", the coastline is more jagged.~~ These factors cause the heterogeneous spatial pattern of area and flow speed changes in sector "West" as compared to the eastern sectors.

Kunz et al. (2012) observed thinning at the glacier termini along the western AP, by analyzing airborne and spaceborne stereo imagery in the period 1947-2010. Two of the twelve studied glaciers are located within our study area; Leonardo Glacier (1968-2010) and Rozier Glacier (1968-2010). An acceleration and terminus retreat can be caused by frontal thinning as shown by Benn et al. (2007). However, Benn et al. (2007) also point out that changes in ice thickness do not necessarily affect the ice flow and that calving front positions and ice dynamics are strongly dependent on the fjord and glacier geometries, derived from modeling results which have higher uncertainties especially for smaller basins.

The large number of glaciers in this sector is analyzed by means of a hierarchical cluster analysis (Section 3.4) and assorted into four groups based on ~~the dissimilarities~~the resulting dendrogram ~~, resulting in the dendrogram plotted in (~~Fig. 6~~)~~. Boxplots of the individual input variables of each group are shown in Fig. 7. The correlation between the observed ice dynamics and the glacier geometries of each group are discussed in the following sections (see also Fig. 7).

**Group 1 (14 glaciers):**

Most glaciers experienced acceleration ~~over the study~~ in the period 1992-2014. The majority of the glacier basins are “very top-heavy” or “top-heavy” (median *HI* = -1.8), stretching from sea level up to 1892 m on average. The $b_{clim}$ increases toward higher altitudes (van Wessem et al., 2016) and highest values are found in ~~regions~~ the zone between 1000 and 1700 m a.s.l~~.~~. Consequently these glaciers receive high mass input in their large high altitude accumulation ~~region~~areas~~s~~. The accumulation is known to have significantly increased on the AP by 20% since 1850 (Thomas et al., 2008). Pritchard and Vaughan (2007) reported that only a small fraction of the acceleration can be attributed to glacier thickening due to increased mass input. Up-glacier thickening combined with frontal thinning (reported by Kunz et al., 2012) leads to a steepening of the glacier and an increase in driving stress, resulting in faster ice flow (Meier and Post, 1987) as observed in this study. Moreover, a thinning of the terminus reduces the effective basal stress of a tidewater glacier and facilitates faster ice flow (Pritchard and Vaughan, 2007). The flux gate cross sections to catchment size ratios are relatively small, indicating narrowing catchments towards the ice front. The channelized increased ice flow almost compensates for the increased calving rates (due to frontal thinning), resulting in an average recession~~shrinkage~~ of the glaciers by only 0.2% in the period 1985-2015. The high flow speeds may outweigh the calving and lead to ice-front advances as measured at Krebs and TPE46 Glacier. The glacier termini of this group are typically located in narrow fjords (Fig. 5) and are clustered in Charcot, Charlotte and Andvord Bay.

**Group 2 (19 glaciers)**

Glaciers of group 2 are spread all over the study site ~~region~~, with a local clustering in Wilhelmina Bay. Group 2 shows similar $h_{max}$ and *FA* characteristics to group 1. Area changes are also quite small (-0.1%). Most of the glaciers experienced acceleration ~~positive~~ or show a “peaked” evolution of the flow velocities ~~trends~~. In contrast to group 1 the catchments are in general “bottom-heavy” and some are even “very bottom-heavy”. We assume that the constraints are similar to group 1 (increasing $b_{clim}$, frontal thinning and steepening). However, the additional mass accumulation in the upper areas~~regions~~ is smaller due to the “bottom-heavy” glacier geometries. Consequently, the imbalance due to the frontal thinning and up-glacier mass gain is less pronounced as in group 1 and numerous glaciers (“peak” type) started to decelerate after the speed-up, indicating that these glaciers are adjusting to the new boundary conditions.

**Group 3 (13 glaciers)**

These basins typically show a “bottom-heavy” hypsometry and smaller elevation ranges (in average up to 1103 m a.s.l.). Thus, $b_{clim}$ is relatively low. The smaller mean ice thickness at the termini (161 m, compared to 211 m of all glaciers) of group 3 implies less interaction with the ocean, leading to a small average frontal retreat of ~0.1%. The low frontal ablation does not significantly affect the ice flow, probably due to the flat glacier topography and the low mass input. Consequently, the flow speed is in general stable or even slightly decreases in the observation period. Glaciers of group 3 usually face the open ocean, and do not terminate in narrow fjords (especially in the northern part, Trinity Peninsula).

**Group 4 (3 glaciers)**

All basins in this group have a “very bottom-heavy” hypsometry and an elevation range comparable to group 3 glaciers. The *FA* factors are in general higher than in group 3, implying that outflow of the catchments is less channelized and the glacier fronts are long compared to the catchment sizes. Therefore, the largest relative area changes, in average -5.1%, are found at glaciers in group 4. However, the absolute frontal retreat is small and does not significantly affect the glacier flow. Note: Group 4 consists of only three samples, limiting the significance.

## 6 Conclusions

Our analysis expands on previous work (Pritchard and Vaughan, 2007) on ice dynamic changes along the west coast of AP between TPE8 and Bagshawe-Grubb Glacier, both in regard to temporal coverage and analysis methods. It also spatially extends previous work on changes in ice dynamics along the east coast between Eyrie Bay and the Seal Nunataks. The spatially and temporally detailed analysis of changes in ice flow speeds (1992-2014) and ice front positions (1985-2015) reveal varying temporal evolution~~trends~~ in glacier dynamics along the northern AP. The results are in general in line with findings of the previous ~~studies,~~studies; however along the west coast higher overall glacier flow was determined and on the eastern side temporal evolution of~~trends in~~ ice dynamics of 21 glaciers were observed for the first time. A large variety of temporal variations~~trends~~ in glacier dynamics were observed in our studied~~y~~ area~~region~~ and attributed to different forcing and boundary conditions.

On the east side all glacier fronts retreated in the study period (relative to 1985, relative to 1995 for former Larsen-A and Prince Gustav Ice Shelf tributaries, see also Section 5.2), with highest retreat rates observed at former tributaries of the Prince Gustav, Larsen Inlet and Larsen A ice shelves~~(relative to the year of ice shelf disintegration)~~. Moreover, nearly all the glaciers affected by ice shelf disintegration showed similar temporal evolutions~~trends~~ of ice velocities. The glaciers reacted with a strong acceleration to ice shelf break up followed by a deceleration, indicating that the glaciers adjusted or are still adjusting to the new boundary conditions. Glaciers on the east coast north of the former Prince Gustav Ice Shelf showed in general a significant deceleration and a reduction in frontal ablation. Based on the observed warming trend since the 1960s and the subsequent cooling since the mid-2000s in the northern AP, we conclude that the initial recession and speed up of the glaciers took place before the start of our observation and that the glaciers are now close to a new equilibrium.

The average flow speed of the glaciers along the west coast of the Antarctic Peninsula significantly increased in the observation period but the total frontal change was negligible. No general evolution in ice dynamics ~~pattern~~ is obvious~~in the~~

~~ice dynamic changes~~. However, correlations between the changes in ice dynamics and the glacier geometries of the individual catchments were obtained by applying a hierarchical cluster analysis. Thus, the geometry of the individual glacier basin strongly affects the reaction of the glacier to external forcing.

We conclude that for regions with such a strong spatial variation in topographic and climatic parameters as the AP, it is impossible to derive a regional trend in glacier change by simply analyzing individual glaciers in this region. Therefore further detailed observation of the glaciological changes along the AP is needed. Upcoming sensor probably facilitate the region wide measurement of recent surface elevation, since current estimates have got only partial coverage or have got some serious issues due to the complex topography of the AP. Moreover, ~~F~~future activities should link remote sensing derived ice dynamics and glacier extent with ocean parameters and ocean models, as well as regional climate models and ice dynamic models, in order to provide a better quantification of mass changes and physical processes leading to the observed changes.

*Author contributions. T.S. designed the study, processed the SAR data, performed the data analysis and led the writing of the manuscript, in which he received support from all authors. A.C. and A.S. compiled and provided glacier front position data sets. MB initiated the project and coordinated the research.*

*Competing interests.* The authors declare no competing financial interests.

*Acknowledgements.* This work was supported by the Deutsche Forschungsgemeinschaft (DFG) in the framework of the priority programme "Antarctic Research with comparative investigations in Arctic ice areas" by a grant to M.B. (BR 2105/9-1). MB and TS would like to thank the HGF Alliance “Remote Sensing of Earth System Dynamics” (HA-310) and Marie-Curie-Network International Research Staff Exchange Scheme IMCONet (EU FP7-PEOPLE-2012-IRSES) for additional support. Access to satellite data was kindly provided by various space agencies, e.g. under ESA AO 4032, DLR TerraSAR-X Background Mission Antarctic Peninsula & Ice Shelves, TSX AO LAN0013, TanDEM-X Mission TDX AO XTI_GLAC0264, ASF, GLIMS as well as NASA and USGS.

**References**

Barrand, N.E., Hindmarsh, R.C.A., Arthern, R.J., Williams, C.R., Mouginot, J., Scheuchl, B., Rignot, E., Ligtenberg, S.R.M., Van Den Broeke, M.R., Edwards, T.L., Cook, A.J., Simonsen, S.B., 2013a. Computing the volume response of the Antarctic Peninsula ice sheet to warming scenarios to 2200. J. Glaciol. 59, 397–409. doi:10.3189/2013JoG12J139

Barrand, N.E., Vaughan, D.G., Steiner, N., Tedesco, M., Kuipers Munneke, P., van den Broeke, M.R., Hosking, J.S., 2013b. Trends in Antarctic Peninsula surface melting conditions from observations and regional climate modeling. J. Geophys. Res. Earth Surf. 118, 315–330. doi:10.1029/2012JF002559

Benn, D.I., Evans, D.J.A., 1998. Glaciers & Glaciation. Arnold.

Benn, D.I., Hulton, N.R.J., Mottram, R.H., 2007. "Calving laws", "sliding laws" and the stability of tidewater glaciers. Ann. Glaciol. 46, 123–130. doi:10.3189/172756407782871161

Braun, M., Humbert, A., 2009. Recent Retreat of Wilkins Ice Shelf Reveals New Insights in Ice Shelf Breakup Mechanisms. IEEE Geosci. Remote Sens. Lett. 6, 263–267. https://doi.org/10.1109/LGRS.2008.2011925

Berthier, E., Scambos, T.A., Shuman, C.A., 2012. Mass loss of Larsen B tributary glaciers (Antarctic Peninsula) unabated since 2002. Geophys. Res. Lett. 39, L13501. doi:10.1029/2012GL051755Burgess, E.W., Forster, R.R., Larsen, C.F., Braun, M., 2012. Surge dynamics on Bering Glacier, Alaska, in 2008–2011. The Cryosphere 6, 1251–1262. doi:10.5194/tc-6-1251-2012

Cape, M.R., Vernet, M., Skvarca, P., Marinsek, S., Scambos, T., Domack, E., 2015. Foehn winds link climate-driven warming to ice shelf evolution in Antarctica. J. Geophys. Res. Atmospheres 2015JD023465. Doi: 10.1002/2015JD023465

Cook, A.J., Vaughan, D.G., 2010. Overview of areal changes of the ice shelves on the Antarctic Peninsula over the past 50 years. The Cryosphere 4, 77–98. https://doi.org/10.5194/tc-4-77-2010

Cook, A. ~~j~~J., Vaughan, D. g., Luckman, A. j., Murray, T., 2014. A new Antarctic Peninsula glacier basin inventory and observed area changes since the 1940s. Antarct. Sci. 26, 614–624. doi:10.1017/S0954102014000200

Cook, A.J., Fox, A.J., Vaughan, D.G., Ferrigno, J.G., 2005. Retreating Glacier Fronts on the Antarctic Peninsula over the Past Half-Century. Science 308, 541–544. doi:10.1126/science.1104235

Cook, A.J., Holland, P.R., Meredith, M.P., Murray, T., Luckman, A., Vaughan, D.G., 2016. Ocean forcing of glacier retreat in the western Antarctic Peninsula. Science 353, 283–286. doi:10.1126/science.aae0017

Cook, A.J., Murray, T., Luckman, A., Vaughan, D.G., Barrand, N.E., 2012. A new 100-m Digital Elevation Model of the Antarctic Peninsula derived from ASTER Global DEM: methods and accuracy assessment. Earth Syst. Sci. Data 4, 129–142. doi:10.5194/essd-4-129-2012

Cook, A.J., Vaughan, D.G., 2010. Overview of areal changes of the ice shelves on the Antarctic Peninsula over the past 50 years. The Cryosphere 4, 77–98. doi:10.5194/tc-4-77-2010

Davies, B.J., Carrivick, J.L., Glasser, N.F., Hambrey, M.J., Smellie, J.L., 2012. Variable glacier response to atmospheric warming, northern Antarctic Peninsula, 1988–2009. The Cryosphere 6, 1031–1048. doi:10.5194/tc-6-1031-2012

De Angelis, H., Skvarca, P., 2003. Glacier Surge After Ice Shelf Collapse. Science 299, 1560–1562. doi:10.1126/science.1077987

de Lange, R., Luckman, A., Murray, T., 2007. Improvement of Satellite Radar Feature Tracking for Ice Velocity Derivation by Spatial Frequency Filtering. IEEE Trans. Geosci. Remote Sens. 45, 2309–2318. doi:10.1109/TGRS.2007.896615

Dee, D.P., Uppala, S.M., Simmons, A.J., Berrisford, P., Poli, P., Kobayashi, S., Andrae, U., Balmaseda, M.A., Balsamo, G., Bauer, P., Bechtold, P., Beljaars, A.C.M., van de Berg, L., Bidlot, J., Bormann, N., Delsol, C., Dragani, R., Fuentes, M., Geer, A.J., Haimberger, L., Healy, S.B., Hersbach, H., Hólm, E.V., Isaksen, L., Kållberg, P., Köhler, M., Matricardi, M., McNally, A.P., Monge-Sanz, B.M., Morcrette, J.-J., Park, B.-K., Peubey, C., de Rosnay, P., Tavolato, C., Thépaut, J.-N., Vitart, F., 2011. The ERA-Interim reanalysis: configuration and performance of the data assimilation system. Q. J. R. Meteorol. Soc. 137, 553–597. doi:10.1002/qj.828

Deza, E., Deza, M.M., 2009. Encyclopedia of Distances. Springer Berlin Heidelberg, Berlin, Heidelberg.

Doake, C.S.M., Vaughan, D.G., 1991. Rapid disintegration of the Wordie Ice Shelf in response to atmospheric warming. Nature 350, 328–330. https://doi.org/10.1038/350328a0

Ferrigno, J.G., Cook, A.J., Foley, K.M., Williams, R.S., Swithinbank, C., Fox, A.J., Thomson, J.W., Sievers, J., 2006. Coastal-change and glaciological map of the Trinity Peninsula area and South Shetland Islands, Antarctica, 1843-2001.

Fretwell, P., Pritchard, H.D., Vaughan, D.G., Bamber, J.L., Barrand, N.E., Bell, R., Bianchi, C., Bingham, R.G., Blankenship, D.D., Casassa, G., Catania, G., Callens, D., Conway, H., Cook, A.J., Corr, H.F.J., Damaske, D.,

Formatiert: Deutsch (Deutschland)

Formatiert: Deutsch (Deutschland)

Damm, V., Ferraccioli, F., Forsberg, R., Fujita, S., Gim, Y., Gogineni, P., Griggs, J.A., Hindmarsh, R.C.A., Holmlund, P., Holt, J.W., Jacobel, R.W., Jenkins, A., Jokat, W., Jordan, T., King, E.C., Kohler, J., Krabill, W., Riger-Kusk, M., Langley, K.A., Leitchenkov, G., Leuschen, C., Luyendyk, B.P., Matsuoka, K., Mouginot, J., Nitsche, F.O., Nogi, Y., Nost, O.A., Popov, S.V., Rignot, E., Rippin, D.M., Rivera, A., Roberts, J., Ross, N., Siegert, M.J., Smith, A.M., Steinhage, D., Studinger, M., Sun, B., Tinto, B.K., Welch, B.C., Wilson, D., Young, D.A., Xiangbin, C., Zirizzotti, A., 2013. Bedmap2: improved ice bed, surface and thickness datasets for Antarctica. The Cryosphere 7, 375–393. doi:10.5194/tc-7-375-2013

Goodwin, B.P., 2013. Recent Environmental Changes on the Antarctic Peninsula as Recorded in an ice core from the Bruce Plateau. The Ohio State University.

Holland, P.R., Brisbourne, A., Corr, H.F.J., McGrath, D., Purdon, K., Paden, J., Fricker, H.A., Paolo, F.S., Fleming, A.H., 2015. Oceanic and atmospheric forcing of Larsen C Ice-Shelf thinning. The Cryosphere 9, 1005–1024. doi:10.5194/tc-9-1005-2015

Huber, J., Cook, A.J., Paul, F., Zemp, M., 2017. A complete glacier inventory of the Antarctic Peninsula based on Landsat 7 images from 2000 to 2002 and other preexisting data sets. Earth Syst. Sci. Data 9, 115–131. doi:10.5194/essd-9-115-2017

Hulbe, C.L., MacAyeal, D.R., Denton, G.H., Kleman, J., Lowell, T.V., 2004. Catastrophic ice shelf breakup as the source of Heinrich event icebergs. Paleoceanography 19, PA1004. doi:10.1029/2003PA000890

Huss, M., Farinotti, D., 2014. A high-resolution bedrock map for the Antarctic Peninsula. The Cryosphere 8, 1261–1273. doi:10.5194/tc-8-1261-2014

Jiskoot, H., Curran, C.J., Tessler, D.L., Shenton, L.R., 2009. Changes in Clemenceau Icefield and Chaba Group glaciers, Canada, related to hypsometry, tributary detachment, length–slope and area–aspect relations. Ann. Glaciol. 50, 133–143. doi:10.3189/172756410790595796

Kaufman, L., Rousseeuw, P.J., 1990. Finding groups in data: an introduction to cluster analysis, Wiley series in probability and mathematical statistics. Wiley, New York.

Kunz, M., King, M.A., Mills, J.P., Miller, P.E., Fox, A.J., Vaughan, D.G., Marsh, S.H., 2012. Multi-decadal glacier surface lowering in the Antarctic Peninsula. Geophys. Res. Lett. 39, L19502. doi:10.1029/2012GL052823

Lance, G.N., Williams, W.T., 1967. A general theory of classificatory sorting strategies: II. Clustering systems. Comput. J. 10, 271–277. doi:10.1093/comjnl/10.3.271

Lai, Z.M., Huang, M.H., 1989. A numerical classification of glaciers in China by means of glaciological indices at the qeuilibrium line. Snow Cover Glacier Var. Proc. Baltim. Symp.

Marshall, G.J., Orr, A., van Lipzig, N.P.M., King, J.C., 2006. The Impact of a Changing Southern Hemisphere Annular Mode on Antarctic Peninsula Summer Temperatures. J. Clim. 19, 5388–5404. doi:10.1175/JCLI3844.1

McNabb, R.W., Hock, R., O'Neel, S., Rasmussen, L.A., Ahn, Y., Braun, M., Conway, H., Herreid, S., Joughin, I., Pfeffer, W.T., Smith, B.E., Truffer, M., 2012. Using surface velocities to calculate ice thickness and bed topography: a case study at Columbia Glacier, Alaska, USA. J. Glaciol. 58, 1151–1164. doi:10.3189/2012JoG11J249

Meier, M.F., Post, A., 1987. Fast tidewater glaciers. J. Geophys. Res. Solid Earth 92, 9051–9058. doi:10.1029/JB092iB09p09051

Meredith, M.P., King, J.C., 2005. Rapid climate change in the ocean west of the Antarctic Peninsula during the second half of the 20th century. Geophys. Res. Lett. 32, L19604. doi:10.1029/2005GL024042

Milligan, G.W., Cooper, M.C., 1988. A study of standardization of variables in cluster analysis. J. Classif. 5, 181–204. doi:10.1007/BF01897163

Motyka, R.J., Truffer, M., 2007. Hubbard Glacier, Alaska: 2002 closure and outburst of Russell Fjord and postflood conditions at Gilbert Point. J. Geophys. Res. Earth Surf. 112, F02004. doi:10.1029/2006JF000475

Oliva, M., Navarro, F., Hrbáček, F., Hernández, A., Nývlt, D., Pereira, P., Ruiz-Fernández, J., Trigo, R., 2017. Recent regional climate cooling on the Antarctic Peninsula and associated impacts on the cryosphere. Sci. Total Environ. 580, 210–223. doi:10.1016/j.scitotenv.2016.12.030

Potocki, M., Mayewski, P.A., Kurbatov, A., Handley, M., Simoes, J.C., Jaña, R., 2011. Detailed Glaciochemical Records from a Northern Antarctic Peninsula Site - Detroit Plateau. AGU Fall Meet. Abstr. 43.

Pritchard, H.D., Vaughan, D.G., 2007. Widespread acceleration of tidewater glaciers on the Antarctic Peninsula. J. Geophys. Res. 112. doi:10.1029/2006JF000597

Pudsey, C.J., Evans, J., Domack, E.W., Morris, P., Valle, R.A.D., 2001. Bathymetry and acoustic facies beneath the former Larsen-A and Prince Gustav ice shelves, north-west Weddell Sea. Antarct. Sci. 13, 312–322. doi:10.1017/S095410200100044X

Rack, W., Rott, H., 2003. Further retreat of the northern Larsen Ice Shelf and collapse of Larsen B, in: 16th International Workshop of the Forum for Research on Ice Shelf Processes (FRISP), June 25.

Rack, W., Rott, H., Nagler, T., Skvarca, P., 1998. Areal Changes and Motion of Northern Larsen Ice Shelf, Antarctic Peninsula, in: Geoscience and Remote Sensing Symposium Proceedings, 1998. IGARSS'98. 1998 IEEE International. IEEE, pp. 2243–2245.

Rack, W., Rott, H., 2004. Pattern of retreat and disintegration of the Larsen B ice shelf, Antarctic Peninsula. Ann. Glaciol. 39, 505–510.

Rankl, M., Kienholz, C., Braun, M., 2014. Glacier changes in the Karakoram region mapped by multimission satellite imagery. The Cryosphere 8, 977–989. doi:10.5194/tc-8-977-2014

**Formatiert:** Deutsch (Deutschland)

Rau, F., Braun, M., 2002. The regional distribution of the dry-snow zone on the Antarctic Peninsula north of 70°S. Ann. Glaciol. 34, 95–100. doi:10.3189/172756402781817914

Rignot, E., Casassa, G., Gogineni, P., Krabill, W., Rivera, A., Thomas, R., 2004. Accelerated ice discharge from the Antarctic Peninsula following the collapse of Larsen B ice shelf. Geophys. Res. Lett. 31. doi:10.1029/2004GL020697

Rott, H., Abdel Jaber, W., Wuite, J., Scheiblauer, S., Floricioiu, D., van Wessem, J.M., Nagler, T., Miranda, N., van den Broeke, M.R., 2017. Changing pattern of ice flow and mass balance for glaciers discharging into the Larsen A and B embayments, Antarctic Peninsula, 2011 to 2016. Cryosphere Discuss 2017, 1–34. https://doi.org/10.5194/tc-2017-259

**Formatiert:** Englisch (USA)

Rott, H., Floricioiu, D., Wuite, J., Scheiblauer, S., Nagler, T., Kern, M., 2014. Mass changes of outlet glaciers along the Nordensjköld Coast, northern Antarctic Peninsula, based on TanDEM-X satellite measurements. Geophys. Res. Lett. 2014GL061613. doi:10.1002/2014GL061613

Rott, H., Müller, F., Nagler, T., Floricioiu, D., 2011. The imbalance of glaciers after disintegration of Larsen-B ice shelf, Antarctic Peninsula. The Cryosphere 5, 125–134. doi:10.5194/tc-5-125-2011

Rott, H., Skvarca, P., Nagler, T., 1996. Rapid Collapse of Northern Larsen Ice Shelf, Antarctica. Science 271, 788–792. https://doi.org/10.1126/science.271.5250.788

Rott, H., Wuite, J., Floricioiu, D., Nagler, T., Scheiblauer, S., 2015. Synergy of TanDEM-X DEM differencing and input-output method for glacier monitoring, in: 2015 IEEE International Geoscience and Remote Sensing Symposium

(IGARSS). Presented at the 2015 IEEE International Geoscience and Remote Sensing Symposium (IGARSS), pp. 5216–5219. doi:10.1109/IGARSS.2015.7327010

Sagredo, E.A., Lowell, T.V., 2012. Climatology of Andean glaciers: A framework to understand glacier response to climate change. Glob. Planet. Change 101–109.

Scambos, T., Hulbe, C., Fahnestock, M., 2003. Climate-Induced Ice Shelf Disintegration in the Antarctic Peninsula, in: Domack, E., Levente, A., Burnet, A., Bindschadler, R., Convey, P., Kirby,  tthew (Eds.), Antarctic Peninsula Climate Variability: Historical and Paleoenvironmental Perspectives. American Geophysical Union, pp. 79–92.

Scambos, T.A., Berthier, E., Haran, T., Shuman, C.A., Cook, A.J., Ligtenberg, S.R.M., Bohlander, J., 2014. Detailed ice loss pattern in the northern Antarctic Peninsula: widespread decline driven by ice front retreats. The Cryosphere 8, 2135–2145. doi:10.5194/tc-8-2135-2014

Scambos, T.A., Bohlander, J., Shuman, C.A., Skvarca, P., 2004. Glacier acceleration and thinning after ice shelf collapse in the Larsen B embayment, Antarctica. Geophys. Res. Lett. 31. doi:10.1029/2004GL020670

Seehaus, T., Marinsek, S., Helm, V., Skvarca, P., Braun, M., 2015. Changes in ice dynamics, elevation and mass discharge of Dinsmoor–Bombardier–Edgeworth glacier system, Antarctic Peninsula. Earth Planet. Sci. Lett. 427, 125–135. doi:10.1016/j.epsl.2015.06.047

Seehaus, T.C., Marinsek, S., Skvarca, P., van Wessem, J.M., Reijmer, C.H., Seco, J.L., Braun, M.H., 2016. Dynamic Response of Sjögren Inlet Glaciers, Antarctic Peninsula, to Ice Shelf Breakup Derived from Multi-Mission Remote Sensing Time Series. Front. Earth Sci. 4. doi:10.3389/feart.2016.00066

Skvarca, P., Rack, W., Rott, H., Donángelo, T.I., 1999. Climatic trend and the retreat and disintegration of ice shelves on the Antarctic Peninsula: an overview. Polar Res. 18, 151–157.

Skvarca, P., Rack, W., Rott, H., Ibarzábal y Donángelo, T., 1998. Evidence of recent climatic warming on the eastern Antarctic Peninsula. Ann. Glaciol. 27, 628–632.

Skvarca, P., Rott, H., Nagler, T., 1995. Satellite imagery, a base line for glacier variation study on James Ross Island, Antarctica. Ann. Glaciol. 21, 291–296.

Strozzi, T., Luckman, A., Murray, T., Wegmuller, U., Werner, C.L., 2002. Glacier motion estimation using SAR offset-tracking procedures. IEEE Trans. Geosci. Remote Sens. 40, 2384–2391. doi:10.1109/TGRS.2002.805079

Thomas, E.R., Marshall, G.J., McConnell, J.R., 2008. A doubling in snow accumulation in the western Antarctic Peninsula since 1850. Geophys. Res. Lett. 35. doi:10.1029/2007GL032529

Turner, J., 2002. Spatial variability of Antarctic Peninsula net surface mass balance. J. Geophys. Res. 107. doi:10.1029/2001JD000755

Turner, J., Colwell, S.R., Marshall, G.J., Lachlan-Cope, T.A., Carleton, A.M., Jones, P.D., Lagun, V., Reid, P.A., Iagovkina, S., 2005. Antarctic climate change during the last 50 years. Int. J. Climatol. 25, 279–294. doi:10.1002/joc.1130

Turner, J., Lu, H., White, I., King, J.C., Phillips, T., Hosking, J.S., Bracegirdle, T.J., Marshall, G.J., Mulvaney, R., Deb, P., 2016. Absence of 21st century warming on Antarctic Peninsula consistent with natural variability. Nature 535, 411–415. doi:10.1038/nature18645

van Lipzig, N.P.M., King, J.C., Lachlan-Cope, T.A., van den Broeke, M.R., 2004. Precipitation, sublimation, and snow drift in the Antarctic Peninsula region from a regional atmospheric model. J. Geophys. Res. Atmospheres 109, D24106. doi:10.1029/2004JD004701

van Lipzig, N.P.M., Meijgaard, E. van, Oerlemans, J., 2002. The spatial and temporal variability of the surface mass balance in Antarctica: results from a regional atmospheric climate model. Int. J. Climatol. 22, 1197–1217. doi:10.1002/joc.798

van Wessem, J.M., Ligtenberg, S.R.M., Reijmer, C.H., van de Berg, W.J., van den Broeke, M.R., Barrand, N.E., Thomas, E.R., Turner, J., Wuite, J., Scambos, T.A., van Meijgaard, E., 2016. The modelled surface mass balance of the Antarctic Peninsula at 5.5 km horizontal resolution. The Cryosphere 10, 271–285. doi:10.5194/tc-10-271-2016

van der Veen, C.J., 2002. Calving glaciers. Prog. Phys. Geogr. 26, 96–122. doi:10.1191/0309133302pp327ra

Walker, K.-M., Zenone, C., 1988. Multitemporal Landsat multispectral scanner and thematic mapper data of the Hubbard Glacier region, southeast Alaska. Photogramm. Eng. Remote Sens. 54, 373–376.

Ward, J.H., 1963. Hierarchical Grouping to Optimize an Objective Function. J. Am. Stat. Assoc. 58, 236–244. doi:10.1080/01621459.1963.10500845

Wendt, J., Rivera, A., Wendt, A., Bown, F., Zamora, R., Casassa, G., Bravo, C., 2010. Recent ice-surface-elevation changes of Fleming Glacier in response to the removal of the Wordie Ice Shelf, Antarctic Peninsula. Ann. Glaciol. 51, 97–102.

Wuite, J., Rott, H., Hetzenecker, M., Floricioiu, D., De Rydt, J., Gudmundsson, G.H., Nagler, T., Kern, M., 2015. Evolution of surface velocities and ice discharge of Larsen B outlet glaciers from 1995 to 2013. The Cryosphere 9, 957–969. doi:10.5194/tc-9-957-2015

**Figures**

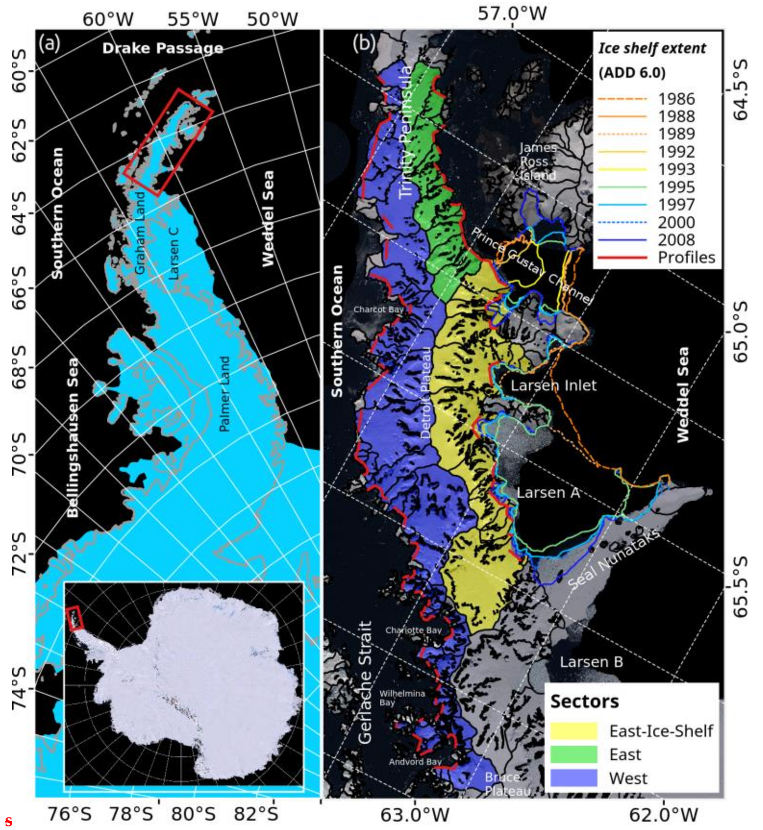


**Figure 1.** Panels **(a)** Location of study site on the Antarctic Peninsula and on the Antarctic continent (inset). Panel **(b)**. Separation of study site in 3 sectors and retreat states of Prince-_Gustav and Larsen A ice shelves. Red lines: profiles at glacier front for velocity measurements. Map base, Landsat LIMA Mosaic ~~©~~ USGS, NASA, BAS, NSF, coastlines (ice shelf extent) and catchment delineations from SCAR Antarctic Digital Database 6.0.

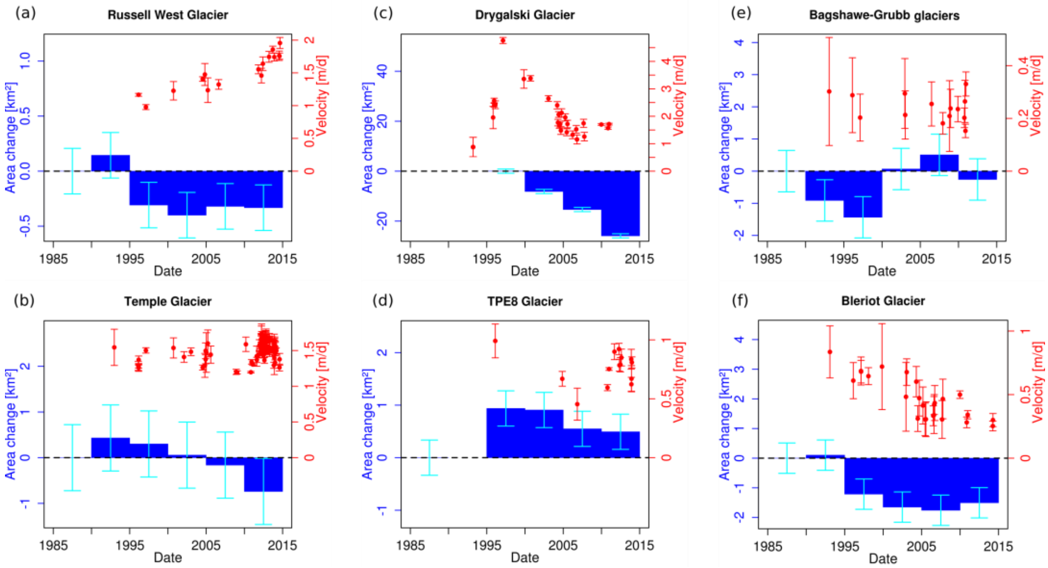


**Figure 2.** Temporal ~~trend~~evolution of surface velocity (red) and area (blue) changes of selected glaciers in the study area ~~region~~ for each velocity change category (see Table 3).

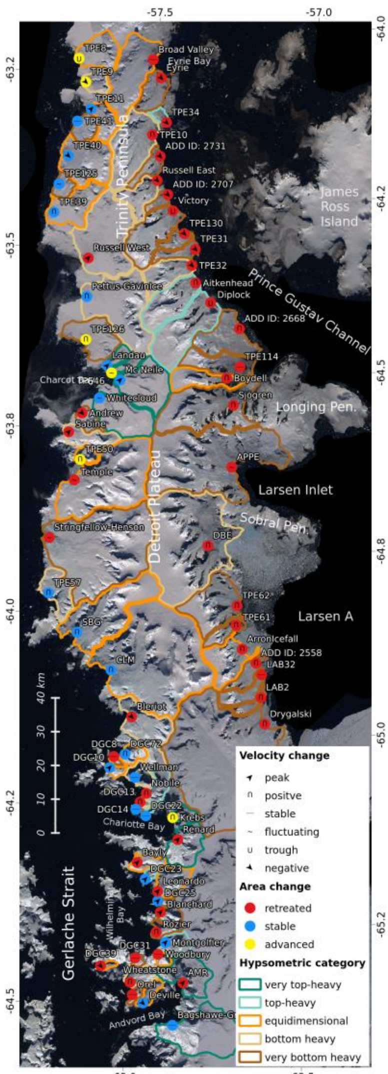


**Figure 3.** Categorizations of glaciers based on the~~to~~ temporal variations of~~trends in~~ area changes (dots) and flow velocities (symbols). Colors of catchment delineation indicate Hypsometric categories according to Jiskoot et al. (2009). Background: Landsat LIMA Mosaic ~~©~~ USGS, NASA, BAS, NSF

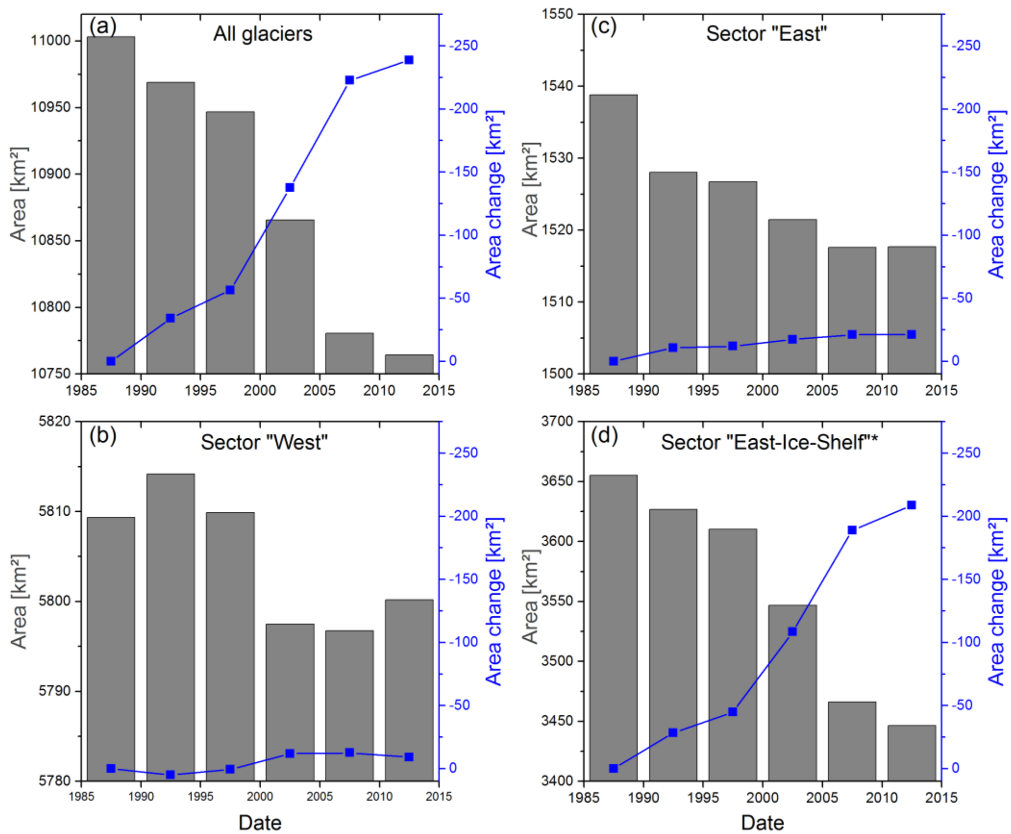


**Figure 4.** Total glacier area (gray bars) of the whole study site (Panel **(a)**) and of the individual sectors (Panels **(b)-(d)**) in the period 1985-2015. Changes in glacier area (blue points) are relative to the measurements in time interval 1985-1990. Note the different scaling of the le~~s~~ft y-axes. *In sector "East-Ice-Shelf", area changes before 1995 are only measured at Larsen Inlet tributaries (APPE glaciers).

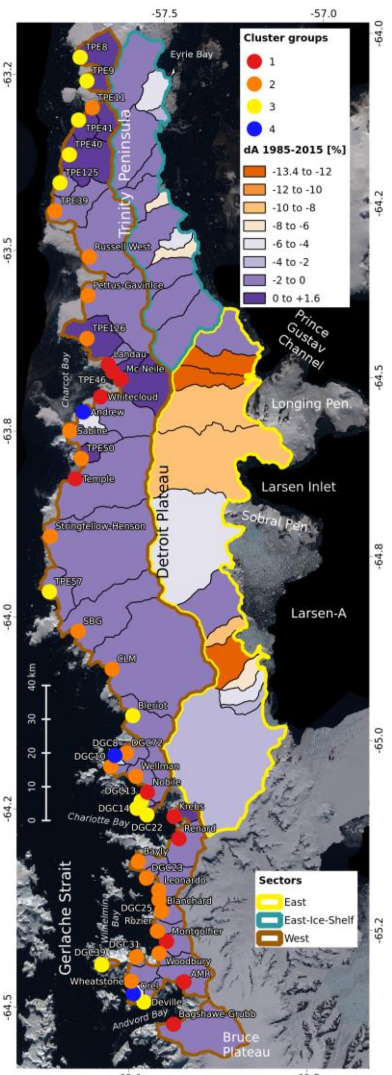


**Figure 5.** Spatial distribution of glacier types along the west coast. Glaciers are group based on a hierarchical cluster analysis (dots). In Section 5.3 the characteristics of the groups are discussed in detail. Individual glacier catchment colors: relative area change in the period 1985-2015. Colored polygon outlines: Boundaries of the three ~~regional~~ sectors. Background: Landsat LIMA Mosaic ~~©~~ USGS, NASA, BAS, NSF

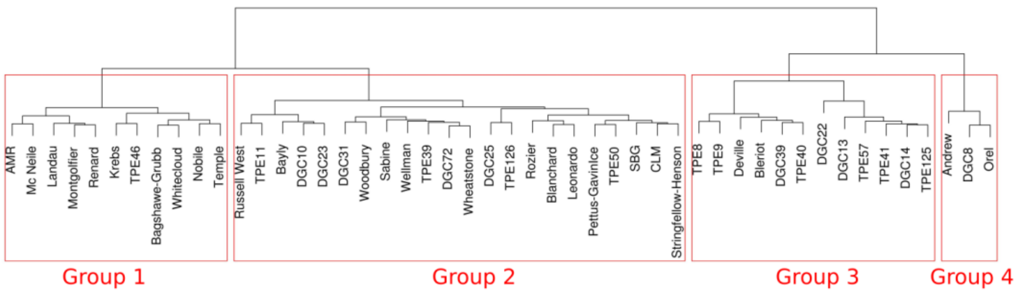


**Figure 6.** Dendrogram of hierarchical cluster analysis of glaciers in sector "West". The glaciers are assorted in four groups (red rectangles). See also Section 5.3.

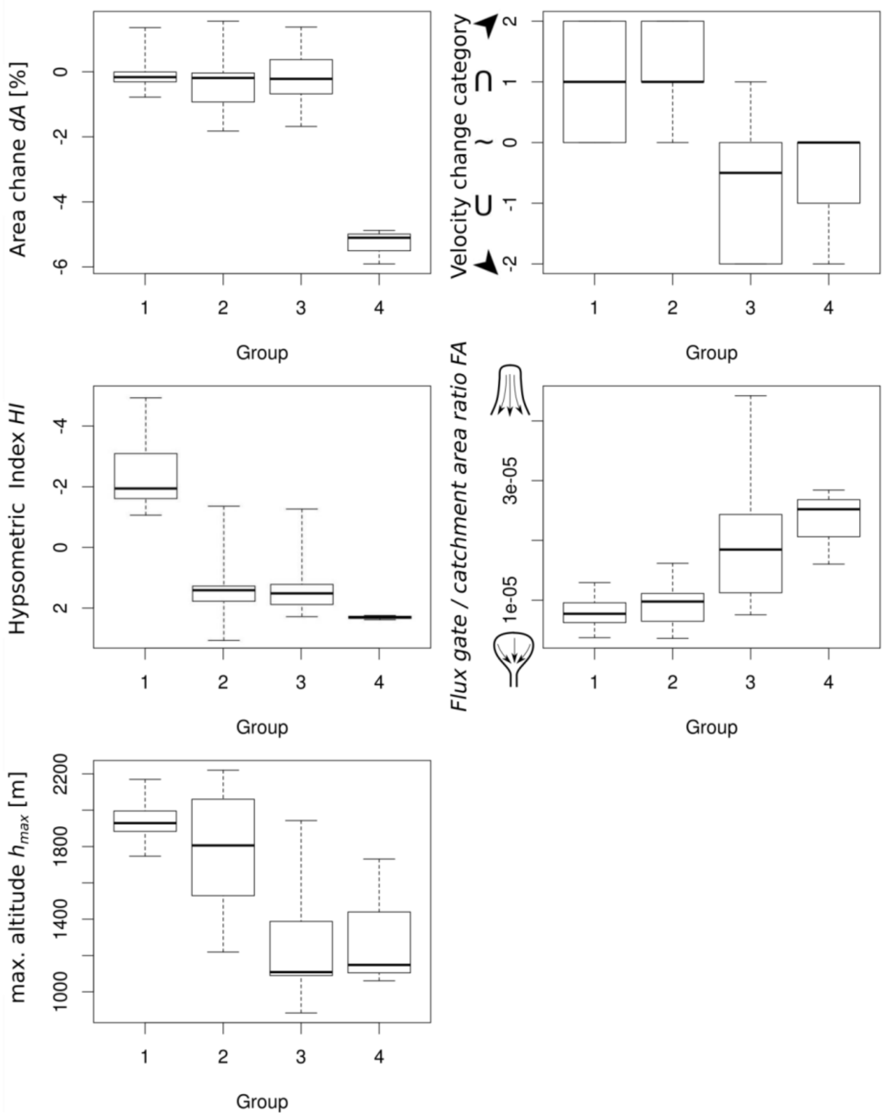


**Figure 7.** Boxplots of cluster analysis input variables (Sector "West") for each group. Whiskers extend to the most extreme data points.

## Tables

**Table 1. A**bbreviations of glacier names

| Abbreviation | Glacier names |
|---|---|
| AMR | Arago-Moser-Rudolph |
| APPE | Albone-Pyke-Polaris-Eliason |
| CLM | Cayley-Lilienthal-Mouillard |
| DBE | Dinsmoor-Bombardier-Edgeworth |
| SBG | Sikorsky-Breguet-Gregory |

**Table 2.** Overview of SAR sensors and specifications used in this study.

| Platform | Sensor | Mode | SAR band | Repetition cycle [d] | Time interval | Ground range resolution [m]* | Tracking patch sizes [p x p]+ | Tracking step size [p x p]+ | Mean uncertainty of tracking results [m/d] |
|---|---|---|---|---|---|---|---|---|---|
| ERS-1/2 | SAR | IM | C band | 35/1 | 08. December 1992<br>02. April 2010 | 30 | 48x240<br>64x320 | 5x25 | 0.15±0.10 |
| RADARSAT 1 | SAR | ST | C band | 24 | 10. September 2000<br>03. September 2006 | 30 | 48x192<br>64x256 | 5x20 | 0.11±0.03 |
| Envisat | ASAR | IM | C band | 35 | 05. December 2003<br>16. August 2009 | 30 | 32x160<br>64x320<br>128x640 | 5x25 | 0.12±0.05 |
| ALOS | PALSAR | FBS | L band | 46 | 18. May 2006<br>17. March 2011 | 10 | 64x192<br>96x192<br>128x384 | 10x30 | 0.05±0.06 |
| TerraSAR-X TanDEM-X | SAR | SM | X band | 11 | 14. October 2008<br>22. December 2014 | 3 | 128x128<br>256x256<br>512x512 | 25x25 | 0.06±0.04 |

* ~~nominal~~nominal resolution; depending on the incidence angle.

+ ~~I~~intensity tracking parameters are provided in pixels [p] in slant range geometry.

**Table 3.** Description of velocity change categories.

| Category | Description | Rating* |
|---|---|---|
| positive | General increase of flow speed | 2 |
| peak | Increase of flow speed with subsequent deceleration | 1 |
| stable | Variability of measurements < 0.25 $m\ d^{-1}$ | 0 |
| fluctuating | Short term speed-ups and deceleration, no clear trend | 0 |
| trough | Decrease of flow speed with subsequent acceleration | -1 |
| negative | General decrease of flow speed | -2 |

*~~R~~ratings used for cluster analysis Section 3.4

**Table 4.** Hypsometric Index and glacier basin category descriptions.

| Hypsometric Index (*HI*)* | Hypsometric categories | Number of Glaciers |
|---|---|---|
| *HI* < -1.5 | Very top-heavy | 8 |
| -1.5 < *HI* < -1.2 | Top-heavy | 7 |
| -1.2 < *HI* < 1.2 | Equidimensional | 18 |
| 1.2 < *HI* < 1.5 | Bottom-heavy | 13 |
| *HI* > 1.5 | Very bottom-heavy | 28 |

*according to Jiskoot et al., (2009)

**Table 5.** Summary of observed parameters for each sector and all glaciers.

| Sector | East | East-Ice-Shelf | West | All glaciers |
|---|---|---|---|---|
| *N* | 13 | 13 | 48 | 74 |
| $l_f$ [m] | 85114 | 127909 | 268763 | 481786 |
| $A_{1985-1990}$ [km²] | 1538.78 | 3655.13 | 5809.33 | 11003.23 |
| $A_{2010-2015}$ [km²] | 1517.71 | 3446.54 | 5800.18 | 10764.42 |
| $dA$ [km²] | -21.07 | -208.59 | -9.14 | -238.81 |
| $dt$ [a] | 18.~~79~~22 | 19.05 | 19.58~~20~~ | 19.25 |
| $v_S$ [m d$^{-1}$] | 0.~~995~~729 | 0.480~~480~~ | 0.42~~7~~8 | 0.490~~537~~ |
| $v_E$ [m d$^{-1}$] | 0.~~307~~306 | 0.562~~1~~ | 0.605 | 0.545 |
| $dv$ [m d$^{-1}$] | -0.423~~688~~ | 0.081 | 0.177 | 0.055~~08~~ |
| $n_v$ | 277~~319~~ | 5~~84~~50 | 1~~600~~429 | 2~~503~~256 |

*N* – number of studied glaciers

$l_f$ – length of ice front

A – g~~G~~lacier area in the respective period (subscript)*

dA – ~~C~~change in glacier area between 1985 and 2015*

dt~~:~~ - mean time period of velocity measurements

$v_S$ – mean of earliest velocity measurements (1992-1996)

$v_E$ – mean of latest velocity measurements (2010-2014)

dv – mean velocity change

$n_v$ – sum of velocity measurements in the observation period (dt)

*since 1995 for the former Larsen-A and Prince Gustav Ice Shelf tributaries (see Section 5.2)

# Supplement to

# Detailed analysis of changes in glacier dynamics in the northern Antarctic Peninsula since 1985

Thorsten Seehaus[1], Alison Cook[2], Aline B. Silva[3], Matthias Braun[1]

[1] Institute of Geography, Friedrich-Alexander-University Erlangen-Nuremberg, Wetterkreuz 15, 91058 Erlangen, Germany
[2] Department of Geography, Durham University, Lower Mountjoy South Road, Durham DH1 3LE, United Kingdom
[3] Laboratório de Monitoramento da Criosfera, Universidade Federal do Rio Grande, Av. Itália, km 8, 96203-900, Rio Grande – RS. Brazil

Correspondence to: Thorsten Seehaus (*thorsten.seehaus@fau.de*)

**Overview:**

**Section S1: Velocity change measurements**

**Figures:**

**Figure S1-S74: Temporal changes in flow speed (median values of measurements along the terminus profiles) and glacier area ~~and flow speed~~**

**Figure S75-S148: Temporal changes in flow speed (measured at maximum ice thickness at the terminus profiles) and glacier area**

**Figure S149-S156:~~Figure S74:~~ Surface velocity across the terminus and respective median values of Drygalski, Bagshawe-Grubb, Bleriot, DGC14, Russell West, Temple and TPE8 glaciers ~~Glacier~~**

**Figure S157-S160: Velocity fields obtained from ERS, ENVISAT, ALOS PALSAR and TerraSAR/TanDEM-X data**

**Figure S161: Categorizations of glaciers based on the temporal variations of area changes and flow velocities (measured at maximum ice thickness at the terminus profiles)**

**Figure S162: Spatial distribution of glacier types along the west coast (Cluster analysis based on velocity measurements at the maximum ice thickness at the terminus profiles)**

**Figure S163: Boxplots of cluster analysis (velocity measurements at the maximum ice thickness at the terminus profiles)**

**Figure S164: Dendrogram of hierarchical cluster analysis (velocity measurements at the maximum ice thickness at the terminus profiles)**

**Tables:**

**~~Table S1: Uncertainties of intensity tracking results~~**

**Table S~~2~~1: Observed parameters of the individual glaciers (median velocities along terminus profiles)**

**Table S2: Observed parameter of the individual glaciers (velocities measured at maximum ice thickness at terminus profiles)**

**Table S~~1~~3: Uncertainties of intensity tracking results**

**S1: Velocity change measurements**

Two approaches to measure and analyze the temporal changes in flow velocities of the studied glaciers are evaluated. For the first approach, the flow velocities are extracted along across glacier profiles (see. Fig. 1 in the manuscript) close to the terminus and the median values along the profiles are calculated (see also Section 3.2 in the manuscript). For the second approach, the flow velocities are measured at the location of the maximum ice thickness at the respective across glacier terminus profile (same as for the 1st approach). The ice thickness information is taken from the Huss and Farinotti (2014) ice thickness reconstruction dataset of the Antarctic Peninsula.

The temporal evolution of the ice velocities of all observed glaciers is plotted in Fig. S1-S74 (for 1st approach) and Fig. S75-S148 (for the 2nd approach). Velocity profiles with partial profile coverage or large data gaps are sorted out using the 1st approach. These data voids usually occur towards the lateral parts of the glacier (e.g. regions affected by SAR shadow, caused by the valley side walls), whereas the maximum ice thickness is usually found towards the center of the terminus. Therefore, some more velocity measurements are obtained using the 2nd approach (2256 measurement for the 1st approach; 2736 measurements for the 2nd approach; see Table S1 and S2).

The temporal changes in flow speed of all studied glaciers are categorized according to Table 3 (manuscript) for both approaches (see. Table S1 and S2). The same categories are addressed to 50 glaciers (68%) by both approaches. Taking the 1st approach as reference; the largest mismatch (9 glaciers) between both approaches is found for the category “stable”. However, most of these “mismatched” glaciers are categorized as “fluctuating” glaciers, using obtained by the second approach (Note: This mismatch does not influencing the subsequent cluster analysis, since both velocity change categories have got the same numerical rating for the cluster analysis, see manuscripts Section 3.4 and Table 3). For both approaches, the same threshold of 0.25 m/d for the temporal variability of the measurements is applied for the category “stable”, in order to carry out a comparable analysis. However, the comparison of Fig. S1-S74 and S75-S148 shows that the magnitude of the temporal variability of the flow speed is typically higher for the 2nd approach, since the values obtained using the 1st approach are smoothed by averaging along the profiles.

Small differences in the mean velocity change rate (*dv* in %) in the observation period are found for Sector “East” (-58.0% for 1st approach, -69% for 2nd approach) and “West” (+41.3% for 1st approach, +44.5% for 2nd approach). At sector “EastIS”, an average increase in flow speed by +26.5% for the 1st approach and +41.0% for the 2nd approach is obtained. This divergence can be explained by the different forcing at sector “EastIS”. The glaciers were buttressed by the Larsen-A and Prince Gustav ice shelves until they broke up in 1995. The subsequent acceleration of the glaciers led to changes in the across glacier velocity profiles (see Fig. S149). Highest acceleration is found towards the center of the glacier terminus (where usually the ice thickness is maximum). Thus, the change of the glacier types from ice shelf terminating to tide water glaciers differently affects both velocity measuring methods and leads to the deviation. However, a general acceleration is revealed by both approaches.

The impact of the velocity measuring approach on the cluster analysis (Section 3.4, manuscript) is little. The results of the cluster analysis (boxplots, dendrogram and the spatial distribution of the glacier groups) using the 1st velocity measuring approach are presented in the manuscript and the results using the 2nd velocity measuring approach are shown in Fig. S162-S164. Forty two out of 48 glaciers are assorted to equal groups. Compared to the grouping based on the 1st velocity measuring approach, group 2 lost 6 glaciers using the 2nd velocity measuring approach. Two glaciers are attributed to group 1 and four glaciers to group 3. Hence, these glaciers are only assorted to neighboring groups, which have got the highest similarity to the original group.

To sum it up, both velocity measuring approaches reveal comparable results at our study region. The results of both approaches are provided in this supplement in order to facilitate a better comparison with results from other studies. As discussed above, the shape of the across glacier velocity profiles can change over time and the peak positon as well (see Fig. S149-S156). Moreover, the maximum ice thickness does not necessarily overlap with the peak in the velocity profiles, since the ice thickness estimates have also got a significant uncertainty. These cases can impact the observed temporal evolution of the flow speed using a fixed position to measure the velocities, as performed by applying the 2nd velocity measuring approach (at maximum ice thickness at the terminus profile) or by other studies using manually defined measuring positions. Therefore, we decided to use the results of the 1st approach for the detailed analysis and discussion in the manuscript, since it takes into account the changes in flow speed across the whole glacier terminus and, in our opinion, this method is more representative for the changes in ice dynamics and ice discharge of a glacier system.

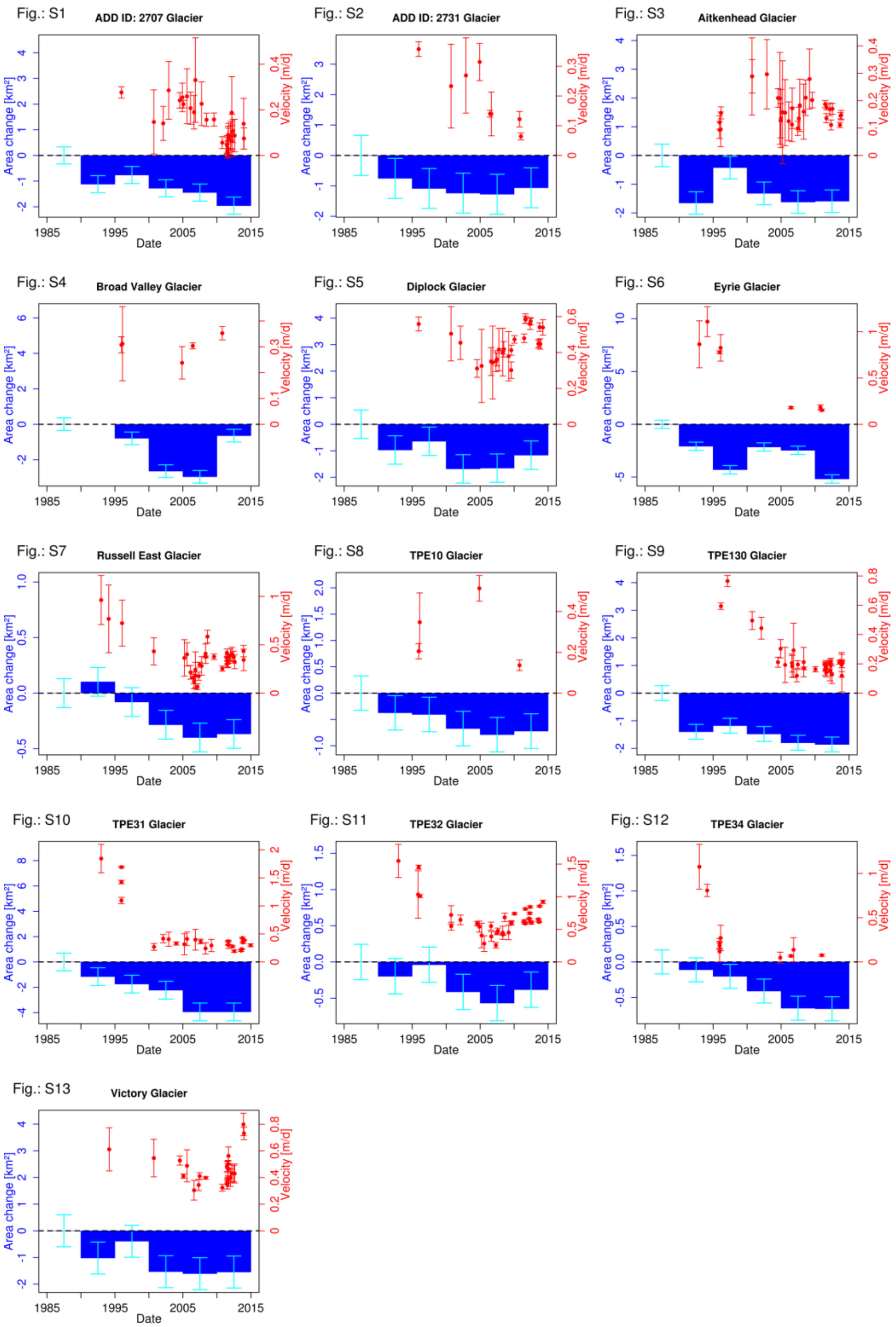


**Figure S1-S13.**~~:~~ Temporal ~~trend~~changes of surface velocity (median values of measurements along terminus profiles) (red) and area (blue) changes of glaciers in sector "East".

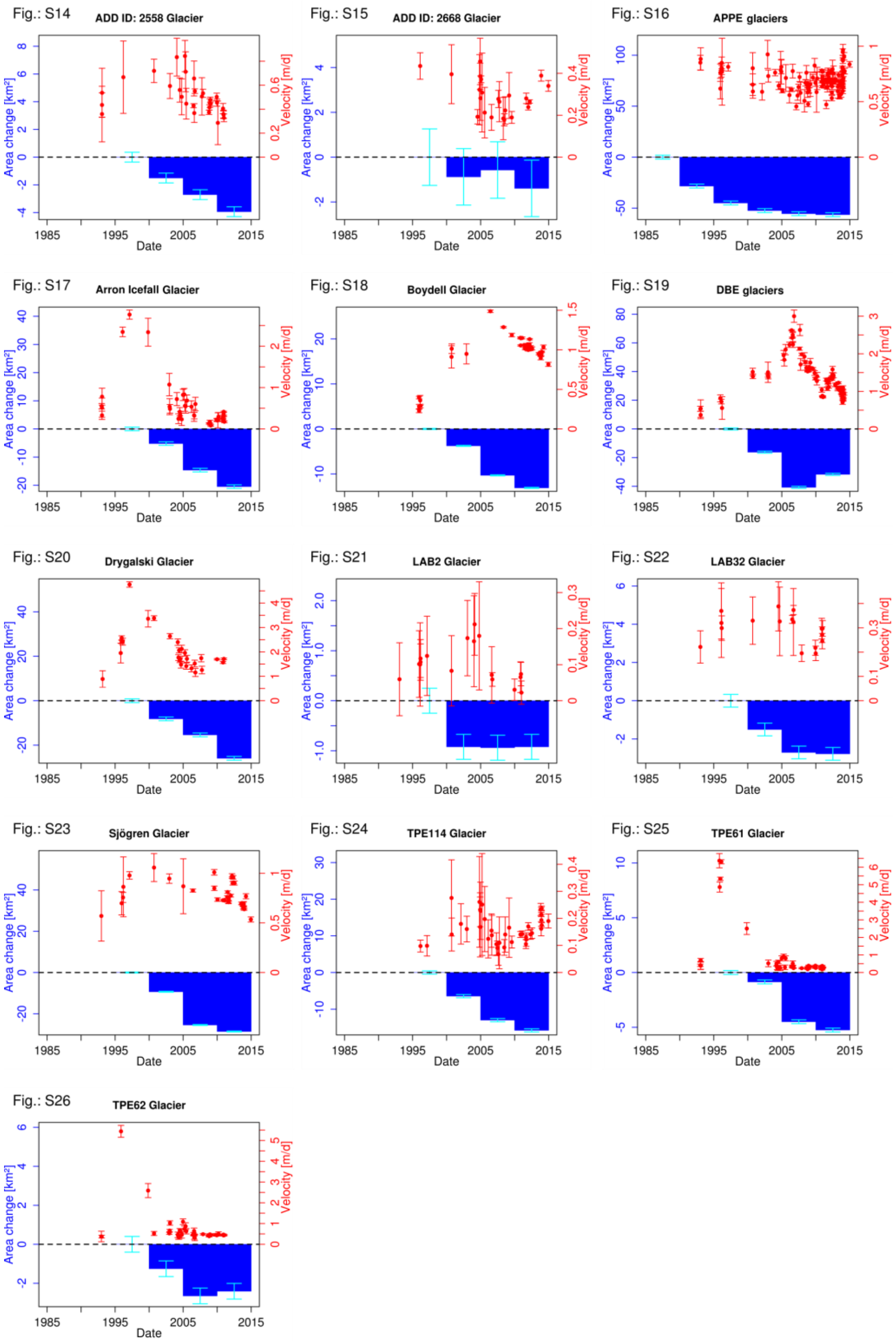


**Figure S14-S26.:** Temporal changes of surface velocity (median values of measurements along terminus profiles) (red) and area (blue) changes of glaciers in sector "East-Ice-Shelf".

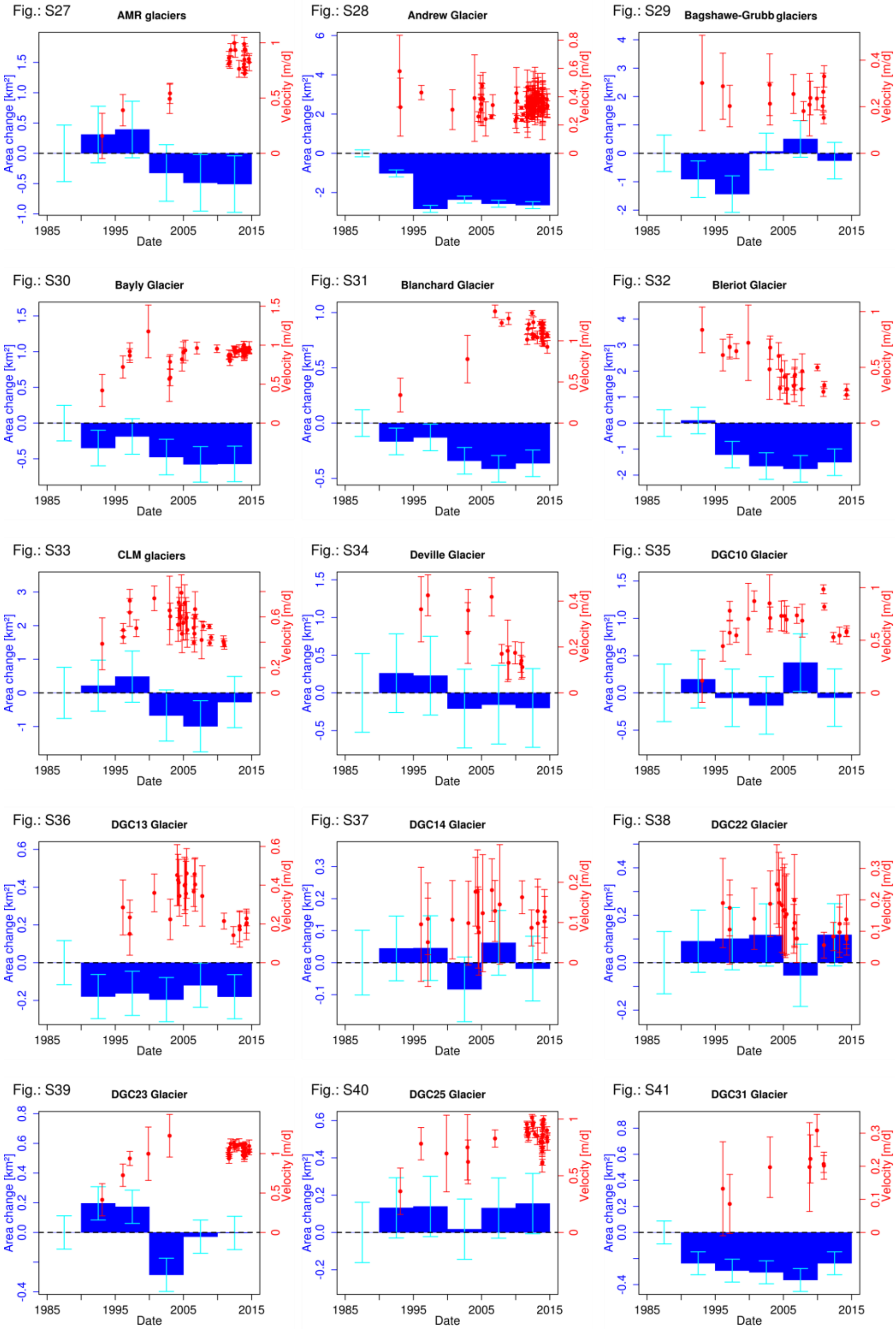


**Figure S27-S41.** Temporal changes of surface velocity (median values of measurements along terminus profiles) (red) and area (blue) changes of glaciers in sector "West".

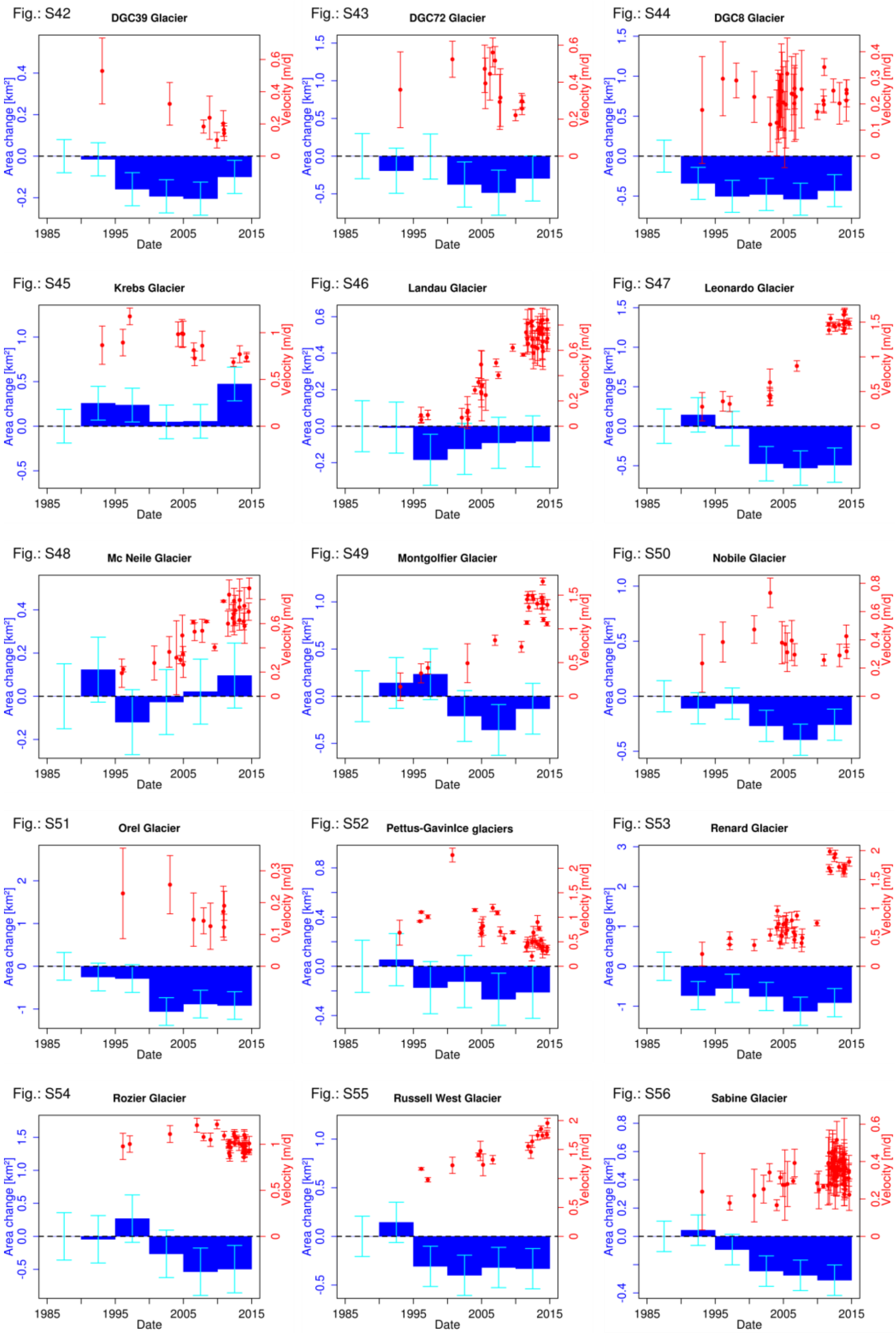


**Figure S42-S56.:** Temporal changes of surface velocity (median values of measurements along terminus profiles) (red) and area (blue) changes of glaciers in sector "West".

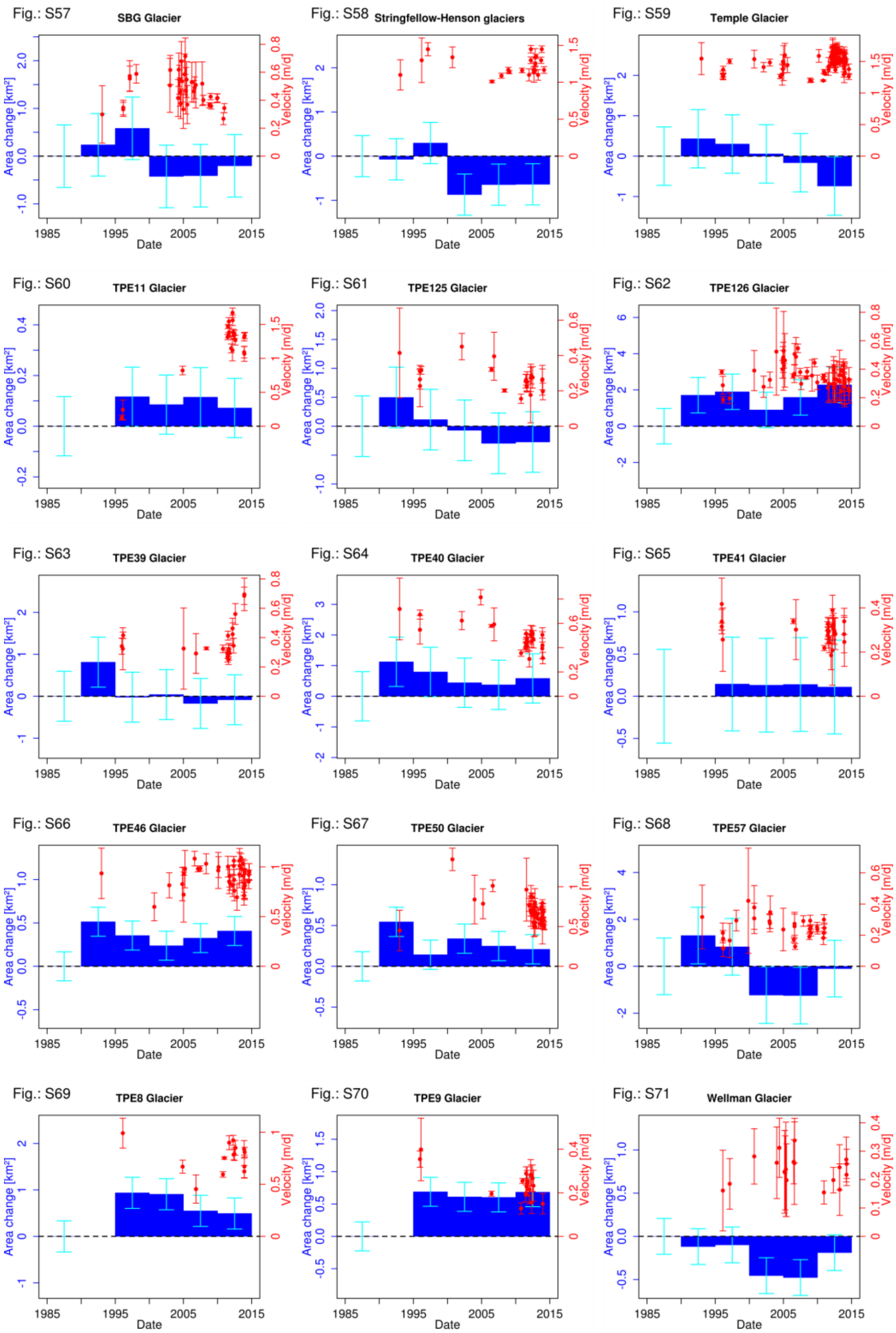


**Figure S57-S71.:** Temporal changes of surface velocity (median values of measurements along terminus profiles) (red) and area (blue) changes of glaciers in sector "West".

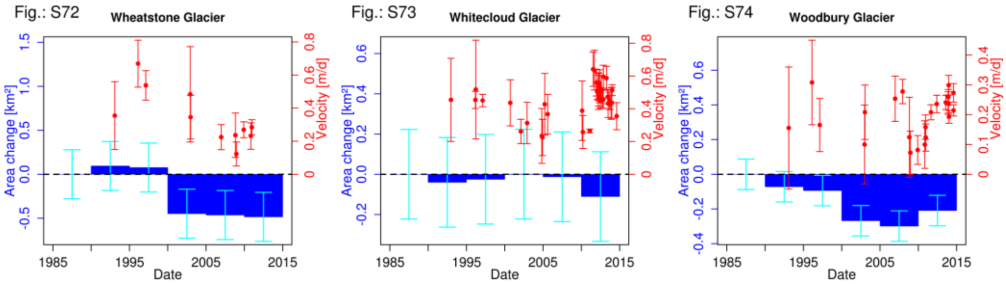


**Figure S72-S74.** Temporal changes of surface velocity (median values of measurements along terminus profiles) (red) and area (blue) changes of glaciers in sector "West".

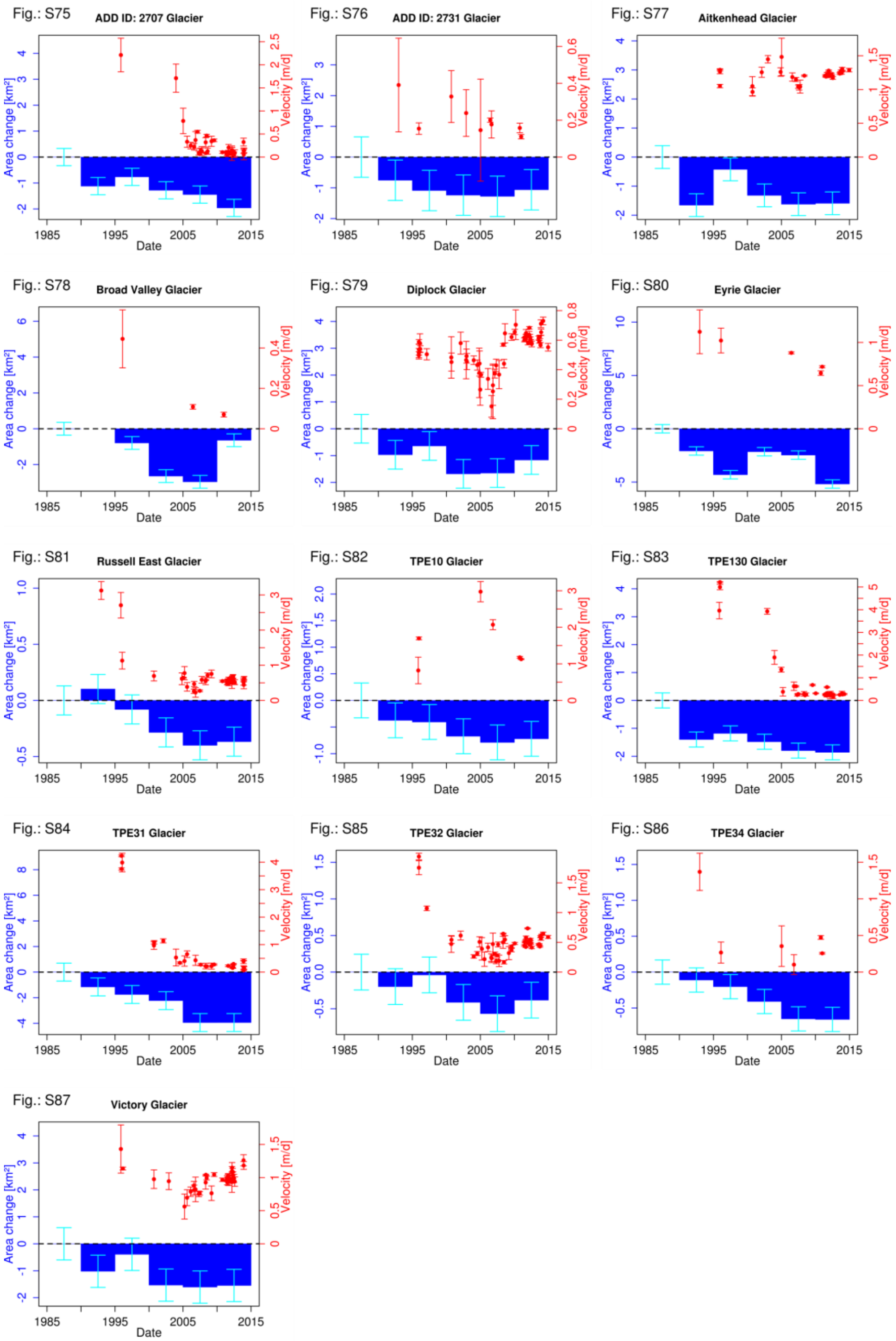


**Figure S75-S87.** Temporal trend of surface velocity measured at maximum ice thickness at terminus profiles (red) and area (blue) changes of glaciers in sector "East".

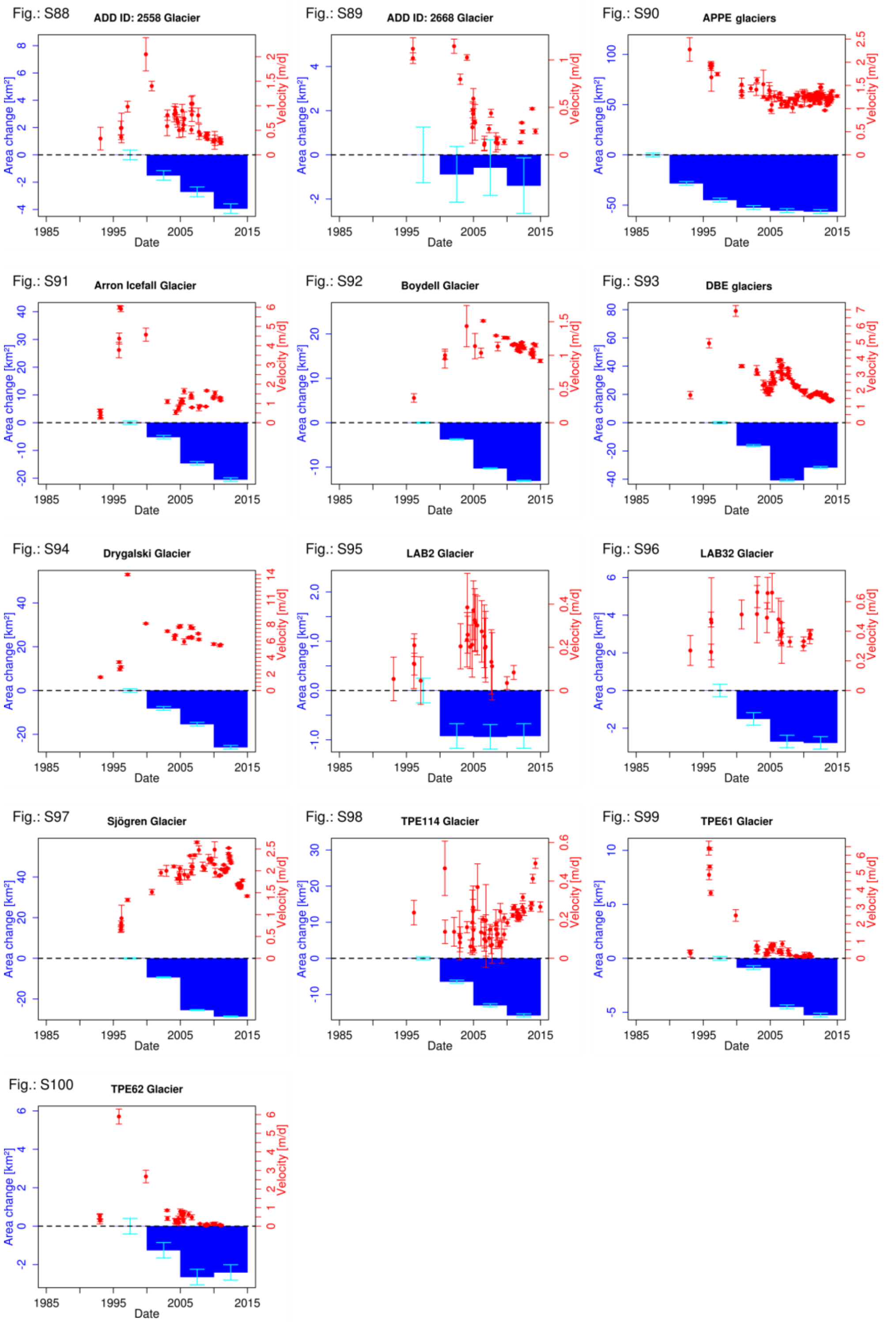


**Figure S88-S100.** Temporal trend of surface velocity measured at maximum ice thickness at terminus profiles (red) and area (blue) changes of glaciers in sector "EastIS".

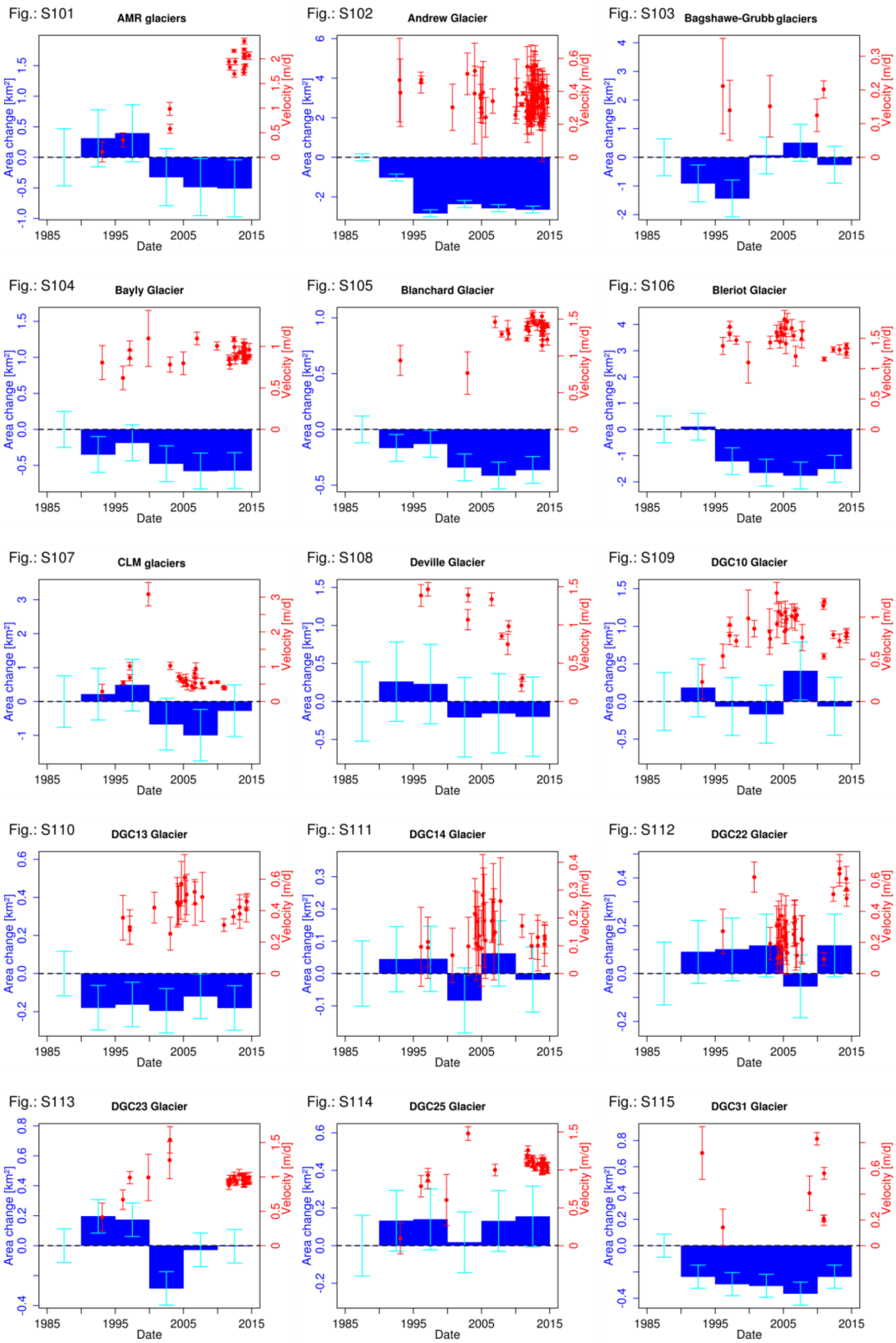


Figure S101-S115. Temporal trend of surface velocity measured at maximum ice thickness at terminus profiles (red) and area (blue) changes of glaciers in sector "West".

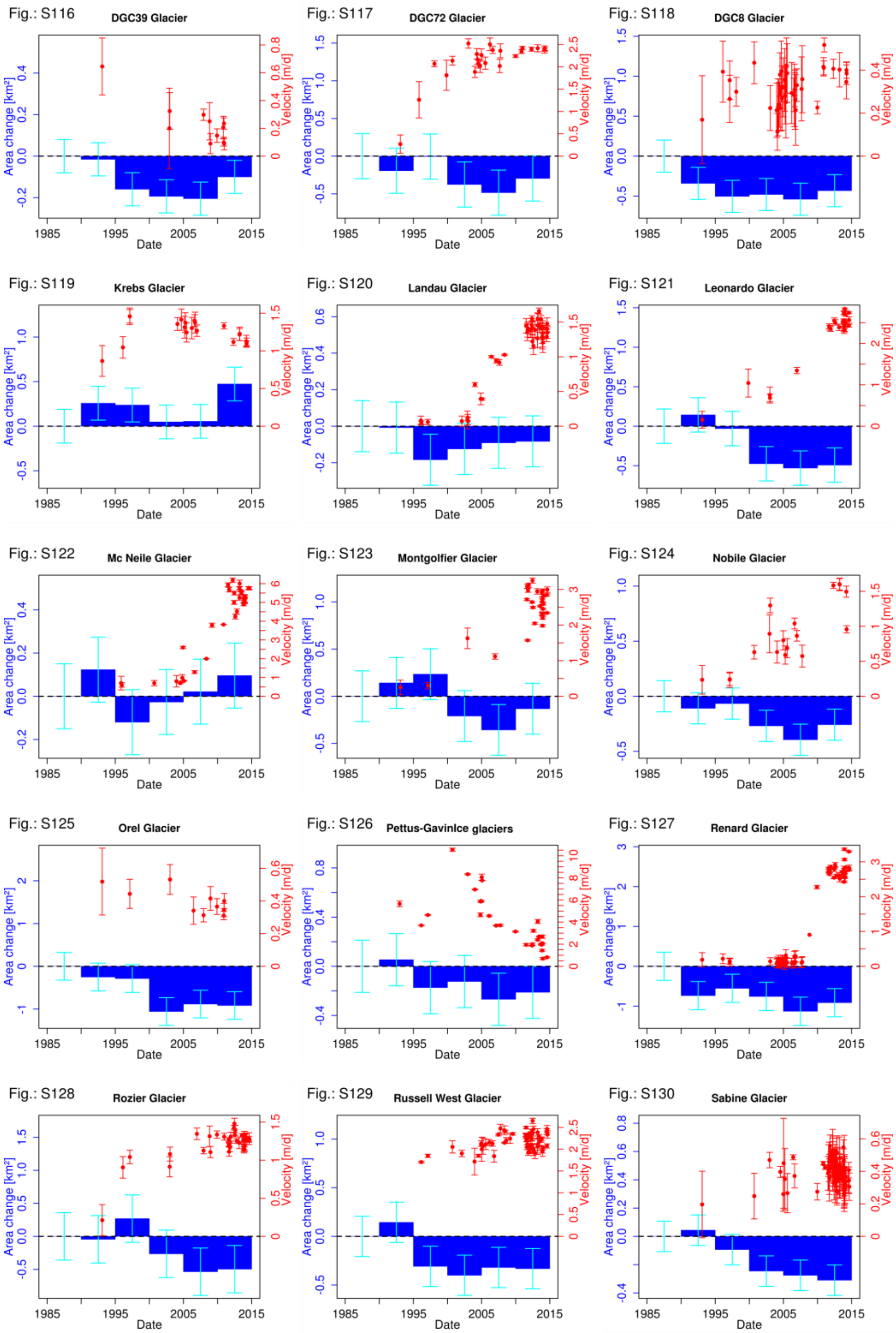


**Figure S116-S130.** Temporal trend of surface velocity measured at maximum ice thickness at terminus profiles (red) and area (blue) changes of glaciers in sector "West".

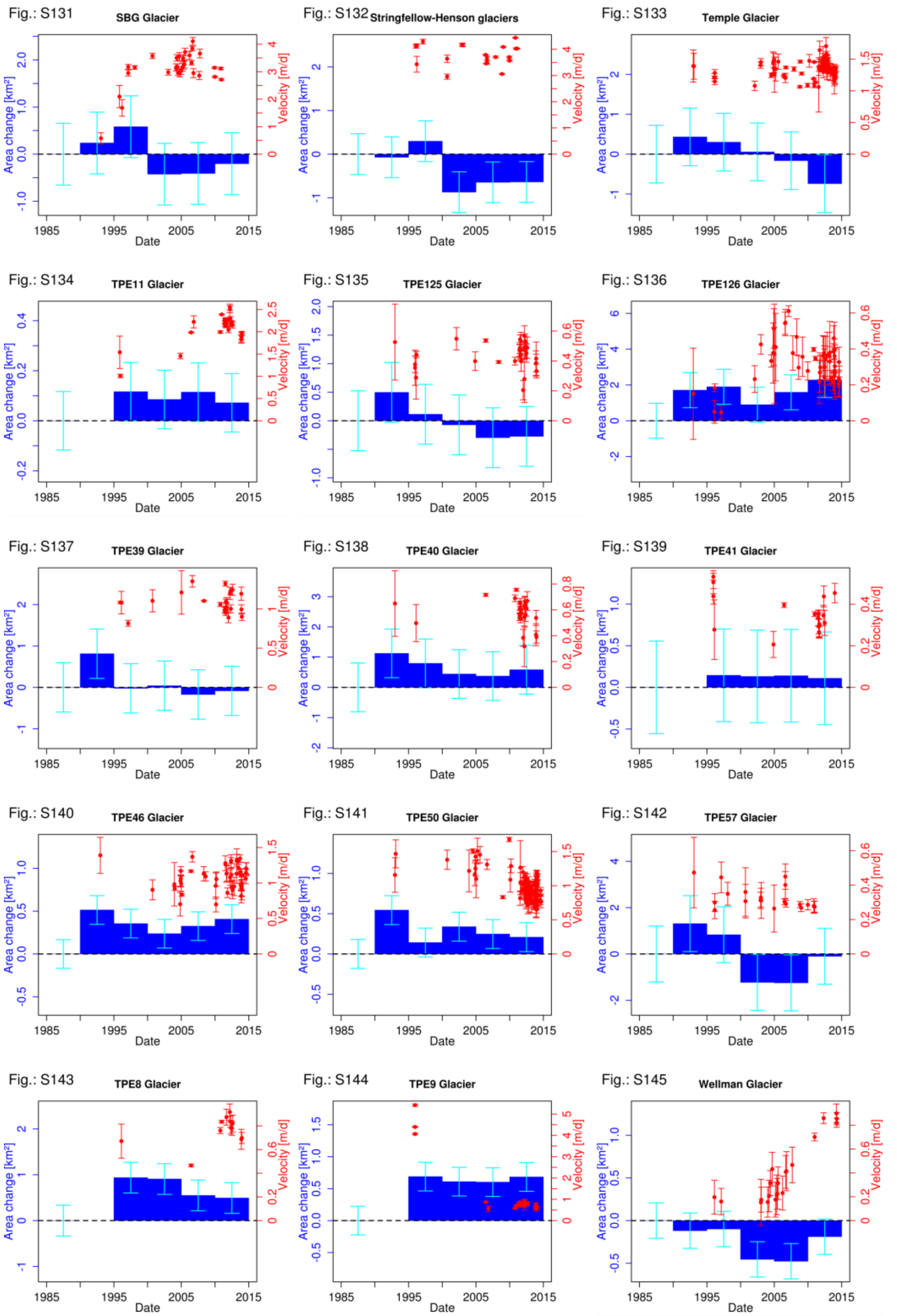


**Figure S131-S145.** Temporal trend of surface velocity measured at maximum ice thickness at terminus profiles (red) and area (blue) changes of glaciers in sector "West".

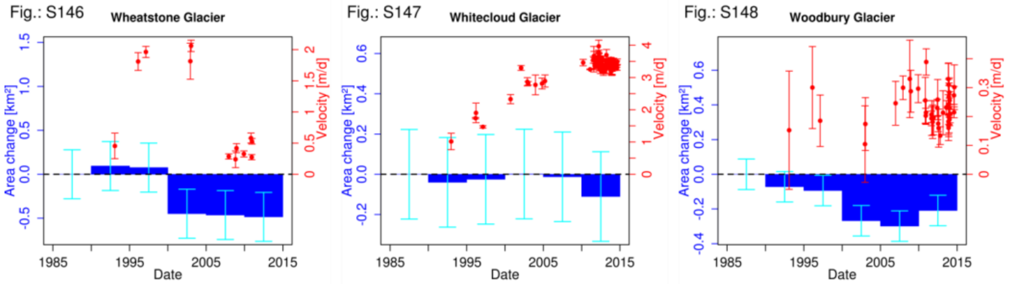


**Figure S146-S148.** Temporal trend of surface velocity measured at maximum ice thickness at terminus profiles (red) and area (blue) changes of glaciers in sector "West".

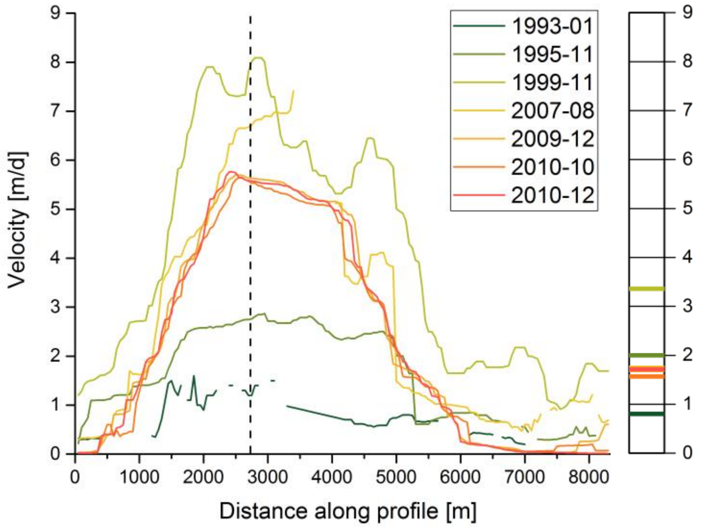


**Figure S149.~~75:~~** Surface velocity across the terminus of Drygalski Glacier (left) and median values of each profile (right). Dashed line: maximum ice thickness of across glacier profile

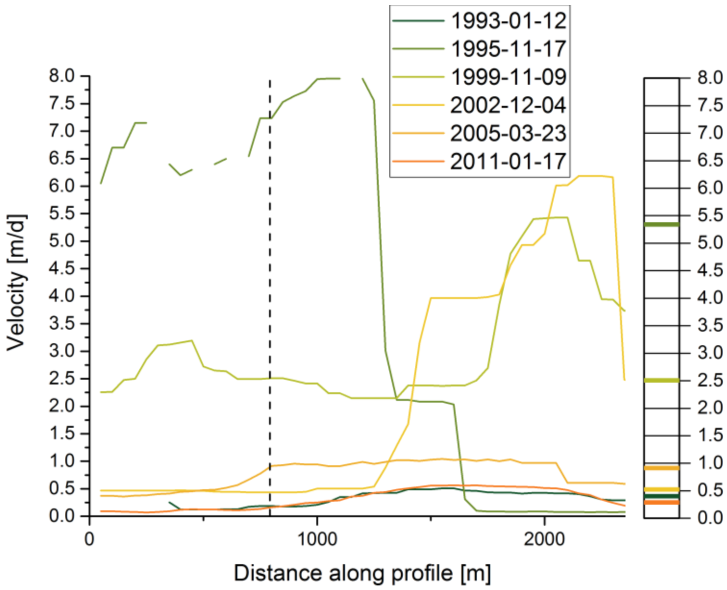


**Figure S150.** Surface velocity across the terminus of TPE61 Glacier (left) and median values of each profile (right). Dashed line: maximum ice thickness of across glacier profile

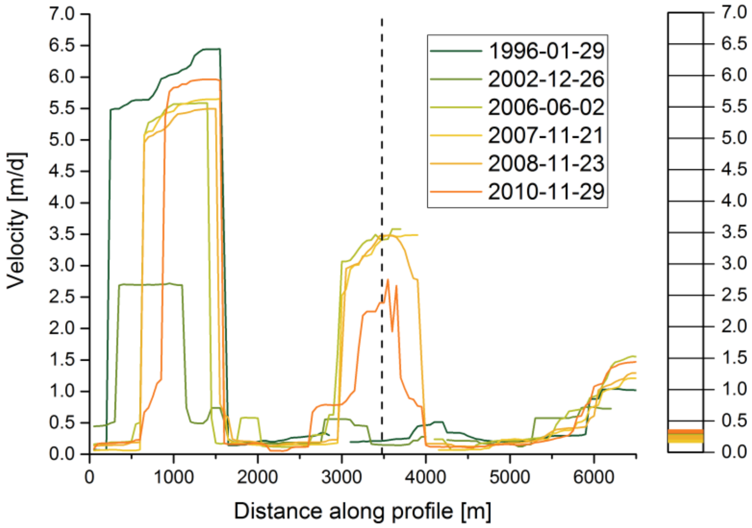


**Figure S151.** Surface velocity across the terminus of Bagshawe-Grubb glaciers (left) and median values of each profile (right). Dashed line: maximum ice thickness of across glacier profile

**Formatiert:** Block, Zeilenabstand: 1.5 Zeilen

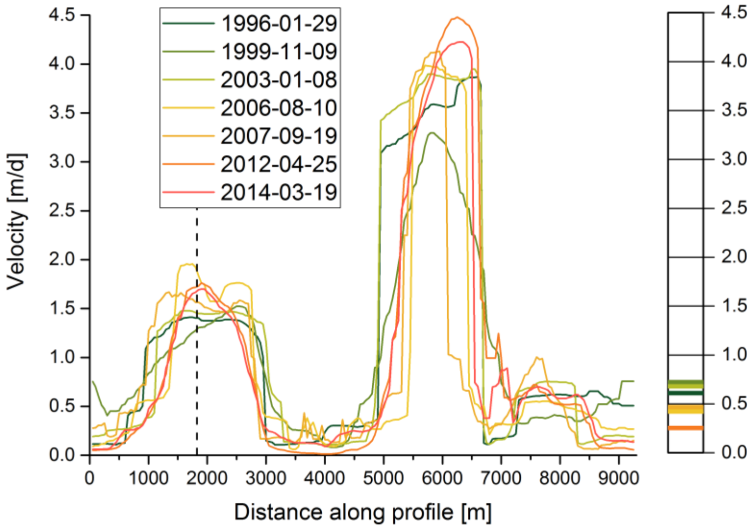


**Figure S152.** Surface velocity across the terminus of Bleriot Glacier (left) and median values of each profile (right). Dashed line: maximum ice thickness of across glacier profile

**Formatiert:** Block, Zeilenabstand: 1.5 Zeilen

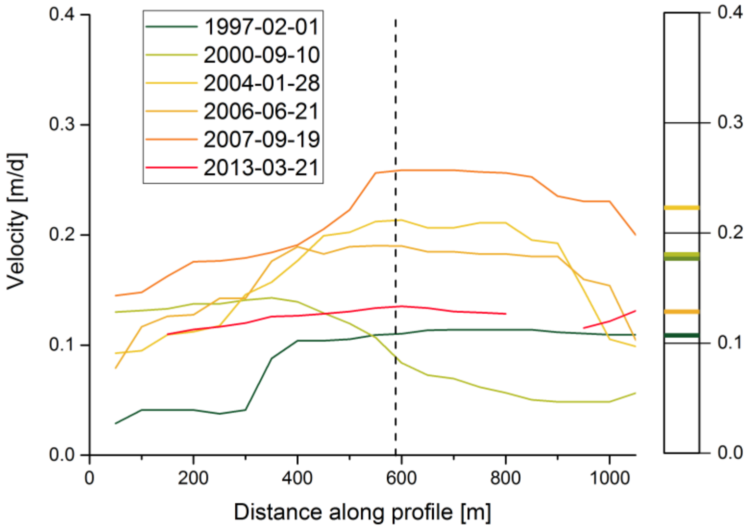


Figure S153. Surface velocity across the terminus of DGC14 Glacier (left) and median values of each profile (right). Dashed line: maximum ice thickness of across glacier profile

Formatiert: Block, Zeilenabstand: 1.5 Zeilen

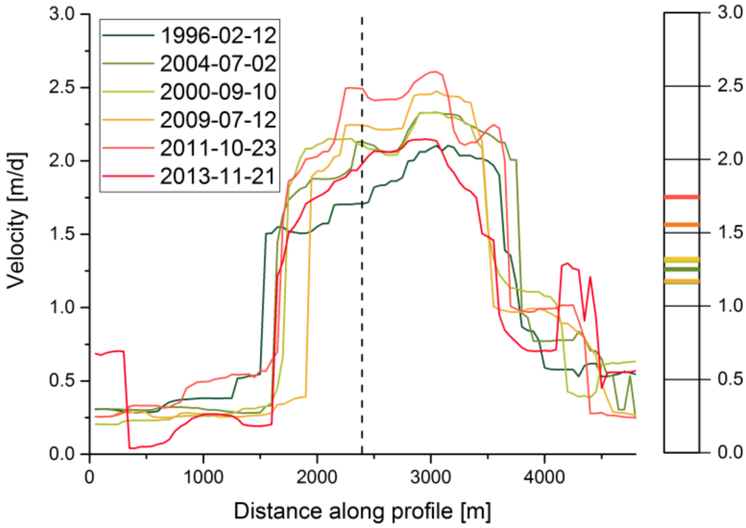


Figure S154. Surface velocity across the terminus of Russell West Glacier (left) and median values of each profile (right). Dashed line: maximum ice thickness of across glacier profile

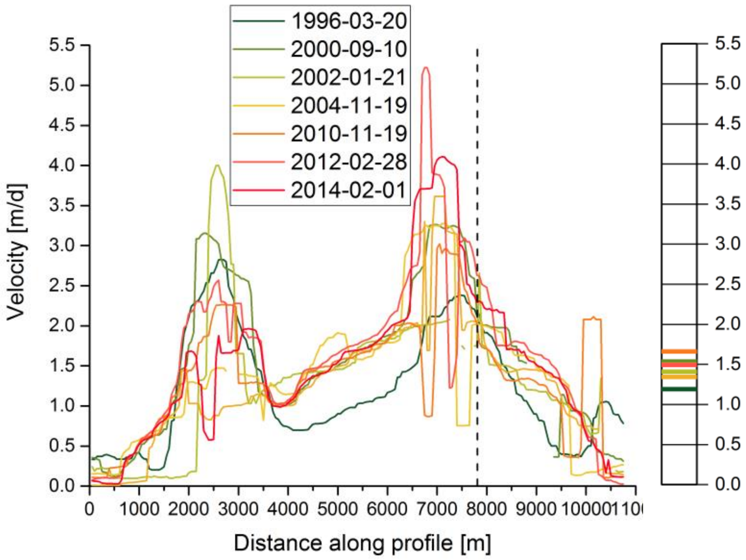


Figure S155. Surface velocity across the terminus of Temple Glacier (left) and median values of each profile (right). Dashed line: maximum ice thickness of across glacier profile

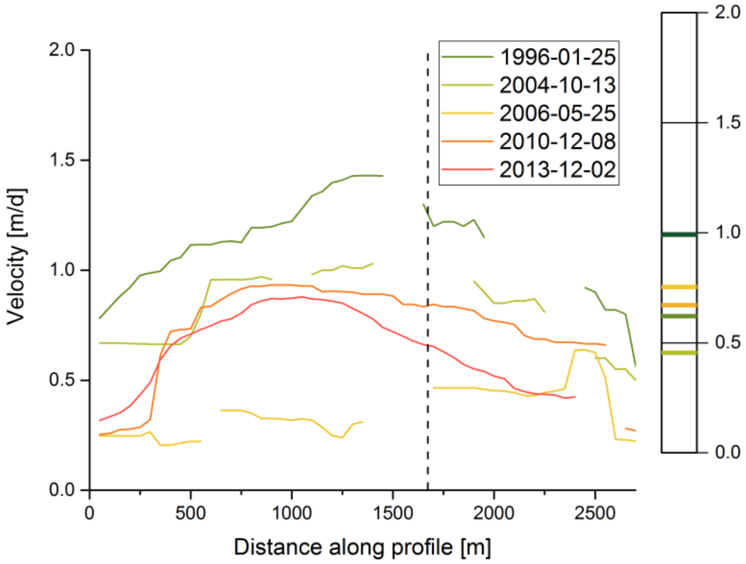


Figure S156. Surface velocity across the terminus of TPE8 Glacier (left) and median values of each profile (right). Dashed line: maximum ice thickness of across glacier profile

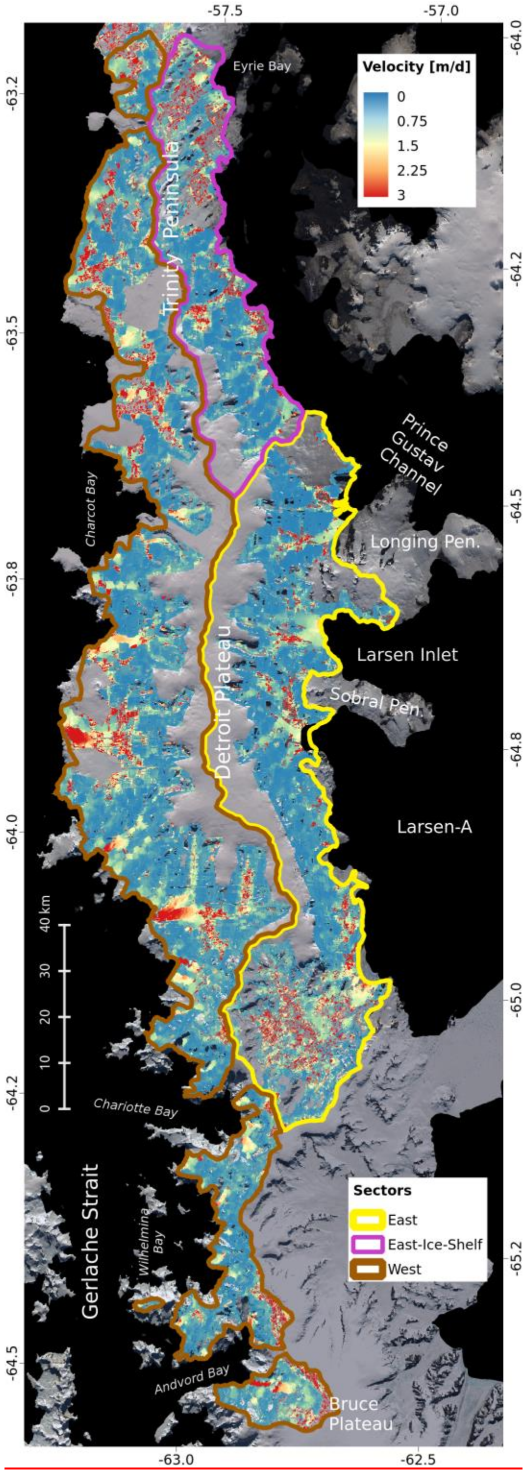


**Figure S157.** Surface velocity fields of outlet glaciers derived from multiple ERS SAR acquisitions (1996-1997). Background: Landsat LIMA Mosaic USGS, NASA, BAS, NSF. Note: Red speckle patterns indicate erroneous tracking results (noise).

**Formatiert:** Schriftart: 10 Pt.

**Formatiert:** Schriftart: 10 Pt., Nicht Fett

**Formatiert:** Schriftart: 10 Pt., Nicht Fett

**Formatiert:** Schriftart: (Standard) Arial, 10 Pt.

**Formatiert:** Schriftart: (Standard) Arial, 10 Pt.

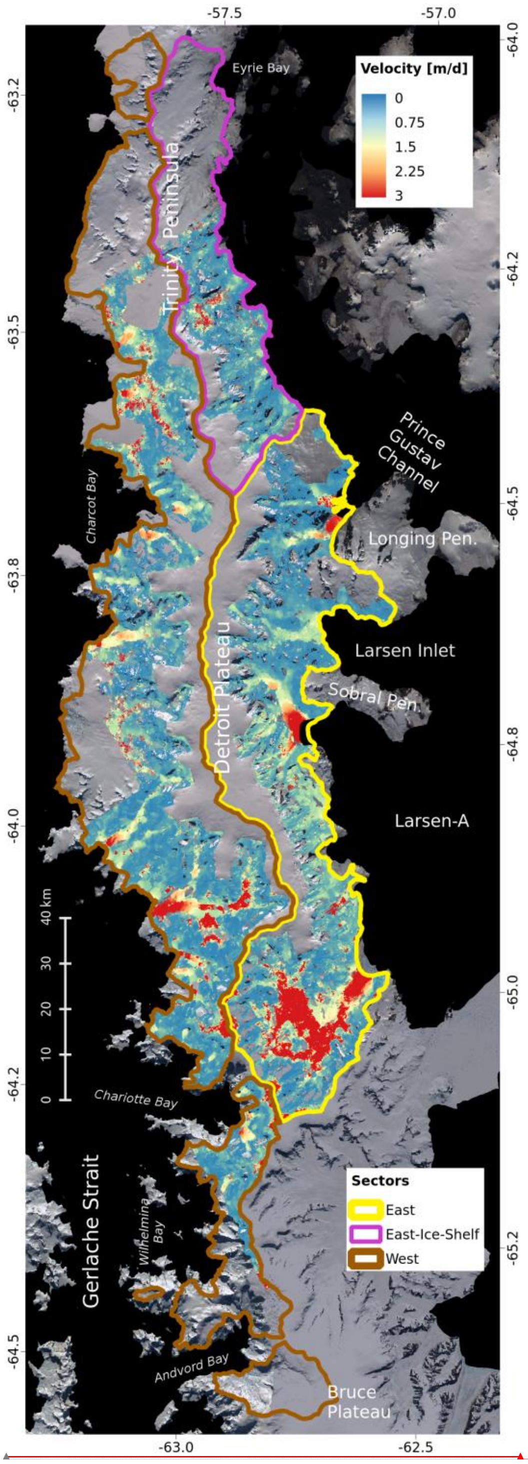


**Figure S158.** Surface velocity fields of outlet glaciers derived from multiple ENVISAT SAR acquisitions (2005-2006). Background: Landsat LIMA Mosaic USGS, NASA, BAS, NSF. Note: Red speckle patterns indicate erroneous tracking results (noise).

**Formatiert:** Schriftart: (Standard) Times New Roman

**Formatiert:** Standard

**Formatiert:** Schriftart: (Standard) Times New Roman

**Formatiert:** Schriftart: 10 Pt.

**Formatiert:** Schriftart: 10 Pt., Nicht Fett

**Formatiert:** Schriftart: 10 Pt., Nicht Fett

**Formatiert:** Schriftart: 10 Pt., Nicht Fett

**Formatiert:** Schriftart: 10 Pt., Nicht Fett

**Formatiert:** Schriftart: (Standard) Arial, 10 Pt.

**Formatiert:** Schriftart: (Standard) Arial, 10 Pt., Unterschneidung ab 1.5 Pt.

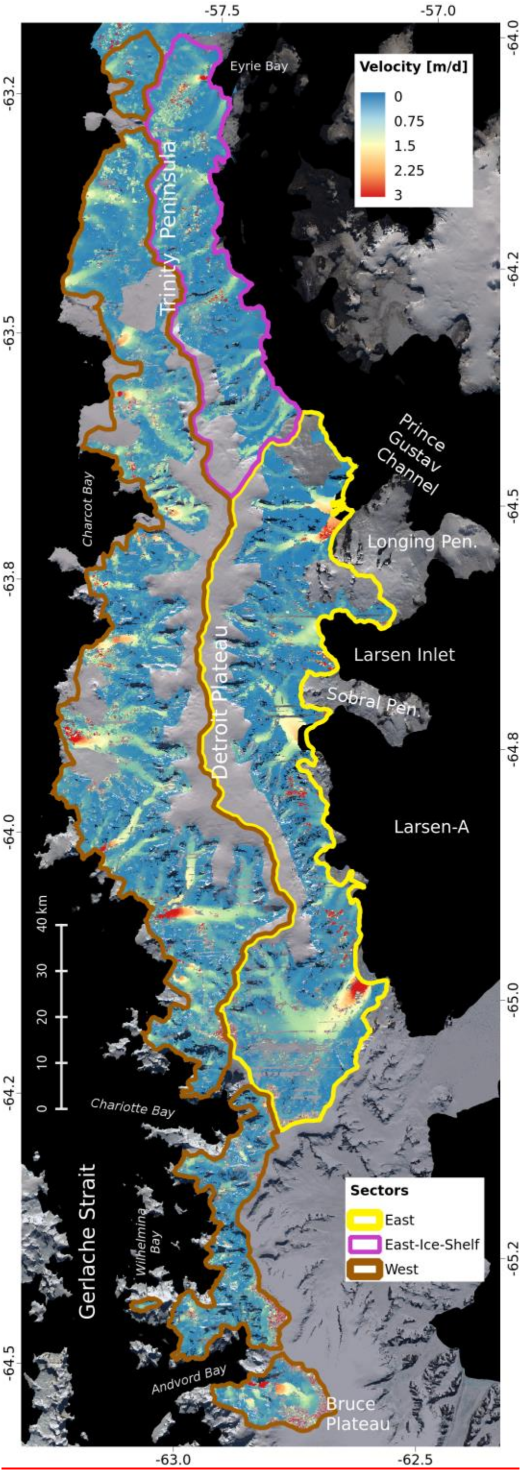


**Figure S159.** Surface velocity fields of outlet glaciers derived from multiple ALOS PALSAR acquisitions (2008-2010). Background: Landsat LIMA Mosaic USGS, NASA, BAS, NSF. Note: Red speckle patterns indicate erroneous tracking results (noise).

Formatiert: Schriftart: 10 Pt.

Formatiert: Schriftart: 10 Pt., Nicht Fett

Formatiert: Schriftart: 10 Pt., Nicht Fett

Formatiert: Schriftart: 10 Pt., Nicht Fett

Formatiert: Schriftart: 10 Pt., Nicht Fett

Formatiert: Schriftart: (Standard) Arial, 10 Pt.

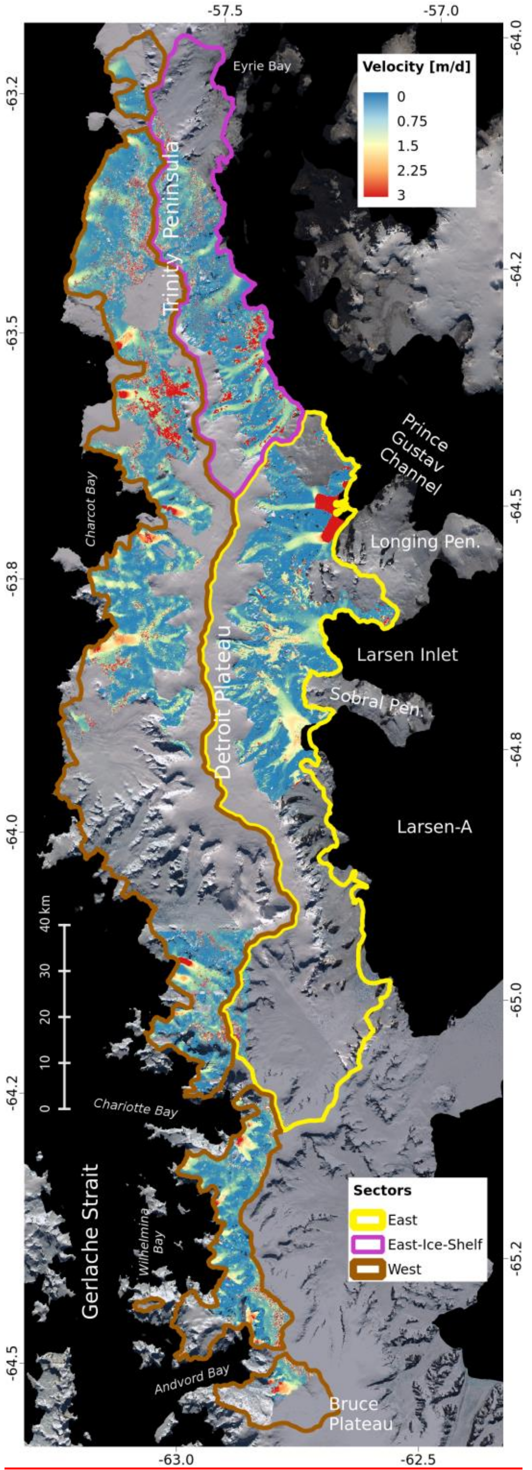


**Figure S160.** Surface velocity fields of outlet glaciers derived from multiple TerraSAR/TanDEM-X SAR acquisitions (2011-2012). Background: Landsat LIMA Mosaic USGS, NASA, BAS, NSF. Note: Red speckle patterns indicate erroneous tracking results (noise).

**Formatiert:** Schriftart: (Standard) Arial, 10 Pt.

**Formatiert:** Schriftart: (Standard) Arial, 10 Pt., Nicht Fett

**Formatiert:** Schriftart: (Standard) Arial, 10 Pt., Nicht Fett

**Formatiert:** Schriftart: (Standard) Arial, 10 Pt., Nicht Fett

**Formatiert:** Schriftart: (Standard) Arial, 10 Pt., Nicht Fett

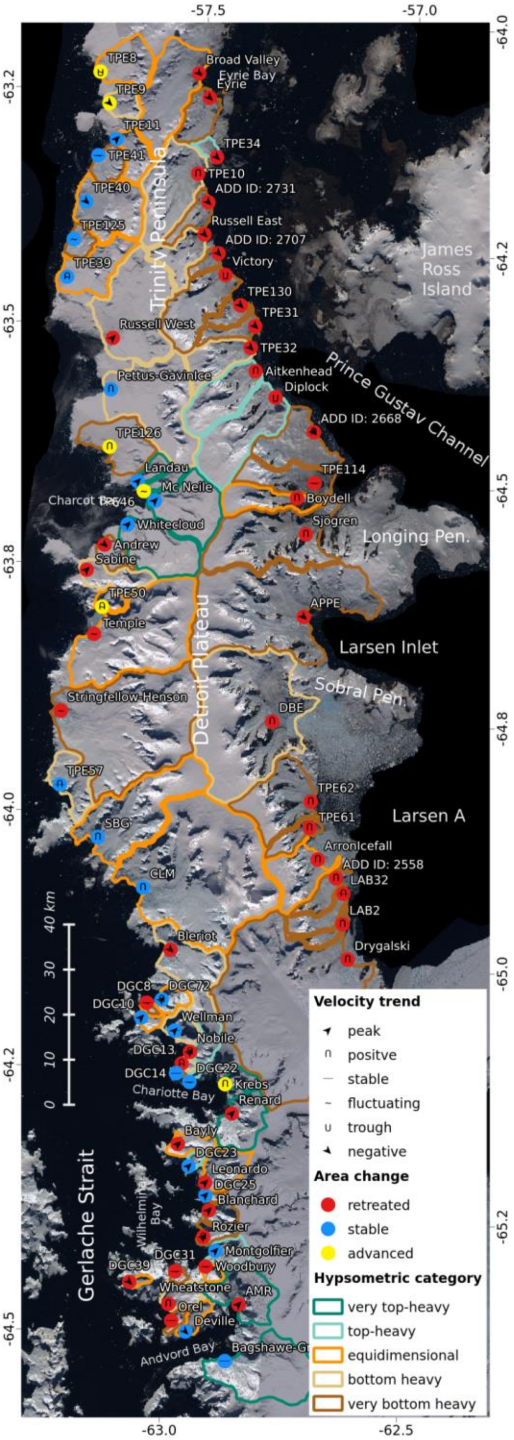


**Figure S161.** Categorizations of glaciers based on the temporal variations of area changes (dots) and flow velocities measured at the maximum ice thickness at the terminus profiles (symbols). Colors of catchment delineation indicate Hypsometric categories according to Jiskoot et al. (2009). Background: Landsat LIMA Mosaic USGS, NASA, BAS, NSF

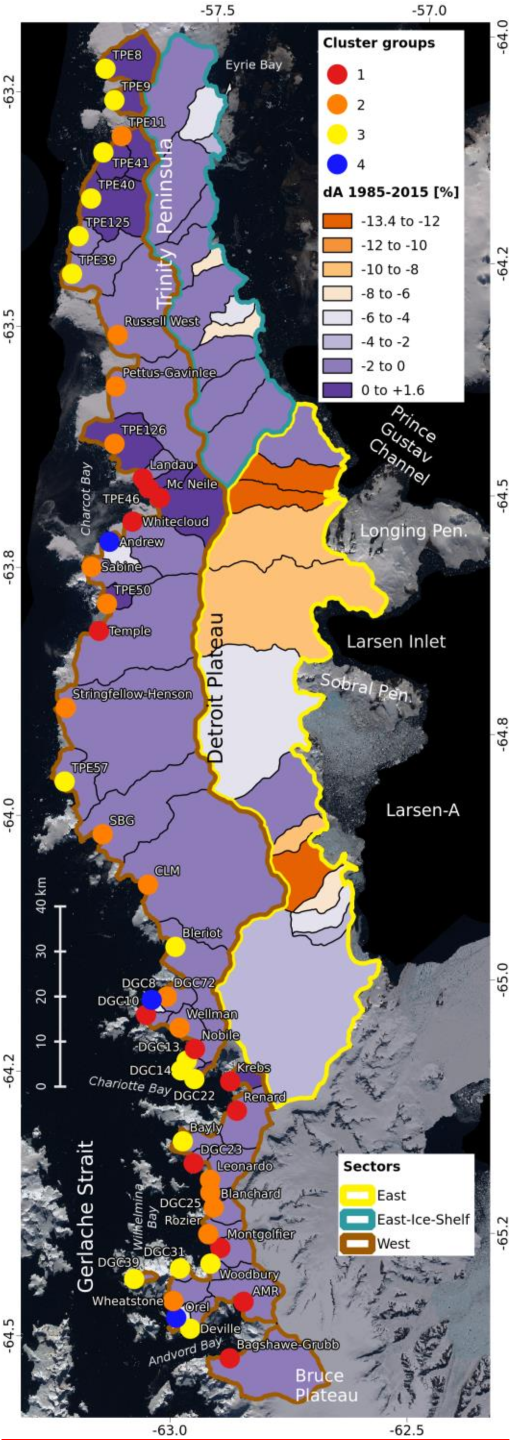


**Figure S162.** Spatial distribution of glacier types along the west coast (based on velocity measurements at the maximum ice thickness at the terminus profiles). Glaciers are group based on a hierarchical cluster analysis (dots). Individual glacier catchment colors: relative area change in the period 1985-2015. Colored polygon outlines: Boundaries of the three sectors. Background: Landsat LIMA Mosaic USGS, NASA, BAS, NSF



**Formatiert:** Zeilenabstand: 1.5 Zeilen

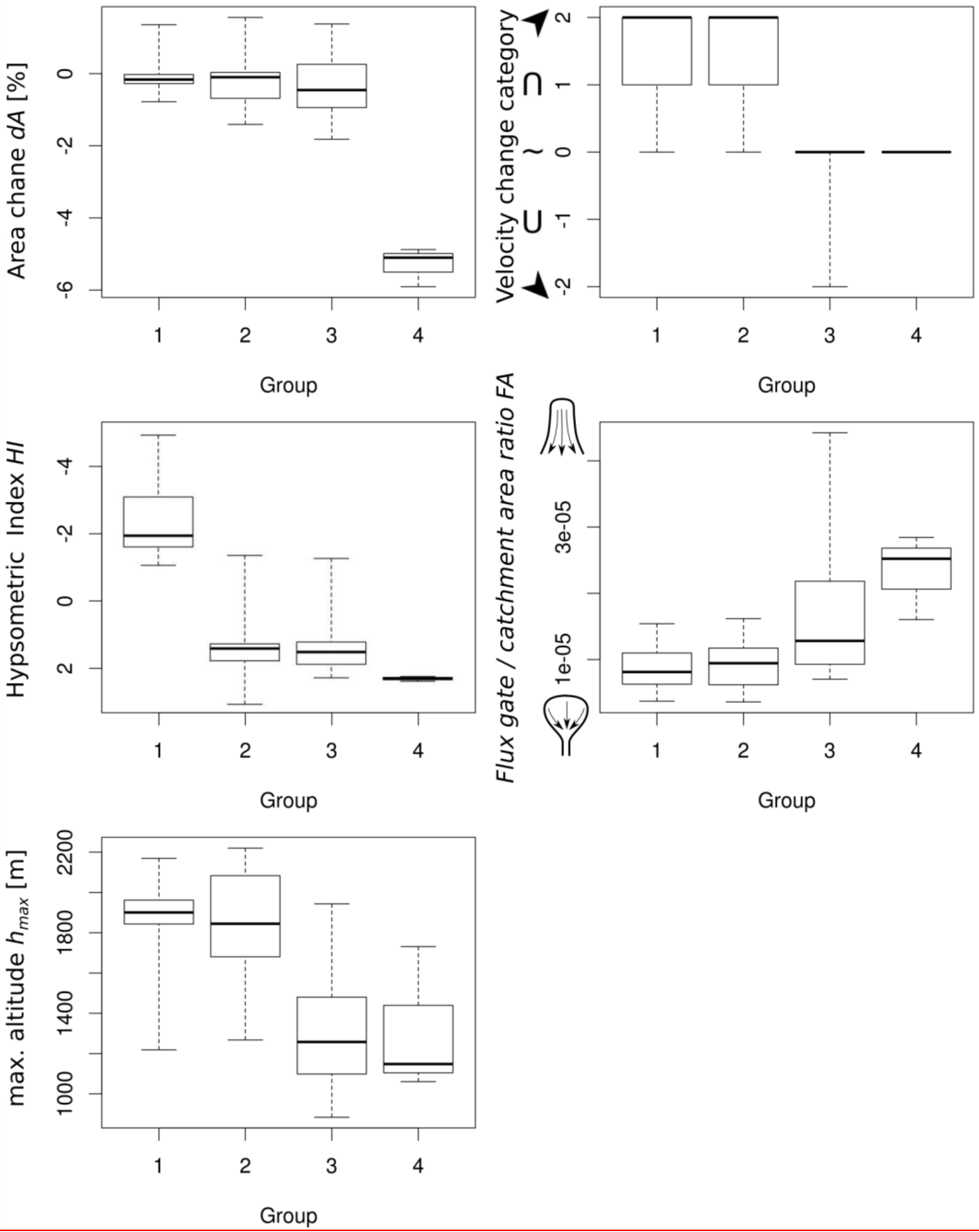


**Figure S163.** Boxplots of cluster analysis input variables (Sector "West") for each group. Whiskers extend to the most extreme data points. Velocities were measured at the maximum ice thickness at the terminus profiles.

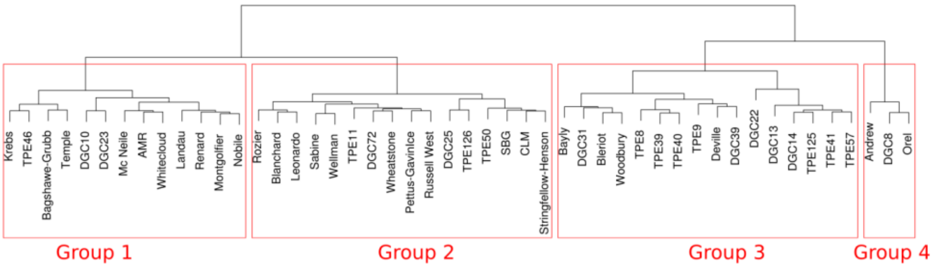


**Figure S164.** Dendrogram of hierarchical cluster analysis of glaciers in sector "West" coast (based on velocity measurements at the maximum ice thickness at the terminus profiles). The glaciers are assorted in four groups (red rectangles). See also Section 5.3.

**Formatiert:** Schriftart: (Standard) Arial

**Formatiert:** Zeilenabstand:  1.5 Zeilen

**Table S1:** Observed parameters of the individual glaciers (median velocities measured along terminus profiles). Table continues on next page.

| Sector | Basin | $l_t$ [m] | $A_{1985-1990}$ [km²] | $A_{2010-2015}$ [km²] | $dA$ [km²] | Area change category | Date $v_S$ [yyyy-mm-dd] | Date $v_E$ [yyyy-mm-dd] | $dt$ [a] | $v_S$ [m d$^{-1}$] | $v_E$ [m d$^{-1}$] | $dv$ [m d$^{-1}$] | $dv$ [%] | $n_v$ | Vel. change category | $h_{max}$ [m a.s.l.] | $HI$ | Hypsometric category | $FA$ | Group |
|---|---|---|---|---|---|---|---|---|---|---|---|---|---|---|---|---|---|---|---|---|
| East | ADD ID: 2707 | 5535 | 28.78 | 26.82 | -1.96 | retreated | 1995-12-18 | 2013-12-24 | 18.03 | 0.276 | 0.107 | -0.170 | -61.375 | 31 | decreased | 1278 | 5.14 | very bottom-heavy | 0.0056 | |
| | ADD ID: 2731 | 10955 | 56.92 | 55.85 | -1.06 | retreated | 1995-12-18 | 2010-12-31 | 15.05 | 0.358 | 0.093 | -0.265 | -73.985 | 8 | decreased | 1327 | 2.93 | very bottom-heavy | 0.0055 | |
| | Aitkenhead | 6532 | 156.70 | 155.11 | -1.59 | retreated | 1995-12-18 | 2013-11-04 | 17.89 | 0.108 | 0.145 | 0.037 | 34.679 | 32 | peak | 1746 | -1.23 | top-heavy | 0.0024 | |
| | Broad Valley | 5948 | 246.73 | 246.08 | -0.64 | retreated | 1995-12-18 | 2010-10-17 | 14.84 | 0.310 | 0.353 | 0.043 | 13.815 | 5 | stable | 1118 | -1.02 | equidimensional | 0.0005 | |
| | Diplock | 8916 | 235.30 | 234.14 | -1.16 | retreated | 1995-12-18 | 2014-03-27 | 18.28 | 0.559 | 0.449 | -0.110 | -19.743 | 27 | trough | 1845 | -1.44 | top-heavy | 0.0017 | |
| | Eyrie | 6570 | 89.53 | 84.35 | -5.18 | retreated | 1992-12-25 | 2010-12-31 | 18.03 | 0.865 | 0.169 | -0.696 | -80.499 | 7 | decreased | 1076 | 2.39 | very bottom-heavy | 0.0035 | |
| | Russell East | 2156 | 93.75 | 93.38 | -0.37 | retreated | 1992-12-25 | 2013-12-07 | 20.96 | 0.963 | 0.389 | -0.573 | -59.559 | 34 | decreased | 1370 | 1.48 | bottom-heavy | 0.0035 | |
| | TPE10 | 5465 | 225.96 | 225.24 | -0.72 | retreated | 1995-12-20 | 2010-10-17 | 14.84 | 0.277 | 0.137 | -0.140 | -50.635 | 4 | peak | 1386 | 1.43 | bottom-heavy | 0.0033 | |
| | TPE130 | 4493 | 40.58 | 38.72 | -1.86 | retreated | 1996-02-29 | 2013-12-24 | 17.83 | 0.680 | 0.201 | -0.479 | -70.498 | 33 | peak | 983 | 2.07 | very bottom-heavy | 0.0076 | |
| | TPE31 | 11684 | 52.70 | 48.76 | -3.94 | retreated | 1992-12-25 | 2014-12-16 | 21.99 | 1.844 | 0.344 | -1.500 | -81.352 | 25 | decreased | 1490 | 3.50 | very bottom-heavy | 0.0076 | |
| | TPE32 | 4071 | 108.63 | 108.24 | -0.38 | retreated | 1992-12-25 | 2014-03-27 | 21.27 | 1.549 | 0.755 | -0.794 | -51.271 | 36 | decreased | 1646 | 1.46 | bottom-heavy | 0.0037 | |
| | TPE34 | 2814 | 22.91 | 22.25 | -0.66 | retreated | 1992-12-25 | 2010-12-31 | 18.03 | 1.076 | 0.076 | -1.000 | -92.937 | 10 | decreased | 500 | -1.37 | top-heavy | 0.0023 | |
| | Victory | 9975 | 180.30 | 178.75 | -1.55 | retreated | 1994-02-28 | 2013-12-24 | 19.83 | 0.612 | 0.765 | 0.153 | 25.078 | 25 | trough | 1645 | 2.11 | very bottom-heavy | 0.0041 | |
| Summary | mean | | | | | | | | 18.22 | 0.729 | 0.306 | -0.423 | -57.983 | | | 1339 | | | | |
| East | sum | 85114 | 1538.78 | 1517.71 | -21.07 | | | | | | | | | 277 | | | | | | |
| East-Ice-Shelf | ADD ID: 2558 | 5890 | 60.2433 | 56.31 | -3.94 | retreated | 1993-01-29 | 2010-12-29 | 17.93 | 0.435 | 0.353 | -0.082 | -18.758 | 30 | peak | 1840 | 9.08 | very bottom-heavy | 0.0067 | |
| | ADD ID: 2668 | 20996 | 162.324 | 160.93 | -1.39 | retreated | 1996-02-13 | 2014-12-16 | 18.85 | 0.435 | 0.340 | -0.095 | -21.821 | 23 | peak | 1342 | 2.88 | very bottom-heavy | 0.0041 | |
| | APPE | 31872 | 696.24 | 639.85 | -56.39 | retreated | 1993-01-12 | 2014-12-16 | 21.94 | 0.869 | 0.853 | -0.015 | -1.766 | 114 | fluctuating | 1964 | 1.82 | very bottom-heavy | 0.0003 | |
| | Arron Icefall | 10557 | 152.356 | 131.88 | -20.48 | retreated | 1993-01-12 | 2011-01-22 | 18.04 | 0.532 | 0.288 | -0.244 | -45.793 | 39 | peak | 1979 | -1.08 | equidimensional | 0.0061 | |
| | Boydell | 1954 | 108.039 | 94.95 | -13.09 | retreated | 1995-12-18 | 2014-12-16 | 19.01 | 0.290 | 0.975 | 0.685 | 236.007 | 37 | peak | 1842 | -1.07 | equidimensional | 0.0009 | |
| | DBE | 12140 | 658.91 | 627.24 | -31.67 | retreated | 1993-01-12 | 2014-02-27 | 21.14 | 0.535 | 0.950 | 0.415 | 77.569 | 85 | peak | 2167 | 1.37 | bottom-heavy | 0.0011 | |
| | Drygalski | 14018 | 990.41 | 964.49 | -25.92 | retreated | 1993-01-29 | 2010-12-29 | 17.93 | 0.951 | 1.641 | 0.219 | 72.572 | 29 | peak | 2043 | 1.60 | very bottom-heavy | 0.0003 | |
| | LAB2 | 4157 | 38.3889 | 37.47 | -0.92 | retreated | 1993-01-29 | 2010-12-29 | 17.93 | 0.060 | 0.065 | 0.006 | 9.726 | 17 | peak | 1779 | 3.76 | very bottom-heavy | 0.0046 | |
| | LAB32 | 5534 | 66.3816 | 63.60 | -2.78 | retreated | 1993-01-12 | 2010-12-29 | 17.97 | 0.221 | 0.284 | 0.063 | 28.300 | 17 | stable | 1841 | 3.21 | very bottom-heavy | 0.0046 | |
| | Sjögren | 3838 | 329.298 | 300.73 | -28.57 | retreated | 1992-12-25 | 2014-12-16 | 21.99 | 0.570 | 0.638 | 0.068 | 11.897 | 36 | peak | 1926 | 1.97 | very bottom-heavy | 0.0014 | |
| | TPE114 | 7310 | 126.385 | 110.61 | -15.78 | retreated | 1996-02-29 | 2014-12-16 | 18.81 | 0.098 | 0.190 | 0.092 | 93.627 | 39 | stable | 1759 | 2.96 | very bottom-heavy | 0.0014 | |
| | TPE61 | 2943 | 54.3413 | 49.09 | -5.25 | retreated | 1993-01-12 | 2011-01-22 | 18.04 | 0.406 | 0.276 | -0.130 | -31.942 | 42 | peak | 1981 | 2.78 | very bottom-heavy | 0.0022 | |
| | TPE62 | 6700 | 211.811 | 209.40 | -2.41 | retreated | 1992-12-25 | 2011-01-22 | 18.09 | 0.372 | 0.448 | 0.076 | 20.424 | 42 | peak | 2118 | 2.43 | very bottom-heavy | 0.0013 | |
| Summary | mean | | | | | | | | 19.05 | 0.444 | 0.562 | 0.118 | 26.480 | | | 1891 | | | | |
| East-Ice-Shelf | sum | 127909 | 3655.13 | 3446.54 | -208.59 | | | | | | | | | 550 | | | | | | |
| West | AMR | 7773 | 137.24 | 136.73 | -0.51 | retreated | 1993-02-01 | 2014-08-22 | 21.57 | 0.157 | 0.837 | 0.679 | 431.515 | 21 | increased | 1884 | -3.82 | very top-heavy | 0.0021 | 1 |
| | Andrew | 2951 | 47.05 | 44.41 | -2.64 | retreated | 1992-12-25 | 2014-08-27 | 21.68 | 0.453 | 0.358 | -0.095 | -21.030 | 107 | decreased | 1731 | 1.99 | very bottom-heavy | 0.0057 | 4 |
| | Bagshawe-Grubb | 10720 | 280.43 | 280.17 | -0.26 | stable | 1993-02-01 | 2010-12-22 | 17.90 | 0.302 | 0.233 | -0.069 | -22.782 | 14 | stable | 2169 | -2.88 | very top-heavy | 0.0019 | 1 |
| | Bayly | 4149 | 47.89 | 47.32 | -0.57 | retreated | 1993-02-01 | 2014-08-22 | 21.57 | 0.419 | 0.912 | 0.493 | 117.584 | 42 | increased | 1529 | -1.06 | equidimensional | 0.0027 | 2 |
| | Blanchard | 2005 | 38.00 | 37.63 | -0.36 | retreated | 1993-02-01 | 2014-08-22 | 21.57 | 0.341 | 1.084 | 0.744 | 218.153 | 30 | increased | 2060 | 1.53 | very bottom-heavy | 0.0025 | 2 |
| | Bleriot | 8527 | 182.20 | 180.69 | -1.50 | retreated | 1993-02-01 | 2014-04-10 | 21.20 | 0.836 | 0.300 | -0.536 | -64.134 | 25 | decreased | 1943 | 1.28 | bottom-heavy | 0.0019 | 3 |
| | CLM | 12682 | 809.85 | 809.58 | -0.27 | stable | 1993-02-01 | 2010-12-29 | 17.92 | 0.388 | 0.396 | 0.008 | 2.157 | 34 | peak | 2191 | 1.13 | equidimensional | 0.0016 | 2 |
| | Deville | 8699 | 34.99 | 34.79 | -0.20 | stable | 1996-02-15 | 2010-12-22 | 14.86 | 0.364 | 0.127 | -0.237 | -65.116 | 12 | decreased | 1389 | -1.19 | equidimensional | 0.0025 | 3 |
| | DGC10 | 6423 | 23.47 | 23.40 | -0.06 | stable | 1993-02-01 | 2014-04-10 | 21.20 | 0.116 | 0.580 | 0.465 | 401.477 | 20 | increased | 1219 | -1.10 | equidimensional | 0.0064 | 2 |
| | DGC13 | 1950 | 10.95 | 10.76 | -0.18 | retreated | 1996-02-15 | 2014-04-10 | 18.16 | 0.285 | 0.205 | -0.081 | -28.256 | 24 | peak | 901 | 1.28 | bottom-heavy | 0.0071 | 3 |
| | DGC14 | 1684 | 5.66 | 5.64 | -0.02 | stable | 1996-02-15 | 2014-04-10 | 18.16 | 0.096 | 0.113 | 0.018 | 18.626 | 20 | stable | 884 | 1.90 | very bottom-heavy | 0.0109 | 3 |
| | DGC22 | 2188 | 8.98 | 9.10 | 0.12 | stable | 1996-02-15 | 2014-04-10 | 18.16 | 0.190 | 0.084 | -0.106 | -55.993 | 24 | stable | 1113 | -1.24 | top-heavy | 0.0148 | 3 |
| | DGC23 | 1868 | 15.92 | 15.91 | 0.00 | stable | 1993-02-01 | 2014-08-22 | 21.57 | 0.414 | 1.025 | 0.611 | 147.314 | 36 | increased | 1379 | -1.33 | top-heavy | 0.0023 | 2 |
| | DGC25 | 2693 | 14.12 | 14.27 | 0.15 | stable | 1993-02-01 | 2014-08-22 | 21.57 | 0.363 | 0.820 | 0.457 | 125.807 | 37 | increased | 1850 | 1.52 | very bottom-heavy | 0.0028 | 2 |
| | DGC31 | 1466 | 13.30 | 13.06 | -0.24 | retreated | 1996-02-15 | 2010-12-11 | 14.83 | 0.132 | 0.204 | 0.072 | 54.579 | 8 | stable | 1488 | 1.86 | very bottom-heavy | 0.0029 | 2 |
| | DGC39 | 1331 | 15.07 | 14.97 | -0.10 | retreated | 1993-02-01 | 2010-12-22 | 17.90 | 0.529 | 0.164 | -0.365 | -69.044 | 8 | decreased | 1472 | 1.02 | equidimensional | 0.0040 | 3 |
| | DGC72 | 4990 | 38.39 | 38.09 | -0.30 | stable | 1993-02-01 | 2010-12-29 | 17.92 | 0.359 | 0.695 | 0.336 | 93.651 | 13 | peak | 1706 | 1.17 | equidimensional | 0.0027 | 2 |
| | DGC8 | 3340 | 9.34 | 8.91 | -0.43 | retreated | 1993-02-01 | 2014-04-10 | 21.20 | 0.177 | 0.241 | 0.064 | 36.012 | 32 | stable | 1061 | 2.07 | very bottom-heavy | 0.0094 | 4 |
| | Krebs | 3152 | 34.80 | 35.27 | 0.47 | advanced | 1993-02-01 | 2014-04-10 | 21.20 | 0.866 | 0.738 | -0.128 | -14.780 | 13 | peak | 2029 | -2.00 | very top-heavy | 0.0006 | 1 |
| | Landau | 2330 | 33.99 | 33.90 | -0.08 | stable | 1996-02-13 | 2014-08-27 | 18.55 | 0.069 | 0.727 | 0.658 | 954.866 | 48 | increased | 1747 | -1.79 | very top-heavy | 0.0027 | 1 |
| | Leonardo | 3632 | 84.22 | 83.72 | -0.49 | retreated | 1993-02-01 | 2014-08-22 | 21.57 | 0.281 | 1.493 | 1.212 | 431.732 | 24 | increased | 2106 | 1.06 | equidimensional | 0.0009 | 2 |
| | Mc Neile | 2507 | 184.56 | 184.66 | 0.10 | stable | 1995-12-19 | 2014-08-27 | 18.70 | 0.207 | 0.699 | 0.492 | 237.738 | 30 | increased | 1882 | -4.58 | very top-heavy | 0.0006 | 1 |
| | Montgolfier | 4486 | 55.20 | 55.06 | -0.13 | stable | 1993-02-01 | 2014-08-22 | 21.57 | 0.141 | 1.371 | 1.230 | 872.806 | 21 | increased | 1929 | -1.32 | top-heavy | 0.0022 | 1 |
| | Nobile | 2361 | 57.04 | 56.78 | -0.26 | retreated | 1993-02-01 | 2014-04-10 | 21.20 | 0.233 | 0.372 | 0.139 | 59.586 | 13 | peak | 1901 | -1.28 | top-heavy | 0.0018 | 1 |
| | Orel | 5399 | 19.02 | 18.11 | -0.92 | retreated | 1996-02-15 | 2010-12-22 | 14.86 | 0.229 | 0.172 | -0.057 | -25.010 | 8 | stable | 1148 | 1.95 | very bottom-heavy | 0.0066 | 4 |
| | Pettus-GavinIce | 3535 | 330.88 | 330.67 | -0.21 | stable | 1992-12-25 | 2014-08-05 | 21.62 | 0.686 | 0.385 | -0.301 | -43.827 | 33 | peak | 1846 | 1.24 | bottom-heavy | 0.0030 | 2 |

| Sector | Basin | $l_f$ [m] | $A_{1985-1990}$ [km²] | $A_{2010-2015}$ [km²] | $dA$ [km²] | Area change category | Date vs [yyyy-mm-dd] | Date vE [yyyy-mm-dd] | dt [a] | vS [m d-1] | vE [m d-1] | dv [m d-1] | dv [%] | nv | Vel. change category | $h_{max}$ [m a.s.l.] | $HI$ | Hypsometric category | $FA$ | Group |
|---|---|---|---|---|---|---|---|---|---|---|---|---|---|---|---|---|---|---|---|---|
| | Renard | 5904 | 118.15 | 117.24 | -0.91 | retreated | 1993-02-01 | 2014-08-22 | 21.57 | 0.212 | 1.698 | 1.486 | 699.238 | 36 | increased | 2043 | -1.82 | very top-heavy | 0.0011 | 1 |
| | Rozier | 5984 | 35.57 | 35.07 | -0.50 | retreated | 1996-02-15 | 2014-08-22 | 18.53 | 0.977 | 0.944 | -0.033 | -3.420 | 38 | peak | 2061 | 2.70 | very bottom-heavy | 0.0036 | 2 |
| | Russell West | 3450 | 329.28 | 328.95 | -0.33 | retreated | 1996-02-29 | 2014-08-27 | 18.50 | 1.072 | 1.759 | 0.687 | 64.111 | 16 | increased | 1645 | 1.44 | bottom-heavy | 0.0028 | 2 |
| | Sabine | 1795 | 83.09 | 82.78 | -0.31 | retreated | 1993-02-01 | 2014-08-27 | 21.58 | 0.239 | 0.348 | 0.109 | 45.520 | 82 | increased | 1843 | 1.21 | bottom-heavy | 0.0070 | 2 |
| | SBG | 10917 | 327.95 | 327.75 | -0.20 | stable | 1993-02-01 | 2010-12-29 | 17.92 | 0.298 | 0.306 | 0.007 | 2.395 | 34 | peak | 2220 | 1.08 | equidimensional | 0.0047 | 2 |
| | Stringfellow-Henson | 7775 | 670.38 | 669.74 | -0.64 | retreated | 1993-02-01 | 2014-02-28 | 21.09 | 1.100 | 1.233 | 0.132 | 12.029 | 22 | fluctuating | 2167 | 1.55 | very bottom-heavy | 0.0026 | 2 |
| | Temple | 12056 | 453.96 | 453.22 | -0.74 | retreated | 1992-12-25 | 2014-08-11 | 21.64 | 1.544 | 1.516 | -0.028 | -1.821 | 90 | fluctuating | 1962 | -1.06 | equidimensional | 0.0031 | 1 |
| | TPE11 | 1947 | 70.06 | 70.13 | 0.07 | stable | 1995-12-20 | 2013-12-24 | 18.02 | 0.184 | 1.203 | 1.018 | 552.655 | 20 | increased | 1268 | 1.05 | equidimensional | 0.0028 | 2 |
| | TPE125 | 8741 | 40.41 | 40.13 | -0.27 | stable | 1992-12-25 | 2013-12-24 | 21.01 | 0.415 | 0.260 | -0.155 | -37.319 | 22 | fluctuating | 1104 | 1.82 | very bottom-heavy | 0.0116 | 3 |
| | TPE126 | 16295 | 145.52 | 147.80 | 2.28 | advanced | 1995-12-19 | 2014-08-27 | 18.70 | 0.287 | 0.306 | 0.019 | 6.542 | 58 | peak | 1655 | 2.20 | very bottom-heavy | 0.0060 | 2 |
| | TPE39 | 9931 | 139.49 | 139.40 | -0.08 | stable | 1995-12-19 | 2013-12-07 | 17.98 | 0.341 | 0.690 | 0.348 | 102.092 | 21 | peak | 1384 | 1.13 | equidimensional | 0.0051 | 2 |
| | TPE40 | 13405 | 184.11 | 184.69 | 0.58 | stable | 1992-12-25 | 2013-12-24 | 21.01 | 0.718 | 0.406 | -0.312 | -43.414 | 27 | decreased | 1386 | 1.01 | equidimensional | 0.0059 | 3 |
| | TPE41 | 9256 | 53.13 | 53.24 | 0.11 | stable | 1995-12-19 | 2013-12-07 | 17.98 | 0.326 | 0.281 | -0.046 | -13.987 | 26 | stable | 1094 | 1.98 | very bottom-heavy | 0.0107 | 3 |
| | TPE46 | 2785 | 33.94 | 34.34 | 0.41 | advanced | 1992-12-25 | 2014-08-27 | 21.68 | 0.935 | 0.881 | -0.054 | -5.756 | 42 | fluctuating | 1843 | -1.86 | very top-heavy | 0.0026 | 1 |
| | TPE50 | 2987 | 31.32 | 31.53 | 0.21 | advanced | 1992-12-25 | 2014-02-28 | 21.19 | 0.450 | 0.517 | 0.067 | 14.899 | 46 | peak | 1839 | 1.13 | equidimensional | 0.0023 | 2 |
| | TPE57 | 20111 | 100.43 | 100.34 | -0.10 | stable | 1993-02-01 | 2010-12-29 | 17.92 | 0.317 | 0.230 | -0.087 | -27.382 | 29 | peak | 1132 | 1.31 | bottom-heavy | 0.0090 | 3 |
| | TPE8 | 5582 | 111.74 | 112.24 | 0.49 | advanced | 1996-02-11 | 2013-12-24 | 17.88 | 0.991 | 0.739 | -0.252 | -25.395 | 14 | trough | 1104 | 1.19 | equidimensional | 0.0035 | 3 |
| | TPE9 | 3735 | 48.96 | 49.64 | 0.68 | advanced | 1995-12-20 | 2013-12-24 | 18.02 | 0.377 | 0.150 | -0.227 | -60.233 | 17 | decreased | 1085 | 1.41 | bottom-heavy | 0.0057 | 3 |
| | Wellman | 3449 | 48.67 | 48.48 | -0.19 | stable | 1996-02-15 | 2014-04-10 | 18.16 | 0.161 | 0.255 | 0.094 | 58.300 | 19 | stable | 1772 | 1.47 | bottom-heavy | 0.0037 | 2 |
| | Wheatstone | 4642 | 52.66 | 52.18 | -0.48 | retreated | 1993-02-01 | 2010-12-22 | 17.90 | 0.355 | 0.258 | -0.097 | -27.262 | 11 | peak | 1569 | 1.21 | bottom-heavy | 0.0029 | 2 |
| | Whitecloud | 3711 | 177.77 | 177.66 | -0.11 | stable | 1992-12-25 | 2014-08-11 | 21.64 | 0.454 | 0.481 | 0.027 | 5.848 | 39 | fluctuating | 1950 | -2.94 | very top-heavy | 0.0013 | 1 |
| | Woodbury | 1464 | 20.24 | 20.03 | -0.21 | retreated | 1993-02-01 | 2014-08-11 | 21.54 | 0.155 | 0.239 | 0.084 | 53.784 | 23 | stable | 1862 | 1.02 | equidimensional | 0.0024 | 2 |
| Summary | mean | | | | | | | | 19.58 | 0.428 | 0.605 | 0.177 | 41.334 | | | 1636 | | | | |
| West | sum | 268763 | 5809.33 | 5800.18 | -9.14 | | | | | | | | | 1429 | | | | | | |
| Summary | mean | | | | | | | | 19.25 | 0.484 | 0.545 | 0.061 | 12.646 | | | 1629 | | | | |
| all glaciers | sum | 481786 | 11003.23 | 10764.42 | -238.81 | | | | | | | | | 2256 | | | | | | |

$l_f$ – length of ice front

$A$ – ~~G~~glacier area in the respective period*

$dA$ – c~~C~~hange in glacier area between 1985 and 2015*

Area change category – see definition in Section 4.1

Date $v_s$ - date of first velocity measurement

Date $v_E$ – date of last velocity measurement

$dt$ - mean time period of velocity measurements

$v_s$ – mean of earliest velocity measurements (1992-1996)

$v_E$ – mean of latest velocity measurements (2010-2014)

$dv$ – mean velocity change

$n_v$ – sum of velocity measurements in the observation period ($dt$)

Velocity change category – see definition in Table 3

$h_{max}$ – average maximum altitude of individual basins

$HI$ – Hypsometric Index of the basin

Hypsometric category – see Table 4

$FA$ – f~~F~~lux gate to catchment size ratio

Group – ~~C~~classification of glaciers in sector “West” according to the hierarchical cluster analysis in Section 4.4.

*since 1995 for the former Larsen-A and Prince Gustav Ice Shelf tributaries (see Section 5.2)

**Table S2:** Observed parameters of the individual glaciers derived from velocity data measured at maximum ice thickness at the terminus profiles. Table continues on next page.

Formatiert: Table, Block

| Sector | Basin | Date $v_S$ [yyyy-mm-dd] | Date $v_E$ [yyyy-mm-dd] | $dt$ [a] | $v_S$ [m d$^{-1}$] | $v_E$ [m d$^{-1}$] | $dv$ [m d$^{-1}$] | $dv$ [%] | $n_v$ | Vel. change category | Longitude [°] | Latitude [°] | Group |
|---|---|---|---|---|---|---|---|---|---|---|---|---|---|
| East | ADD ID: 2707 | 1995-11-14 | 2013-12-24 | 18.12 | 2.212 | 0.140 | -2.072 | -93.676 | 40 | decreased | -58.3480 | -63.7806 | |
| | ADD ID: 2731 | 1992-12-25 | 2010-12-31 | 18.03 | 0.391 | 0.134 | -0.256 | -65.654 | 9 | decreased | -58.1603 | -63.6990 | |
| | Aitkenhead | 1995-12-18 | 2014-12-16 | 19.01 | 1.266 | 1.280 | 0.014 | 1.134 | 34 | peak | -58.6712 | -63.9561 | |
| | Broad Valley | 1996-02-11 | 2010-12-31 | 14.90 | 0.445 | 0.070 | -0.375 | -84.243 | 3 | decreased | -57.6730 | -63.5434 | |
| | Diplock | 1995-12-18 | 2014-12-16 | 19.01 | 0.538 | 0.641 | 0.103 | 19.140 | 52 | trough | -58.7446 | -64.0382 | |
| | Eyrie | 1992-12-25 | 2010-12-31 | 18.03 | 1.123 | 0.682 | -0.442 | -39.311 | 5 | decreased | -57.7725 | -63.5999 | |
| | Russell East | 1992-12-25 | 2013-12-24 | 21.01 | 3.127 | 0.552 | -2.575 | -82.350 | 39 | decreased | -58.2950 | -63.7328 | |
| | TPE10 | 1995-11-14 | 2010-12-31 | 15.14 | 1.258 | 1.154 | -0.105 | -8.327 | 6 | peak | -58.0911 | -63.6559 | |
| | TPE130 | 1995-11-14 | 2014-03-27 | 18.38 | 4.998 | 0.273 | -4.725 | -94.540 | 50 | decreased | -58.4762 | -63.8652 | |
| | TPE31 | 1995-12-18 | 2013-12-24 | 18.03 | 3.986 | 0.169 | -3.816 | -95.756 | 25 | decreased | -58.5084 | -63.9136 | |
| | TPE32 | 1995-12-19 | 2014-12-16 | 19.01 | 1.848 | 0.625 | -1.223 | -66.185 | 49 | decreased | -58.5985 | -63.9253 | |
| | TPE34 | 1992-12-25 | 2010-12-31 | 18.03 | 1.369 | 0.365 | -1.004 | -73.345 | 6 | decreased | -57.9752 | -63.6675 | |
| | Victory | 1995-11-14 | 2013-12-02 | 18.06 | 1.284 | 1.222 | -0.062 | -4.852 | 37 | trough | -58.3952 | -63.8057 | |
| Summary | mean | | | 18.06 | 1.834 | 0.562 | -1.272 | -69.360 | | | | | |
| East | sum | | | | | | | | 355 | | | | |
| East-Ice-Shelf | ADD ID: 2558 | 1993-01-29 | 2010-12-29 | 17.93 | 0.332 | 0.297 | -0.035 | -10.600 | 39 | peak | -60.4713 | -64.6331 | |
| | ADD ID: 2668 | 1995-12-19 | 2014-03-27 | 18.28 | 1.068 | 0.367 | -0.701 | -65.626 | 24 | decreased | -58.7338 | -64.0949 | |
| | APPE | 1992-12-25 | 2014-12-16 | 21.99 | 2.276 | 1.230 | -1.046 | -45.972 | 126 | decreased | -59.5048 | -64.3030 | |
| | Arron Icefall | 1993-01-12 | 2010-12-29 | 17.97 | 0.479 | 1.298 | 0.819 | 170.781 | 30 | peak | -60.4392 | -64.5916 | |
| | Boydell | 1996-02-13 | 2014-12-16 | 18.85 | 0.367 | 1.149 | 0.782 | 213.226 | 37 | peak | -59.0689 | -64.1694 | |
| | DBE | 1993-01-29 | 2014-02-27 | 21.09 | 1.710 | 1.392 | -0.318 | -18.603 | 115 | peak | -59.9281 | -64.3595 | |
| | Drygalski | 1993-01-29 | 2010-12-29 | 17.93 | 1.610 | 5.490 | 3.879 | 240.893 | 22 | peak | -60.7602 | -64.7437 | |
| | LAB2 | 1993-01-29 | 2010-12-29 | 17.93 | 0.053 | 0.084 | 0.030 | 56.272 | 23 | peak | -60.6258 | -64.6894 | |
| | LAB32 | 1993-01-29 | 2010-12-29 | 17.93 | 0.270 | 0.378 | 0.108 | 39.865 | 23 | peak | -60.5046 | -64.6596 | |
| | Sjögren | 1996-02-13 | 2014-12-16 | 18.85 | 0.758 | 1.661 | 0.904 | 119.255 | 61 | peak | -59.1731 | -64.2164 | |
| | TPE114 | 1996-02-13 | 2014-12-16 | 18.85 | 0.237 | 0.379 | 0.143 | 60.225 | 55 | fluctuating | -58.9343 | -64.1937 | |
| | TPE61 | 1993-01-12 | 2011-01-22 | 18.04 | 0.343 | 0.136 | -0.207 | -60.310 | 44 | peak | -60.3090 | -64.5320 | |
| | TPE62 | 1992-12-25 | 2011-01-22 | 18.09 | 0.374 | 0.067 | -0.308 | -82.175 | 40 | peak | -60.1646 | -64.5031 | |
| Summary | mean | | | 18.75 | 0.760 | 1.071 | 0.312 | 41.000 | | | | | |
| East-Ice-Shelf | sum | | | | | | | | 639 | | | | |
| West | AMR | 1993-02-01 | 2014-08-22 | 21.57 | 0.112 | 2.065 | 1.954 | 1750.085 | 18 | increased | -62.3704 | -64.8692 | 1 |
| | Andrew | 1992-12-25 | 2014-08-27 | 21.68 | 0.430 | 0.339 | -0.091 | -21.211 | 112 | fluctuating | -59.7202 | -63.8728 | 4 |
| | Bagshawe-Grubb | 1996-02-15 | 2010-11-29 | 14.80 | 0.211 | 0.163 | -0.048 | -22.789 | 5 | stable | -62.6231 | -64.9147 | 1 |
| | Bayly | 1993-02-01 | 2014-08-22 | 21.57 | 0.806 | 0.886 | 0.080 | 9.931 | 37 | fluctuating | -61.8628 | -64.6094 | 3 |
| | Blanchard | 1993-02-01 | 2014-08-22 | 21.57 | 0.937 | 1.390 | 0.453 | 48.342 | 37 | increased | -62.0656 | -64.7283 | 2 |
| | Bleriot | 1996-02-15 | 2014-04-10 | 18.16 | 1.375 | 1.267 | -0.107 | -7.793 | 27 | fluctuating | -61.1699 | -64.4075 | 3 |
| | CLM | 1993-02-01 | 2010-12-29 | 17.92 | 0.288 | 0.394 | 0.106 | 36.932 | 24 | peak | -60.9489 | -64.3093 | 2 |
| | Deville | 1996-02-15 | 2010-12-22 | 14.86 | 1.386 | 0.259 | -1.127 | -81.322 | 10 | decreased | -62.5725 | -64.8107 | 3 |
| | DGC10 | 1993-02-01 | 2014-04-10 | 21.20 | 0.232 | 0.774 | 0.542 | 234.115 | 30 | increased | -61.4458 | -64.4220 | 1 |
| | DGC13 | 1996-02-15 | 2014-04-10 | 18.16 | 0.354 | 0.457 | 0.102 | 28.864 | 23 | fluctuating | -61.5345 | -64.5383 | 3 |
| | DGC14 | 1996-02-15 | 2014-04-10 | 18.16 | 0.096 | 0.124 | 0.028 | 28.973 | 29 | stable | -61.5777 | -64.5362 | 3 |
| | DGC22 | 1996-02-15 | 2014-04-10 | 18.16 | 0.272 | 0.543 | 0.271 | 99.864 | 33 | fluctuating | -61.5535 | -64.5763 | 3 |
| | DGC23 | 1993-02-01 | 2014-08-22 | 21.57 | 0.414 | 0.960 | 0.545 | 131.621 | 37 | increased | -61.9237 | -64.6491 | 1 |
| | DGC25 | 1993-02-01 | 2014-08-22 | 21.57 | 0.096 | 1.049 | 0.953 | 994.935 | 38 | increased | -62.0029 | -64.7076 | 2 |
| | DGC31 | 1993-02-01 | 2010-12-22 | 17.90 | 0.719 | 0.211 | -0.509 | -70.700 | 7 | fluctuating | -62.3808 | -64.7243 | 3 |
| | DGC39 | 1993-02-01 | 2010-12-22 | 17.90 | 0.645 | 0.153 | -0.493 | -76.339 | 11 | decreased | -62.5177 | -64.6534 | 3 |
| | DGC72 | 1993-02-01 | 2014-04-10 | 21.20 | 0.269 | 2.387 | 2.118 | 787.360 | 25 | increased | -61.3022 | -64.4380 | 2 |
| | DGC8 | 1993-02-01 | 2014-04-10 | 21.20 | 0.169 | 0.384 | 0.215 | 127.060 | 40 | fluctuating | -61.3651 | -64.4162 | 4 |
| | Krebs | 1993-02-01 | 2014-04-10 | 21.20 | 0.866 | 1.119 | 0.253 | 29.203 | 20 | peak | -61.5201 | -64.6377 | 1 |
| | Landau | 1996-02-13 | 2014-08-27 | 18.55 | 0.068 | 1.349 | 1.281 | 1876.773 | 43 | increased | -59.3685 | -63.8722 | 1 |
| | Leonardo | 1993-02-01 | 2014-08-22 | 21.57 | 0.155 | 2.523 | 2.368 | 1525.056 | 28 | increased | -61.9568 | -64.6961 | 2 |
| | Mc Neile | 1995-11-14 | 2014-08-27 | 18.80 | 0.650 | 5.146 | 4.496 | 691.683 | 33 | increased | -59.4035 | -63.9233 | 1 |
| | Montgolfier | 1993-02-01 | 2014-08-22 | 21.57 | 0.250 | 2.624 | 2.374 | 949.476 | 31 | increased | -62.2203 | -64.7800 | 1 |
| | Nobile | 1993-02-01 | 2014-04-10 | 21.20 | 0.235 | 1.226 | 0.991 | 421.633 | 18 | increased | -61.4705 | -64.5422 | 1 |
| | Orel | 1993-02-01 | 2010-12-22 | 17.90 | 0.519 | 0.344 | -0.174 | -33.577 | 10 | stable | -62.5638 | -64.7635 | 4 |
| | Pettus-GavinIce | 1992-12-25 | 2014-08-05 | 21.62 | 5.651 | 1.951 | -3.700 | -65.473 | 29 | peak | -59.1464 | -63.7450 | 2 |

| Sector | Basin | Date vs [yyyy-mm-dd] | Date vE [yyyy-mm-dd] | dt [a] | vS [m d-1] | vE [m d-1] | dv [m d-1] | dv [%] | nv | Vel. change category | | | Group |
|---|---|---|---|---|---|---|---|---|---|---|---|---|---|
| | Renard | 1993-02-01 | 2014-08-22 | 21.57 | 0.213 | 1.273 | 1.060 | 498.781 | 42 | increased | -61.6438 | -64.6709 | 2 |
| | Rozier | 1996-02-29 | 2014-08-27 | 21.57 | 1.777 | 2.210 | 0.433 | 24.342 | 59 | increased | -62.1835 | -64.7457 | 2 |
| | Russell West | 1993-02-01 | 2014-08-27 | 18.50 | 0.196 | 0.341 | 0.145 | 73.631 | 105 | increased | -58.8902 | -63.6830 | 2 |
| | Sabine | 1993-02-01 | 2010-12-12 | 21.58 | 0.577 | 2.814 | 2.238 | 388.165 | 31 | peak | -59.8056 | -63.8741 | 2 |
| | SBG | 1996-02-13 | 2011-02-08 | 17.87 | 4.106 | 4.029 | -0.077 | -1.885 | 20 | fluctuating | -60.8223 | -64.1623 | 2 |
| | Stringfellow-Henson | 1992-12-25 | 2014-02-28 | 15.00 | 1.390 | 1.283 | -0.106 | -7.660 | 98 | fluctuating | -60.4311 | -63.9752 | 1 |
| | Temple | 1995-11-14 | 2013-12-24 | 21.19 | 1.272 | 1.881 | 0.609 | 47.843 | 28 | increased | -60.1247 | -63.9419 | 2 |
| | TPE11 | 1992-12-25 | 2013-12-24 | 18.12 | 0.526 | 0.384 | -0.142 | -26.927 | 31 | fluctuating | -58.1397 | -63.4734 | 3 |
| | TPE125 | 1992-12-25 | 2014-08-27 | 21.01 | 0.150 | 0.277 | 0.127 | 84.605 | 50 | peak | -58.6190 | -63.5057 | 2 |
| | TPE126 | 1995-12-19 | 2013-12-24 | 21.68 | 1.081 | 0.993 | -0.088 | -8.144 | 25 | fluctuating | -59.3057 | -63.7796 | 3 |
| | TPE39 | 1992-12-25 | 2013-12-24 | 18.03 | 0.649 | 0.408 | -0.241 | -37.191 | 25 | fluctuating | -58.7693 | -63.5361 | 3 |
| | TPE40 | 1995-12-19 | 2013-12-24 | 21.01 | 0.472 | 0.454 | -0.018 | -3.798 | 17 | fluctuating | -58.3804 | -63.4791 | 3 |
| | TPE41 | 1992-12-25 | 2014-08-27 | 18.03 | 1.390 | 1.025 | -0.365 | -26.229 | 47 | fluctuating | -58.2347 | -63.4585 | 1 |
| | TPE46 | 1992-12-25 | 2014-08-27 | 21.68 | 1.312 | 0.852 | -0.459 | -35.021 | 113 | fluctuating | -59.3930 | -63.8914 | 2 |
| | TPE50 | 1993-02-01 | 2010-12-29 | 21.68 | 0.473 | 0.275 | -0.198 | -41.828 | 22 | stable | -59.9269 | -63.9387 | 3 |
| | TPE57 | 1996-02-11 | 2013-12-24 | 17.92 | 0.671 | 0.692 | 0.021 | 3.134 | 12 | fluctuating | -60.6700 | -64.0238 | 3 |
| | TPE8 | 1995-12-19 | 2013-12-24 | 17.88 | 4.396 | 0.605 | -3.791 | -86.236 | 24 | decreased | -57.9284 | -63.3700 | 3 |
| | TPE9 | 1996-02-15 | 2014-04-10 | 18.03 | 0.196 | 0.855 | 0.658 | 335.252 | 21 | increased | -58.0371 | -63.4244 | 2 |
| | Wellman | 1993-02-01 | 2010-12-22 | 18.16 | 0.455 | 0.530 | 0.075 | 16.501 | 12 | peak | -61.4298 | -64.4846 | 2 |
| | Wheatstone | 1992-12-25 | 2014-08-27 | 17.90 | 1.017 | 3.375 | 2.359 | 232.018 | 99 | increased | -62.5189 | -64.7362 | 1 |
| | Whitecloud | 1993-02-01 | 2014-08-22 | 21.68 | 0.153 | 0.237 | 0.085 | 55.585 | 44 | fluctuating | -59.5585 | -63.9000 | 3 |
| | Woodbury | 1993-02-01 | 2014-08-22 | 21.57 | 0.213 | 1.273 | 1.060 | 498.781 | 42 | increased | -62.3053 | -64.7749 | 2 |
| Summary West | mean | | | 19.65 | 0.831 | 1.200 | 0.369 | 44.461 | | | | | |
| | sum | | | | | | | | 1742 | | | | |
| Summary all glaciers | mean | | | 19.21 | 0.994 | 1.065 | 0.071 | | | | | | |
| | sum | | | | | | | | 2736 | | | | |

Date $v_S$ - date of first velocity measurement

Date $v_E$ – date of last velocity measurement

*dt* - mean time period of velocity measurements

$v_S$ – mean of earliest velocity measurements (1992-1996)

$v_E$ – mean of latest velocity measurements (2010-2014)

*dv* – mean velocity change

$n_v$ – sum of velocity measurements in the observation period (*dt*)

Velocity change category – see definition in Table 3

Latitude/Longitude – ~~p~~position of velocity measurements

Group – ~~c~~classification of glaciers in sector “West” according to the hierarchical cluster analysis in Section 4.4.

**Table S3~~2~~:** Uncertainty $\sigma_v$ of intensity tracking results. Table continues on next pages

| Date [yyyy-mm-dd] | Satellite | $dt$ [d] | $\sigma_v^C$ [m d$^{-1}$] | $n$ | $\sigma_v^I$ [m d$^{-1}$] | $\sigma_v$ [m d$^{-1}$] |
|---|---|---|---|---|---|---|
| 1992-12-25 | ERS | 35 | 0.13 | 9721 | 0.05 | 0.14 |
| 1992-12-25 | ERS | 35 | 0.25 | 23678 | 0.05 | 0.26 |
| 1993-01-12 | ERS | 70 | 0.07 | 9880 | 0.02 | 0.07 |
| 1993-01-29 | ERS | 35 | 0.10 | 6090 | 0.05 | 0.11 |
| 1993-01-29 | ERS | 35 | 0.23 | 4533 | 0.05 | 0.24 |
| 1993-02-01 | ERS | 35 | 0.20 | 6321 | 0.05 | 0.21 |
| 1994-02-01 | ERS | 21 | 0.35 | 22007 | 0.08 | 0.36 |
| 1994-02-18 | ERS | 54 | 0.07 | 28834 | 0.03 | 0.08 |
| 1994-02-28 | ERS | 33 | 0.16 | 26276 | 0.05 | 0.17 |
| 1995-10-31 | ERS | 1* | 0.41 | 150 | 1.60 | 0.41 |
| 1995-11-14 | ERS | 1* | 0.36 | 1961 | 1.60 | 0.36 |
| 1995-11-16 | ERS | 1* | 0.29 | 448 | 1.60 | 0.29 |
| 1995-12-18 | ERS | 71 | 0.02 | 68711 | 0.02 | 0.03 |
| 1995-12-18 | ERS | 70 | 0.03 | 77246 | 0.02 | 0.04 |
| 1995-12-19 | ERS | 71 | 0.02 | 70974 | 0.02 | 0.03 |
| 1995-12-19 | ERS | 70 | 0.06 | 67287 | 0.02 | 0.06 |
| 1995-12-19 | ERS | 69 | 0.12 | 66877 | 0.02 | 0.12 |
| 1995-12-20 | ERS | 70 | 0.04 | 70897 | 0.02 | 0.04 |
| 1995-12-21 | ERS | 70 | 0.08 | 10755 | 0.02 | 0.08 |
| 1995-12-21 | ERS | 69 | 0.09 | 9000 | 0.02 | 0.10 |
| 1996-01-22 | ERS | 1* | 0.24 | 49973 | 1.60 | 0.24 |
| 1996-01-23 | ERS | 1* | 0.34 | 546 | 1.60 | 0.34 |
| 1996-02-11 | ERS | 35 | 0.12 | 10215 | 0.05 | 0.12 |
| 1996-02-11 | ERS | 35 | 0.14 | 8164 | 0.05 | 0.15 |
| 1996-02-13 | ERS | 35 | 0.06 | 23882 | 0.05 | 0.08 |
| 1996-02-15 | ERS | 35 | 0.14 | 9379 | 0.05 | 0.15 |
| 1996-02-29 | ERS | 35 | 0.02 | 39573 | 0.05 | 0.05 |
| 1996-03-03 | ERS | 34 | 0.05 | 18324 | 0.05 | 0.07 |
| 1996-03-03 | ERS | 35 | 0.05 | 18395 | 0.05 | 0.07 |
| 1996-03-20 | ERS | 1* | 0.30 | 9049 | 1.60 | 0.30 |
| 1997-02-13 | ERS | 35 | 0.04 | 44246 | 0.05 | 0.06 |
| 1997-02-15 | ERS | 35 | 0.11 | 14969 | 0.05 | 0.12 |
| 1997-02-18 | ERS | 35 | 0.09 | 6705 | 0.05 | 0.10 |
| 1998-02-03 | ERS | 35 | 0.07 | 3176 | 0.05 | 0.08 |
| 1999-11-09 | ERS | 1* | 0.34 | 4022 | 1.60 | 0.34 |
| 2002-02-07 | ERS | 35 | 0.07 | 9893 | 0.05 | 0.09 |
| 2002-11-29 | ERS | 35 | 0.13 | 61073 | 0.05 | 0.13 |
| 2002-12-03 | ERS | 35 | 0.13 | 19079 | 0.05 | 0.13 |
| 2002-12-08 | ERS | 35 | 0.29 | 1965 | 0.05 | 0.29 |
| 2002-12-21 | ERS | 70 | 0.05 | 21331 | 0.02 | 0.05 |
| 2002-12-21 | ERS | 35 | 0.27 | 3396 | 0.05 | 0.27 |
| 2002-12-26 | ERS | 70 | 0.13 | 2437 | 0.02 | 0.13 |
| 2003-01-07 | ERS | 35 | 0.05 | 24658 | 0.05 | 0.07 |
| 2003-01-08 | ERS | 70 | 0.19 | 4794 | 0.02 | 0.19 |
| 2003-01-12 | ERS | 35 | 0.09 | 2548 | 0.05 | 0.10 |
| 2003-01-25 | ERS | 35 | 0.10 | 14207 | 0.05 | 0.11 |
| 2004-11-01 | ERS | 35 | 0.17 | 30346 | 0.05 | 0.17 |
| 2004-11-17 | ERS | 70 | 0.06 | 71277 | 0.02 | 0.07 |
| 2004-11-19 | ERS | 70 | 0.08 | 32153 | 0.02 | 0.09 |
| 2004-12-06 | ERS | 35 | 0.11 | 33520 | 0.05 | 0.12 |
| 2004-12-24 | ERS | 70 | 0.11 | 34409 | 0.02 | 0.11 |
| 2004-12-25 | ERS | 35 | 0.14 | 12592 | 0.05 | 0.14 |
| 2005-01-10 | ERS | 35 | 0.28 | 23466 | 0.05 | 0.28 |

| Date [yyyy-mm-dd] | Satellite | *dt* [d] | $\sigma_v^C$ [m d$^{-1}$] | *n* | $\sigma_v^T$ [m d$^{-1}$] | $\sigma_v$ [m d$^{-1}$] |
|---|---|---|---|---|---|---|
| 2006-11-03 | ERS | 35 | 0.19 | 56628 | 0.05 | 0.19 |
| 2006-11-04 | ERS | 35 | 0.14 | 70277 | 0.05 | 0.14 |
| 2008-10-29 | ERS | 35 | 0.07 | 9881 | 0.05 | 0.08 |
| 2010-02-08 | ERS | 35 | 0.18 | 18041 | 0.05 | 0.19 |
| 2010-02-26 | ERS | 70 | 0.11 | 19172 | 0.02 | 0.11 |
| 2010-03-15 | ERS | 35 | 0.10 | 23486 | 0.05 | 0.11 |
| 2000-09-22 | R1 | 24 | 0.10 | 20810 | 0.06 | 0.12 |
| 2000-09-22 | R1 | 24 | 0.14 | 33870 | 0.06 | 0.15 |
| 2000-10-01 | R1 | 24 | 0.06 | 30397 | 0.06 | 0.09 |
| 2006-08-22 | R1 | 24 | 0.07 | 57259 | 0.06 | 0.10 |
| 2006-08-22 | R1 | 24 | 0.08 | 21635 | 0.06 | 0.10 |
| 2003-12-22 | ENVISAT | 35 | 0.31 | 38866 | 0.05 | 0.31 |
| 2004-01-09 | ENVISAT | 70 | 0.03 | 61495 | 0.02 | 0.04 |
| 2004-01-10 | ENVISAT | 35 | 0.13 | 1790 | 0.05 | 0.13 |
| 2004-01-28 | ENVISAT | 70 | 0.16 | 1510 | 0.02 | 0.16 |
| 2004-02-14 | ENVISAT | 35 | 0.09 | 1898 | 0.05 | 0.10 |
| 2004-03-20 | ENVISAT | 35 | 0.13 | 3299 | 0.05 | 0.14 |
| 2004-04-24 | ENVISAT | 35 | 0.12 | 3505 | 0.05 | 0.13 |
| 2004-05-29 | ENVISAT | 35 | 0.10 | 3623 | 0.05 | 0.11 |
| 2004-07-03 | ENVISAT | 35 | 0.10 | 3546 | 0.05 | 0.11 |
| 2004-07-19 | ENVISAT | 35 | 0.03 | 60612 | 0.05 | 0.06 |
| 2004-08-07 | ENVISAT | 35 | 0.11 | 3418 | 0.05 | 0.12 |
| 2004-09-11 | ENVISAT | 35 | 0.14 | 3400 | 0.05 | 0.15 |
| 2004-10-16 | ENVISAT | 35 | 0.15 | 3449 | 0.05 | 0.16 |
| 2004-12-06 | ENVISAT | 35 | 0.06 | 63965 | 0.05 | 0.08 |
| 2005-01-28 | ENVISAT | 70 | 0.02 | 62239 | 0.02 | 0.03 |
| 2005-03-05 | ENVISAT | 35 | 0.15 | 2744 | 0.05 | 0.15 |
| 2005-03-21 | ENVISAT | 35 | 0.19 | 64254 | 0.05 | 0.19 |
| 2005-04-09 | ENVISAT | 35 | 0.13 | 2904 | 0.05 | 0.14 |
| 2005-05-14 | ENVISAT | 35 | 0.17 | 3016 | 0.05 | 0.17 |
| 2005-06-18 | ENVISAT | 35 | 0.13 | 3631 | 0.05 | 0.14 |
| 2005-07-23 | ENVISAT | 35 | 0.14 | 2943 | 0.05 | 0.14 |
| 2005-08-08 | ENVISAT | 35 | 0.12 | 68061 | 0.05 | 0.13 |
| 2006-02-15 | ENVISAT | 35 | 0.07 | 61205 | 0.05 | 0.08 |
| 2006-03-25 | ENVISAT | 35 | 0.14 | 2755 | 0.05 | 0.15 |
| 2006-07-08 | ENVISAT | 35 | 0.08 | 3488 | 0.05 | 0.09 |
| 2006-08-09 | ENVISAT | 35 | 0.06 | 60954 | 0.05 | 0.08 |
| 2006-08-12 | ENVISAT | 35 | 0.15 | 3302 | 0.05 | 0.15 |
| 2006-09-16 | ENVISAT | 35 | 0.14 | 3295 | 0.05 | 0.15 |
| 2006-10-21 | ENVISAT | 35 | 0.16 | 2741 | 0.05 | 0.17 |
| 2007-02-18 | ENVISAT | 70 | 0.03 | 71538 | 0.02 | 0.04 |
| 2007-04-29 | ENVISAT | 70 | 0.04 | 65692 | 0.02 | 0.05 |
| 2007-06-20 | ENVISAT | 35 | 0.03 | 63862 | 0.05 | 0.05 |
| 2007-08-12 | ENVISAT | 70 | 0.04 | 61079 | 0.02 | 0.05 |
| 2007-09-01 | ENVISAT | 35 | 0.15 | 3391 | 0.05 | 0.16 |
| 2007-10-03 | ENVISAT | 35 | 0.10 | 61336 | 0.05 | 0.11 |
| 2007-10-06 | ENVISAT | 35 | 0.16 | 3255 | 0.05 | 0.16 |
| 2008-04-30 | ENVISAT | 35 | 0.10 | 63576 | 0.05 | 0.11 |
| 2008-06-22 | ENVISAT | 70 | 0.03 | 57922 | 0.02 | 0.04 |
| 2008-08-13 | ENVISAT | 35 | 0.07 | 60539 | 0.05 | 0.08 |
| 2009-03-11 | ENVISAT | 35 | 0.11 | 64638 | 0.05 | 0.12 |
| 2009-07-29 | ENVISAT | 35 | 0.03 | 61130 | 0.05 | 0.05 |
| 2006-06-10 | ALOS | 46 | 0.02 | 15503 | 0.02 | 0.02 |
| 2006-06-17 | ALOS | 46 | 0.01 | 61958 | 0.02 | 0.02 |
| 2006-06-25 | ALOS | 46 | 0.08 | 581 | 0.02 | 0.09 |
| 2006-07-14 | ALOS | 46 | 0.02 | 9476 | 0.02 | 0.02 |
| 2006-09-21 | ALOS | 92 | 0.02 | 9912 | 0.01 | 0.02 |

| Date [yyyy-mm-dd] | Satellite | *dt* [d] | $\sigma_v^C$ [m d$^{-1}$] | *n* | $\sigma_v^T$ [m d$^{-1}$] | $\sigma_v$ [m d$^{-1}$] |
|---|---|---|---|---|---|---|
| 2006-12-23 | ALOS | 46 | 0.08 | 5135 | 0.02 | 0.08 |
| 2007-12-04 | ALOS | 46 | 0.03 | 10220 | 0.02 | 0.04 |
| 2007-12-14 | ALOS | 46 | 0.04 | 2193 | 0.02 | 0.04 |
| 2008-05-14 | ALOS | 46 | 0.01 | 43889 | 0.02 | 0.02 |
| 2008-10-21 | ALOS | 46 | 0.02 | 10711 | 0.02 | 0.02 |
| 2008-10-31 | ALOS | 46 | 0.13 | 2461 | 0.02 | 0.13 |
| 2008-11-13 | ALOS | 92 | 0.02 | 10861 | 0.01 | 0.02 |
| 2008-11-14 | ALOS | 46 | 0.02 | 33136 | 0.02 | 0.02 |
| 2008-12-06 | ALOS | 46 | 0.04 | 10213 | 0.02 | 0.04 |
| 2008-12-07 | ALOS | 92 | 0.02 | 36230 | 0.01 | 0.02 |
| 2008-12-16 | ALOS | 46 | 0.07 | 2291 | 0.02 | 0.07 |
| 2008-12-29 | ALOS | 92 | 0.02 | 10998 | 0.01 | 0.02 |
| 2008-12-30 | ALOS | 46 | 0.04 | 37661 | 0.02 | 0.04 |
| 2009-01-21 | ALOS | 46 | 0.02 | 10677 | 0.02 | 0.03 |
| 2009-12-02 | ALOS | 46 | 0.05 | 3484 | 0.02 | 0.05 |
| 2009-12-09 | ALOS | 46 | 0.03 | 9707 | 0.02 | 0.03 |
| 2009-12-21 | ALOS | 46 | 0.05 | 2455 | 0.02 | 0.05 |
| 2009-12-26 | ALOS | 46 | 0.03 | 9385 | 0.02 | 0.03 |
| 2010-01-19 | ALOS | 46 | 0.02 | 15505 | 0.02 | 0.02 |
| 2010-10-08 | ALOS | 46 | 0.04 | 620 | 0.02 | 0.04 |
| 2010-10-17 | ALOS | 46 | 0.03 | 79294 | 0.02 | 0.03 |
| 2010-11-06 | ALOS | 46 | 0.08 | 2212 | 0.02 | 0.08 |
| 2010-11-08 | ALOS | 46 | 0.01 | 16076 | 0.02 | 0.02 |
| 2010-11-10 | ALOS | 46 | 0.02 | 422 | 0.02 | 0.03 |
| 2010-11-13 | ALOS | 46 | 0.04 | 9956 | 0.02 | 0.05 |
| 2010-11-29 | ALOS | 92 | 0.03 | 2069 | 0.01 | 0.03 |
| 2010-12-01 | ALOS | 92 | 0.01 | 18027 | 0.01 | 0.01 |
| 2010-12-03 | ALOS | 92 | 0.40 | 426 | 0.01 | 0.40 |
| 2010-12-06 | ALOS | 92 | 0.03 | 10352 | 0.01 | 0.03 |
| 2010-12-11 | ALOS | 92 | 0.04 | 4683 | 0.01 | 0.04 |
| 2010-12-12 | ALOS | 46 | 0.03 | 9480 | 0.02 | 0.04 |
| 2010-12-22 | ALOS | 46 | 0.05 | 1992 | 0.02 | 0.05 |
| 2010-12-26 | ALOS | 46 | 0.02 | 411 | 0.02 | 0.03 |
| 2010-12-29 | ALOS | 46 | 0.03 | 10478 | 0.02 | 0.04 |
| 2010-12-31 | ALOS | 46 | 0.01 | 46824 | 0.02 | 0.02 |
| 2011-01-18 | ALOS | 92 | 0.16 | 430 | 0.01 | 0.16 |
| 2011-02-08 | ALOS | 46 | 0.01 | 17569 | 0.02 | 0.02 |
| 2011-02-10 | ALOS | 46 | 0.01 | 394 | 0.02 | 0.02 |
| 2008-10-19 | TSX/TDX | 11 | 0.05 | 4560 | 0.02 | 0.05 |
| 2008-10-25 | TSX/TDX | 22 | 0.02 | 4362 | 0.01 | 0.02 |
| 2008-10-30 | TSX/TDX | 11 | 0.03 | 4507 | 0.02 | 0.04 |
| 2009-08-01 | TSX/TDX | 11 | 0.02 | 11170 | 0.02 | 0.03 |
| 2009-10-28 | TSX/TDX | 11 | 0.06 | 4220 | 0.02 | 0.07 |
| 2010-10-26 | TSX/TDX | 33 | 0.02 | 2678 | 0.01 | 0.02 |
| 2010-11-01 | TSX/TDX | 44 | 0.02 | 3442 | 0.01 | 0.02 |
| 2010-11-17 | TSX/TDX | 22 | 0.01 | 5995 | 0.01 | 0.01 |
| 2010-11-17 | TSX/TDX | 11 | 0.06 | 3599 | 0.02 | 0.07 |
| 2010-11-28 | TSX/TDX | 99 | 0.01 | 3063 | 0.00 | 0.01 |
| 2010-12-15 | TSX/TDX | 66 | 0.02 | 3476 | 0.00 | 0.02 |
| 2010-12-20 | TSX/TDX | 77 | 0.01 | 3524 | 0.00 | 0.01 |
| 2010-12-20 | TSX/TDX | 55 | 0.01 | 4297 | 0.00 | 0.02 |
| 2010-12-26 | TSX/TDX | 66 | 0.01 | 4341 | 0.00 | 0.01 |
| 2011-01-22 | TSX/TDX | 11 | 0.02 | 4722 | 0.02 | 0.03 |
| 2011-06-25 | TSX/TDX | 22 | 0.01 | 15556 | 0.01 | 0.02 |
| 2011-06-25 | TSX/TDX | 22 | 0.04 | 9886 | 0.01 | 0.04 |
| 2011-07-06 | TSX/TDX | 44 | 0.04 | 10380 | 0.01 | 0.04 |
| 2011-07-16 | TSX/TDX | 22 | 0.04 | 3582 | 0.01 | 0.04 |

| Date [yyyy-mm-dd] | Satellite | *dt* [d] | $\sigma_v^C$ [m d$^{-1}$] | *n* | $\sigma_v^I$ [m d$^{-1}$] | $\sigma_v$ [m d$^{-1}$] |
|---|---|---|---|---|---|---|
| 2011-07-17 | TSX/TDX | 22 | 0.01 | 15712 | 0.01 | 0.02 |
| 2011-07-16 | TSX/TDX | 22 | 0.10 | 1421 | 0.01 | 0.10 |
| 2011-07-17 | TSX/TDX | 22 | 0.03 | 10450 | 0.01 | 0.03 |
| 2011-07-28 | TSX/TDX | 44 | 0.02 | 10607 | 0.01 | 0.02 |
| 2011-08-03 | TSX/TDX | 22 | 0.40 | 614 | 0.01 | 0.40 |
| 2011-08-08 | TSX/TDX | 22 | 0.03 | 10394 | 0.01 | 0.04 |
| 2011-08-14 | TSX/TDX | 44 | 0.14 | 1556 | 0.01 | 0.14 |
| 2011-08-19 | TSX/TDX | 44 | 0.03 | 10054 | 0.01 | 0.03 |
| 2011-08-19 | TSX/TDX | 55 | 0.04 | 2385 | 0.00 | 0.04 |
| 2011-08-24 | TSX/TDX | 22 | 0.03 | 1894 | 0.01 | 0.03 |
| 2011-08-24 | TSX/TDX | 55 | 0.03 | 10578 | 0.00 | 0.03 |
| 2011-08-29 | TSX/TDX | 33 | 0.03 | 1856 | 0.01 | 0.03 |
| 2011-08-30 | TSX/TDX | 22 | 0.02 | 15605 | 0.01 | 0.02 |
| 2011-08-30 | TSX/TDX | 22 | 0.06 | 7157 | 0.01 | 0.06 |
| 2011-09-04 | TSX/TDX | 33 | 0.01 | 15878 | 0.01 | 0.01 |
| 2011-09-09 | TSX/TDX | 11 | 0.06 | 2325 | 0.02 | 0.06 |
| 2011-09-14 | TSX/TDX | 11 | 0.05 | 3667 | 0.02 | 0.05 |
| 2011-09-14 | TSX/TDX | 11 | 0.12 | 1279 | 0.02 | 0.12 |
| 2011-09-15 | TSX/TDX | 11 | 0.03 | 15546 | 0.02 | 0.03 |
| 2011-09-15 | TSX/TDX | 11 | 0.07 | 7819 | 0.02 | 0.07 |
| 2011-09-27 | TSX/TDX | 44 | 0.14 | 2001 | 0.01 | 0.14 |
| 2011-10-01 | TSX/TDX | 33 | 0.02 | 1956 | 0.01 | 0.02 |
| 2011-10-01 | TSX/TDX | 44 | 0.04 | 3582 | 0.01 | 0.04 |
| 2011-10-06 | TSX/TDX | 33 | 0.04 | 3602 | 0.01 | 0.05 |
| 2011-10-06 | TSX/TDX | 33 | 0.11 | 1353 | 0.01 | 0.11 |
| 2011-10-12 | TSX/TDX | 66 | 0.02 | 3453 | 0.00 | 0.02 |
| 2011-10-17 | TSX/TDX | 55 | 0.03 | 3541 | 0.00 | 0.03 |
| 2011-10-23 | TSX/TDX | 11 | 0.06 | 2018 | 0.02 | 0.06 |
| 2011-11-03 | TSX/TDX | 22 | 0.05 | 3533 | 0.01 | 0.05 |
| 2011-11-03 | TSX/TDX | 22 | 0.07 | 1209 | 0.01 | 0.07 |
| 2011-11-25 | TSX/TDX | 22 | 0.03 | 3507 | 0.01 | 0.03 |
| 2011-12-06 | TSX/TDX | 11 | 0.06 | 2432 | 0.02 | 0.06 |
| 2011-12-12 | TSX/TDX | 33 | 0.01 | 13467 | 0.01 | 0.01 |
| 2011-12-13 | TSX/TDX | 44 | 0.05 | 2328 | 0.01 | 0.05 |
| 2011-12-17 | TSX/TDX | 22 | 0.01 | 4172 | 0.01 | 0.02 |
| 2011-12-18 | TSX/TDX | 33 | 0.08 | 2365 | 0.01 | 0.08 |
| 2012-01-03 | TSX/TDX | 11 | 0.01 | 16220 | 0.02 | 0.03 |
| 2012-01-03 | TSX/TDX | 11 | 0.07 | 8576 | 0.02 | 0.07 |
| 2012-01-31 | TSX/TDX | 55 | 0.05 | 2338 | 0.00 | 0.05 |
| 2012-03-09 | TSX/TDX | 11 | 0.02 | 13279 | 0.02 | 0.03 |
| 2012-03-09 | TSX/TDX | 11 | 0.16 | 7483 | 0.02 | 0.16 |
| 2012-03-10 | TSX/TDX | 22 | 0.07 | 2343 | 0.01 | 0.07 |
| 2012-03-15 | TSX/TDX | 22 | 0.01 | 15451 | 0.01 | 0.01 |
| 2012-03-15 | TSX/TDX | 33 | 0.05 | 2290 | 0.01 | 0.05 |
| 2012-03-15 | TSX/TDX | 22 | 0.07 | 7142 | 0.01 | 0.07 |
| 2012-03-20 | TSX/TDX | 11 | 0.08 | 6422 | 0.02 | 0.08 |
| 2012-03-21 | TSX/TDX | 44 | 0.05 | 2265 | 0.01 | 0.05 |
| 2012-03-25 | TSX/TDX | 22 | 0.11 | 1258 | 0.01 | 0.11 |
| 2012-03-26 | TSX/TDX | 55 | 0.05 | 2143 | 0.00 | 0.05 |
| 2012-03-26 | TSX/TDX | 11 | 0.19 | 2259 | 0.02 | 0.19 |
| 2012-04-01 | TSX/TDX | 22 | 0.14 | 2362 | 0.01 | 0.14 |
| 2012-04-06 | TSX/TDX | 33 | 0.06 | 2248 | 0.01 | 0.06 |
| 2012-04-06 | TSX/TDX | 11 | 0.10 | 2316 | 0.02 | 0.10 |
| 2012-04-12 | TSX/TDX | 22 | 0.05 | 2100 | 0.01 | 0.05 |
| 2012-04-17 | TSX/TDX | 22 | 0.02 | 15486 | 0.01 | 0.02 |
| 2012-04-17 | TSX/TDX | 22 | 0.05 | 7244 | 0.01 | 0.05 |
| 2012-04-30 | TSX/TDX | 11 | 0.04 | 1747 | 0.02 | 0.05 |

| Date [yyyy-mm-dd] | Satellite | $dt$ [d] | $\sigma_v^C$ [m d$^{-1}$] | $n$ | $\sigma_v^I$ [m d$^{-1}$] | $\sigma_v$ [m d$^{-1}$] |
|---|---|---|---|---|---|---|
| 2012-05-08 | TSX/TDX | 66 | 0.02 | 3381 | 0.00 | 0.02 |
| 2012-05-09 | TSX/TDX | 22 | 0.02 | 15305 | 0.01 | 0.02 |
| 2012-05-09 | TSX/TDX | 55 | 0.04 | 2344 | 0.00 | 0.04 |
| 2012-05-09 | TSX/TDX | 22 | 0.05 | 6241 | 0.01 | 0.05 |
| 2012-05-13 | TSX/TDX | 77 | 0.02 | 3656 | 0.00 | 0.02 |
| 2012-05-15 | TSX/TDX | 44 | 0.04 | 2221 | 0.01 | 0.04 |
| 2012-05-19 | TSX/TDX | 22 | 0.03 | 3672 | 0.01 | 0.03 |
| 2012-05-19 | TSX/TDX | 22 | 0.10 | 1275 | 0.01 | 0.10 |
| 2012-05-20 | TSX/TDX | 55 | 0.04 | 2375 | 0.00 | 0.04 |
| 2012-05-24 | TSX/TDX | 33 | 0.04 | 1210 | 0.01 | 0.04 |
| 2012-05-30 | TSX/TDX | 33 | 0.03 | 2544 | 0.01 | 0.03 |
| 2012-06-04 | TSX/TDX | 11 | 0.05 | 3532 | 0.02 | 0.06 |
| 2012-06-04 | TSX/TDX | 11 | 0.10 | 1351 | 0.02 | 0.11 |
| 2012-06-05 | TSX/TDX | 33 | 0.01 | 15558 | 0.01 | 0.01 |
| 2012-06-11 | TSX/TDX | 11 | 0.09 | 2222 | 0.02 | 0.09 |
| 2012-06-15 | TSX/TDX | 11 | 0.08 | 3328 | 0.02 | 0.09 |
| 2012-06-15 | TSX/TDX | 11 | 0.10 | 1280 | 0.02 | 0.10 |
| 2012-06-21 | TSX/TDX | 11 | 0.07 | 2621 | 0.02 | 0.07 |
| 2012-06-27 | TSX/TDX | 11 | 0.06 | 7647 | 0.02 | 0.06 |
| 2012-06-28 | TSX/TDX | 44 | 0.04 | 2293 | 0.01 | 0.04 |
| 2012-07-03 | TSX/TDX | 55 | 0.04 | 2350 | 0.00 | 0.04 |
| 2012-07-03 | TSX/TDX | 33 | 0.05 | 2292 | 0.01 | 0.05 |
| 2012-07-09 | TSX/TDX | 44 | 0.04 | 2389 | 0.01 | 0.04 |
| 2012-07-13 | TSX/TDX | 33 | 0.03 | 2765 | 0.01 | 0.03 |
| 2012-07-19 | TSX/TDX | 33 | 0.02 | 15662 | 0.01 | 0.02 |
| 2012-07-25 | TSX/TDX | 11 | 0.09 | 2122 | 0.02 | 0.09 |
| 2012-08-04 | TSX/TDX | 11 | 0.07 | 2545 | 0.02 | 0.07 |
| 2012-08-09 | TSX/TDX | 11 | 0.07 | 3577 | 0.02 | 0.07 |
| 2012-08-09 | TSX/TDX | 11 | 0.12 | 1204 | 0.02 | 0.13 |
| 2012-08-10 | TSX/TDX | 11 | 0.07 | 7151 | 0.02 | 0.07 |
| 2012-08-11 | TSX/TDX | 44 | 0.08 | 2444 | 0.01 | 0.08 |
| 2012-08-16 | TSX/TDX | 55 | 0.04 | 2374 | 0.00 | 0.04 |
| 2012-08-22 | TSX/TDX | 44 | 0.04 | 2230 | 0.01 | 0.04 |
| 2012-09-07 | TSX/TDX | 11 | 0.14 | 1690 | 0.02 | 0.14 |
| 2012-09-23 | TSX/TDX | 33 | 0.05 | 1078 | 0.01 | 0.05 |
| 2012-09-29 | TSX/TDX | 55 | 0.04 | 1597 | 0.00 | 0.04 |
| 2012-09-29 | TSX/TDX | 33 | 0.06 | 2397 | 0.01 | 0.06 |
| 2012-10-05 | TSX/TDX | 44 | 0.08 | 2401 | 0.01 | 0.08 |
| 2012-10-10 | TSX/TDX | 55 | 0.05 | 2372 | 0.00 | 0.05 |
| 2012-10-20 | TSX/TDX | 33 | 0.03 | 2520 | 0.01 | 0.03 |
| 2012-10-21 | TSX/TDX | 11 | 0.09 | 2179 | 0.02 | 0.09 |
| 2012-10-27 | TSX/TDX | 22 | 0.08 | 2296 | 0.01 | 0.08 |
| 2012-11-01 | TSX/TDX | 11 | 0.10 | 2327 | 0.02 | 0.10 |
| 2012-11-01 | TSX/TDX | 33 | 0.17 | 1923 | 0.01 | 0.17 |
| 2012-11-05 | TSX/TDX | 11 | 0.05 | 3446 | 0.02 | 0.05 |
| 2012-11-05 | TSX/TDX | 11 | 0.13 | 1186 | 0.02 | 0.13 |
| 2012-11-07 | TSX/TDX | 44 | 0.05 | 2312 | 0.01 | 0.05 |
| 2012-11-12 | TSX/TDX | 33 | 0.05 | 2364 | 0.01 | 0.06 |
| 2012-11-12 | TSX/TDX | 11 | 0.12 | 2354 | 0.02 | 0.12 |
| 2012-11-18 | TSX/TDX | 22 | 0.07 | 2419 | 0.01 | 0.07 |
| 2012-11-23 | TSX/TDX | 11 | 0.08 | 2204 | 0.02 | 0.09 |
| 2012-12-26 | TSX/TDX | 55 | 0.03 | 2141 | 0.00 | 0.03 |
| 2013-02-23 | TSX/TDX | 77 | 0.01 | 3503 | 0.00 | 0.01 |
| 2013-03-01 | TSX/TDX | 11 | 0.08 | 2802 | 0.02 | 0.08 |
| 2013-03-17 | TSX/TDX | 11 | 0.06 | 3749 | 0.02 | 0.07 |
| 2013-03-17 | TSX/TDX | 11 | 0.14 | 1255 | 0.02 | 0.14 |
| 2013-03-23 | TSX/TDX | 22 | 0.03 | 3632 | 0.01 | 0.03 |

| Date [yyyy-mm-dd] | Satellite | $dt$ [d] | $\sigma_v^C$ [m d$^{-1}$] | $n$ | $\sigma_v^I$ [m d$^{-1}$] | $\sigma_v$ [m d$^{-1}$] |
|---|---|---|---|---|---|---|
| 2013-03-23 | TSX/TDX | 22 | 0.08 | 1196 | 0.01 | 0.08 |
| 2013-03-26 | TSX/TDX | 11 | 0.08 | 1992 | 0.02 | 0.08 |
| 2013-03-28 | TSX/TDX | 11 | 0.17 | 1347 | 0.02 | 0.18 |
| 2013-03-29 | TSX/TDX | 33 | 0.05 | 1148 | 0.01 | 0.05 |
| 2013-04-03 | TSX/TDX | 33 | 0.09 | 2117 | 0.01 | 0.09 |
| 2013-04-10 | TSX/TDX | 22 | 0.06 | 2172 | 0.01 | 0.07 |
| 2013-04-15 | TSX/TDX | 33 | 0.07 | 2237 | 0.01 | 0.07 |
| 2013-04-26 | TSX/TDX | 55 | 0.05 | 2275 | 0.00 | 0.05 |
| 2013-04-26 | TSX/TDX | 11 | 0.12 | 2379 | 0.02 | 0.13 |
| 2013-04-30 | TSX/TDX | 55 | 0.02 | 3261 | 0.00 | 0.03 |
| 2013-06-08 | TSX/TDX | 22 | 0.03 | 3820 | 0.01 | 0.03 |
| 2013-06-08 | TSX/TDX | 22 | 0.04 | 1021 | 0.01 | 0.04 |
| 2013-06-19 | TSX/TDX | 44 | 0.02 | 3719 | 0.01 | 0.02 |
| 2013-06-30 | TSX/TDX | 22 | 0.03 | 3813 | 0.01 | 0.03 |
| 2013-06-30 | TSX/TDX | 22 | 0.09 | 1258 | 0.01 | 0.09 |
| 2013-07-28 | TSX/TDX | 33 | 0.01 | 15233 | 0.01 | 0.02 |
| 2013-08-02 | TSX/TDX | 33 | 0.02 | 2763 | 0.01 | 0.02 |
| 2013-08-25 | TSX/TDX | 33 | 0.05 | 2311 | 0.01 | 0.05 |
| 2013-08-30 | TSX/TDX | 33 | 0.01 | 15399 | 0.01 | 0.01 |
| 2013-09-20 | TSX/TDX | 33 | 0.03 | 3602 | 0.01 | 0.03 |
| 2013-09-20 | TSX/TDX | 33 | 0.05 | 1292 | 0.01 | 0.05 |
| 2013-09-27 | TSX/TDX | 33 | 0.04 | 2235 | 0.01 | 0.04 |
| 2013-10-02 | TSX/TDX | 33 | 0.01 | 15262 | 0.01 | 0.01 |
| 2013-10-23 | TSX/TDX | 33 | 0.02 | 3578 | 0.01 | 0.02 |
| 2013-10-23 | TSX/TDX | 33 | 0.05 | 1283 | 0.01 | 0.05 |
| 2013-10-30 | TSX/TDX | 33 | 0.05 | 2317 | 0.01 | 0.05 |
| 2013-11-02 | TSX/TDX | 11 | 0.02 | 9090 | 0.02 | 0.03 |
| 2013-11-02 | TSX/TDX | 11 | 0.07 | 484 | 0.02 | 0.07 |
| 2013-11-04 | TSX/TDX | 33 | 0.02 | 15102 | 0.01 | 0.02 |
| 2013-11-09 | TSX/TDX | 11 | 0.05 | 2652 | 0.02 | 0.06 |
| 2013-11-10 | TSX/TDX | 55 | 0.04 | 2294 | 0.00 | 0.04 |
| 2013-11-15 | TSX/TDX | 22 | 0.04 | 2878 | 0.01 | 0.05 |
| 2013-11-20 | TSX/TDX | 22 | 0.03 | 3538 | 0.01 | 0.04 |
| 2013-11-20 | TSX/TDX | 33 | 0.04 | 2955 | 0.01 | 0.04 |
| 2013-11-20 | TSX/TDX | 11 | 0.08 | 2846 | 0.02 | 0.08 |
| 2013-11-20 | TSX/TDX | 22 | 0.10 | 1321 | 0.01 | 0.10 |
| 2013-11-21 | TSX/TDX | 11 | 0.08 | 2180 | 0.02 | 0.08 |
| 2013-11-25 | TSX/TDX | 33 | 0.02 | 3312 | 0.01 | 0.02 |
| 2013-11-25 | TSX/TDX | 33 | 0.05 | 1125 | 0.01 | 0.05 |
| 2013-11-26 | TSX/TDX | 11 | 0.03 | 15060 | 0.02 | 0.03 |
| 2013-11-26 | TSX/TDX | 22 | 0.04 | 2825 | 0.01 | 0.04 |
| 2013-11-26 | TSX/TDX | 11 | 0.08 | 6708 | 0.02 | 0.09 |
| 2013-11-27 | TSX/TDX | 22 | 0.08 | 2346 | 0.01 | 0.09 |
| 2013-11-30 | TSX/TDX | 44 | 0.00 | 8207 | 0.01 | 0.01 |
| 2013-12-01 | TSX/TDX | 44 | 0.02 | 3438 | 0.01 | 0.02 |
| 2013-12-01 | TSX/TDX | 33 | 0.03 | 2670 | 0.01 | 0.03 |
| 2013-12-01 | TSX/TDX | 11 | 0.06 | 2893 | 0.02 | 0.06 |
| 2013-12-02 | TSX/TDX | 22 | 0.01 | 14680 | 0.01 | 0.01 |
| 2013-12-02 | TSX/TDX | 33 | 0.04 | 2079 | 0.01 | 0.04 |
| 2013-12-02 | TSX/TDX | 22 | 0.06 | 6620 | 0.01 | 0.06 |
| 2013-12-02 | TSX/TDX | 11 | 0.23 | 1957 | 0.02 | 0.24 |
| 2013-12-06 | TSX/TDX | 11 | 0.05 | 3548 | 0.02 | 0.06 |
| 2013-12-06 | TSX/TDX | 11 | 0.15 | 1322 | 0.02 | 0.15 |
| 2013-12-07 | TSX/TDX | 11 | 0.02 | 14924 | 0.02 | 0.03 |
| 2013-12-07 | TSX/TDX | 22 | 0.04 | 2905 | 0.01 | 0.04 |
| 2013-12-07 | TSX/TDX | 11 | 0.11 | 8347 | 0.02 | 0.11 |
| 2013-12-08 | TSX/TDX | 22 | 0.08 | 2021 | 0.01 | 0.08 |

| Date [yyyy-mm-dd] | Satellite | *dt* [d] | $\sigma_v^C$ [m d$^{-1}$] | *n* | $\sigma_v^T$ [m d$^{-1}$] | $\sigma_v$ [m d$^{-1}$] |
|---|---|---|---|---|---|---|
| 2013-12-12 | TSX/TDX | 22 | 0.03 | 3508 | 0.01 | 0.03 |
| 2013-12-12 | TSX/TDX | 33 | 0.03 | 2814 | 0.01 | 0.03 |
| 2013-12-12 | TSX/TDX | 11 | 0.07 | 3039 | 0.02 | 0.08 |
| 2013-12-12 | TSX/TDX | 22 | 0.09 | 1242 | 0.01 | 0.09 |
| 2013-12-13 | TSX/TDX | 33 | 0.06 | 2306 | 0.01 | 0.06 |
| 2013-12-13 | TSX/TDX | 11 | 0.07 | 2024 | 0.02 | 0.08 |
| 2013-12-17 | TSX/TDX | 11 | 0.02 | 3978 | 0.02 | 0.03 |
| 2013-12-17 | TSX/TDX | 33 | 0.03 | 3323 | 0.01 | 0.03 |
| 2013-12-17 | TSX/TDX | 11 | 0.14 | 1290 | 0.02 | 0.14 |
| 2013-12-18 | TSX/TDX | 33 | 0.01 | 13920 | 0.01 | 0.01 |
| 2013-12-18 | TSX/TDX | 22 | 0.03 | 2741 | 0.01 | 0.04 |
| 2013-12-23 | TSX/TDX | 22 | 0.03 | 3725 | 0.01 | 0.03 |
| 2013-12-23 | TSX/TDX | 11 | 0.05 | 2877 | 0.02 | 0.06 |
| 2013-12-23 | TSX/TDX | 22 | 0.09 | 1118 | 0.01 | 0.10 |
| 2013-12-24 | TSX/TDX | 22 | 0.01 | 14893 | 0.01 | 0.01 |
| 2013-12-24 | TSX/TDX | 22 | 0.05 | 7587 | 0.01 | 0.05 |
| 2013-12-24 | TSX/TDX | 11 | 0.09 | 2342 | 0.02 | 0.09 |
| 2013-12-28 | TSX/TDX | 11 | 0.05 | 3475 | 0.02 | 0.05 |
| 2013-12-28 | TSX/TDX | 11 | 0.14 | 1096 | 0.02 | 0.15 |
| 2013-12-30 | TSX/TDX | 44 | 0.03 | 2034 | 0.01 | 0.03 |
| 2014-01-03 | TSX/TDX | 33 | 0.02 | 2819 | 0.01 | 0.02 |
| 2014-01-04 | TSX/TDX | 55 | 0.04 | 2128 | 0.00 | 0.04 |
| 2014-01-04 | TSX/TDX | 33 | 0.05 | 1939 | 0.01 | 0.05 |
| 2014-01-09 | TSX/TDX | 22 | 0.03 | 2828 | 0.01 | 0.03 |
| 2014-01-10 | TSX/TDX | 44 | 0.03 | 2083 | 0.01 | 0.03 |
| 2014-01-10 | TSX/TDX | 22 | 0.10 | 2104 | 0.01 | 0.10 |
| 2014-01-14 | TSX/TDX | 44 | 0.01 | 3685 | 0.01 | 0.01 |
| 2014-01-15 | TSX/TDX | 33 | 0.05 | 2236 | 0.01 | 0.05 |
| 2014-01-19 | TSX/TDX | 33 | 0.02 | 3652 | 0.01 | 0.02 |
| 2014-01-31 | TSX/TDX | 22 | 0.03 | 2647 | 0.01 | 0.03 |
| 2014-02-27 | TSX/TDX | 44 | 0.03 | 3163 | 0.01 | 0.03 |
| 2014-02-28 | TSX/TDX | 55 | 0.05 | 2235 | 0.00 | 0.05 |
| 2014-03-24 | TSX/TDX | 11 | 0.08 | 1958 | 0.02 | 0.08 |
| 2014-03-27 | TSX/TDX | 11 | 0.03 | 15610 | 0.02 | 0.03 |
| 2014-04-04 | TSX/TDX | 33 | 0.04 | 1921 | 0.01 | 0.04 |
| 2014-04-10 | TSX/TDX | 22 | 0.05 | 1895 | 0.01 | 0.05 |
| 2014-07-25 | TSX/TDX | 11 | 0.07 | 1184 | 0.02 | 0.08 |
| 2014-08-05 | TSX/TDX | 33 | 0.05 | 1130 | 0.01 | 0.05 |
| 2014-08-06 | TSX/TDX | 22 | 0.03 | 2495 | 0.01 | 0.03 |
| 2014-08-11 | TSX/TDX | 33 | 0.02 | 2649 | 0.01 | 0.02 |
| 2014-08-11 | TSX/TDX | 22 | 0.08 | 1340 | 0.01 | 0.08 |
| 2014-08-22 | TSX/TDX | 11 | 0.08 | 3049 | 0.02 | 0.08 |
| 2014-08-27 | TSX/TDX | 11 | 0.08 | 1215 | 0.02 | 0.09 |
| 2014-12-16 | TSX/TDX | 11 | 0.03 | 15265 | 0.02 | 0.03 |

| datasets | Mean values: | | | | | |
|---|---|---|---|---|---|---|
| 382 | All | | 0.07 | 11717 | 0.05 | 0.08 |
| 59 | ERS | | 0.14 | 26475 | 0.04 | 0.15 |
| 5 | R1 | | 0.09 | 32794 | 0.06 | 0.11 |
| 41 | ENVISAT | | 0.11 | 30240 | 0.04 | 0.12 |
| 43 | ALOS | | 0.05 | 13868 | 0.01 | 0.05 |
| 234 | TSX/TDX | | 0.06 | 4414 | 0.01 | 0.06 |

Date - mean date of SAR acquisitions

*dt* - time interval in days between consecutive SAR acquisitions

$\sigma_v^C$ - uncertainty of image coregistration

$\sigma_v^T$ - uncertainty of intensity tracking process

[*] if *dt* = 1d -> $\sigma_v = \sigma_v^C$ see manuscript Section 4.2